

This version of the article has been accepted for publication, after peer review (when applicable) and is subject to Springer Nature's AM terms of use, but is not the Version of Record and does not reflect post-acceptance improvements, or any corrections. The Version of Record is available online at:

http://dx.doi.org/10.1007/978-981-19-9776-1_67

Access to this work was provided by the University of Maryland, Baltimore County (UMBC) ScholarWorks@UMBC digital repository on the Maryland Shared Open Access (MD-SOAR) platform.

Please provide feedback

Please support the ScholarWorks@UMBC repository by emailing scholarworks-group@umbc.edu and telling us what having access to this work means to you and why it's important to you. Thank you.

Flex-Nucleosides – A Strategic Approach to Antiviral Therapeutics

Seley-Radtke, Katherine L. *; Kutz, Christianna H. M.; Thames, Joy E.

*Corresponding author

A. Abstract:

One of the most common classes of drugs are nucleoside analogues, which have long served as a cornerstone for antiviral, antiparasitic, and anticancer treatments. This is due to their close resemblance to the naturally occurring nucleosides found in many biological processes. In terms of antiviral drug design, typically viral proteins or cellular proteins are targeted. Each has its pros and cons; however, both carry the risk of the development of drug resistance, making it imperative that novel and more effective antivirals are developed. This chapter will focus on a specific class of shaped-modified nucleoside analogues called fleximers. These flexible nucleoside analogues possess a split purine ring system, which endows flexibility to the nucleobase scaffold. This flexibility has been shown to be beneficial for increased antiviral activity but also results in broad-spectrum antiviral activity as well as the potential to overcome point mutations related to viral drug resistance. For over two decades now, the fleximer technology has been applied to numerous nucleoside analogues and has led to potent, broad-spectrum activity against a wide array of viruses including flaviviruses, filoviruses, and coronaviruses among others. Their history and development, the various synthetic routes to realize them, and some of the biological data obtained to date for the fleximers will be discussed within this chapter.

B. Fleximers, nucleosides/nucleotides, enzyme inhibitors, antiviral

C. Introduction:

Nucleoside analogues are one of the most common drug types, often used as antivirals or antineoplastic agents.(Seley-Radtke and Yates 2018, Yates and Seley-Radtke 2019) They are an attractive target for drug design due to their implication in biological and cellular processes.(Périgaud, Gosselin et al. 1992, De Clercq 2002, Ouellette and Rawn 2018) When looking at current antiviral drugs that have been approved for clinical use, a vast majority of these are either nucleoside or nucleotide analogues.(De Clercq 2005) Usually, this antiviral activity stems from the nucleoside analogues being able to target specific intracellular biosynthetic events, with selectivity coming from the inhibition of specific virus-associated or virus-induced enzymes that are part of nucleos(t)ide metabolism or from inhibition of enzymes critical for viral replication.(Périgaud, Gosselin et al. 1992, Seley-Radtke 2018, Seley-Radtke and Yates 2018, Yates and Seley-Radtke 2019) Typically, the triphosphate of a nucleoside analogue is the active form.(Périgaud, Gosselin et al. 1992, De Clercq 2002, Seley-Radtke and Yates 2018, Yates and Seley-Radtke 2019) However, due to poor cell membrane permeability, the triphosphate cannot be directly administered.(Périgaud, Gosselin et al. 1992) Instead, nucleoside analogues are administered and are then phosphorylated intracellularly by kinases (**Figure 1**).(De Clercq and Neyts 2009, Seley-Radtke and Yates 2018, Yates and Seley-Radtke 2019)

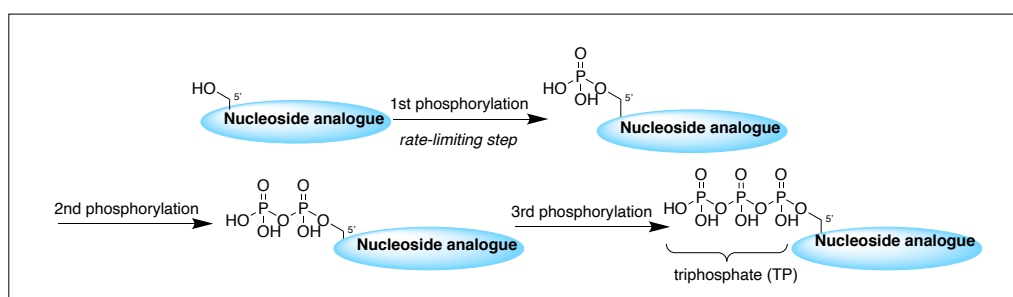


Figure 1. Intracellular activation of nucleoside analogues (conversion to triphosphate form).(Mehellou, Rattan et al. 2018)

Antiviral drug design typically focuses on one of two targets: viral proteins or cellular proteins.(Périgaud, Gosselin et al. 1992, Seley-Radtke and Yates 2018, Yates and Seley-Radtke 2019) By targeting viral proteins, greater specificity is usually observed which leads to lower drug toxicity and off target effects; however, the breadth of the antiviral activity is usually fairly narrow and there is a higher risk for the development of drug resistance.(De Clercq 2002) Conversely, targeting cellular proteins can help reduce the risk of drug resistance and impart more broad-spectrum activity but often comes at the cost of increased toxicity.(De Clercq 2002) Thus, it is critical that new and more effective antivirals are continually developed

in order to combat emerging and reemerging infectious diseases as well as viral resistance.(De Clercq 2002, Seley-Radtke and Yates 2018, Yates and Seley-Radtke 2019)

D. Background and significance:

I. Nucleobase Modifications

When looking at the nucleos(t)ide scaffold (**Figure 2**), its structure can be broken down into four main components: a heterocyclic base (nucleobase), the glycosidic bond, the sugar, and in the case of nucleotides, the phosphate moiety.(Seley-Radtke and Yates 2018) These components represent sites at which many different types of modifications can be made.(De Clercq 2005, De Clercq and Neyts 2009, Seley-Radtke and Yates 2018, Yates and Seley-Radtke 2019) Modifications to the nucleoside structure can then lead to disruption of biological processes such as viral DNA/RNA replication.(De Clercq and Neyts 2009)

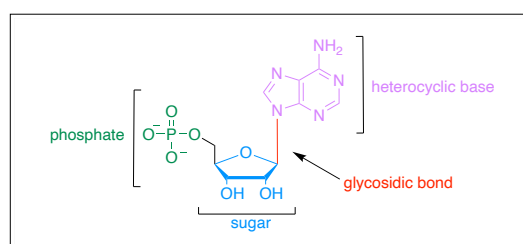


Figure 2. The nucleoside scaffold.

Typically, the nucleos(t)ide analogue is recognized as a substrate by an enzyme involved with replication of the target virus.(Seley, Zhang et al. 2001, Seley, Zhang et al. 2002, De Clercq and Neyts 2009, Tripathi and Bankaitis 2017) Historically, the relationship between an enzyme and substrate recognition was commonly regarded as akin to a lock and key as first introduced by Emil Fischer in 1894.(Fischer 1894, Tripathi and Bankaitis 2017) The substrate, or “key”, should be able to fit into the enzyme binding site, or “lock”, and either compete with the natural substrate and block it from binding, or be incorporated into the growing DNA/RNA chain and result in chain termination.(Fischer 1894, Seley, Zhang et al. 2002, Tripathi and Bankaitis 2017, Seley-Radtke and Yates 2018) Based on this analogy, the substrate must perfectly fit into the enzyme binding site in order to have biological activity.(Fischer 1894, Tripathi and Bankaitis 2017) Substrates that are too large or misshaped would not be able to appropriately fit into the enzyme “lock”.(Fischer 1894, Tripathi and Bankaitis 2017) However, later Daniel Koshland proposed the “induced fit” model which proposed that enzymes actually adjust their shape when interacting with given substrates.(Koshland 1958, Tripathi and Bankaitis 2017) With this model, the enzyme “lock” becomes dynamic when interacting with a set substrate “key”, causing changes to the “keyhole” or binding site.(Koshland 1958, Tripathi and Bankaitis 2017) Thus, when a substrate “key” interacts with the enzyme “lock”, it induces certain conformational changes.(Koshland 1958, Tripathi and Bankaitis 2017) Specific conformational changes then produce the desired result (e.g. biological activity).(Koshland 1958, Tripathi and Bankaitis 2017) Thus the induced fit model accounts for ligands which, based on shape, would appear to be substrates for given enzymes but in reality have little to no interaction.(Koshland 1958, Tripathi and Bankaitis 2017)

Taking into account this induced fit model that has a dynamic “lock” with a rigid “key”, Seley-Radtke hypothesized that a “key” which is more flexible would theoretically be able to adapt to fit into numerous “locks”.(Seley, Zhang et al. 2001, Seley, Zhang et al. 2002, Tripathi and Bankaitis 2017) With this in mind, in 2001 Seley-Radtke introduced a novel class of shaped-modified nucleosides known as “fleximers” (**Figure 3**).(Seley, Zhang et al. 2001, Seley, Zhang et al. 2002)

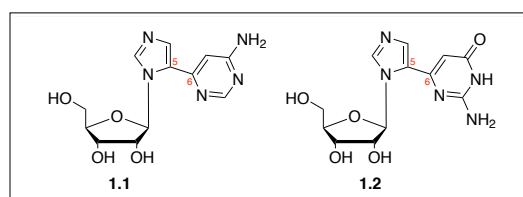


Figure 3. Distal fleximers: Flex-adenosine (1.1, Flex-A) and flex-guanosine (1.2, Flex-G).

To maintain key molecular elements needed for binding site recognition, the goal was to split the bicyclic purine ring system, preserving the structural features involved with hydrogen bonding and enzyme

recognition, while adding flexibility.(Seley, Zhang et al. 2001, Seley, Zhang et al. 2002) The first fleximers featured a split purine ring connected through a carbon-carbon bond between the C-5 of the imidazole moiety and the C-6 of the pyrimidine ring, analogous to Leonard's *dist*-benzo nucleosides.(Leonard, Morrice et al. 1975, Morrice, Sprecker et al. 1975, Seley, Zhang et al. 2001, Seley, Zhang et al. 2002, Seley, Quirk et al. 2003) And thus, the first "fleximers" were created, featuring a 1.50 Å separation between the two nucleobase rings (**Figure 3**). (Seley, Zhang et al. 2002) Those first fleximers became the basis for pursuing various novel fleximer scaffolds that are still being pursued today.

1. Distal Fleximers

As mentioned previously, the first fleximers to be synthesized featured a split purine ring with the carbon-carbon bond occurring between the C-5 of the imidazole moiety and the C-6 of the pyrimidine moiety.(Seley, Zhang et al. 2001) These fleximers later became known as *distal* fleximers. Interestingly, they were conceived as a result of another project going on in the Seley-Radtke group based on the extended purine nucleosides introduced by Nelson Leonard with his *lin*-, *prox*-, and *dist*-benzo nucleosides (**Figure 4**). (Leonard, Morrice et al. 1975, Morrice, Sprecker et al. 1975, Leonard and Hiremath 1986, Seley, Zhang et al. 2001) These benzo-expanded nucleosides were limited by structural rigidity and likely attributed to poor enzyme inhibition.(Leonard, Morrice et al. 1975, Morrice, Sprecker et al. 1975, Leonard and Hiremath 1986)

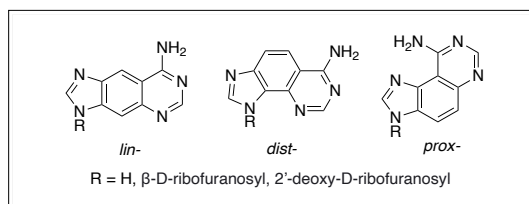
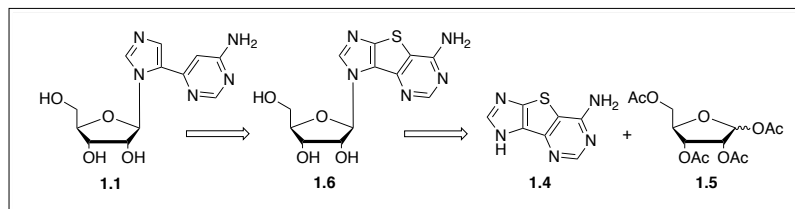


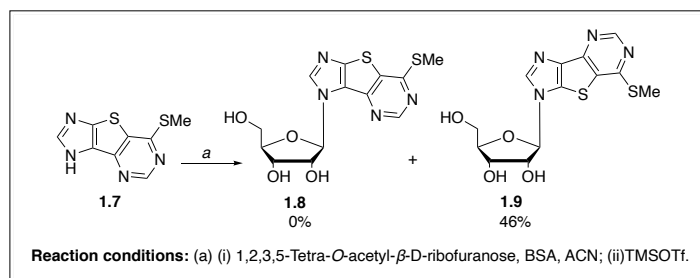
Figure 4. Leonard's benzo-expanded nucleosides.

Initially, Seley-Radtke planned to achieve fleximers **1.1** and **1.2** (**Figure 3**) using Leonard's approach by first constructing the tricyclic base (utilizing a thiophene spacer ring instead of a benzene spacer ring) followed by coupling to a commercially available tetraacetate-protected sugar, shown in **Scheme 1**. (Leonard, Morrice et al. 1975, Seley, Zhang et al. 2001)



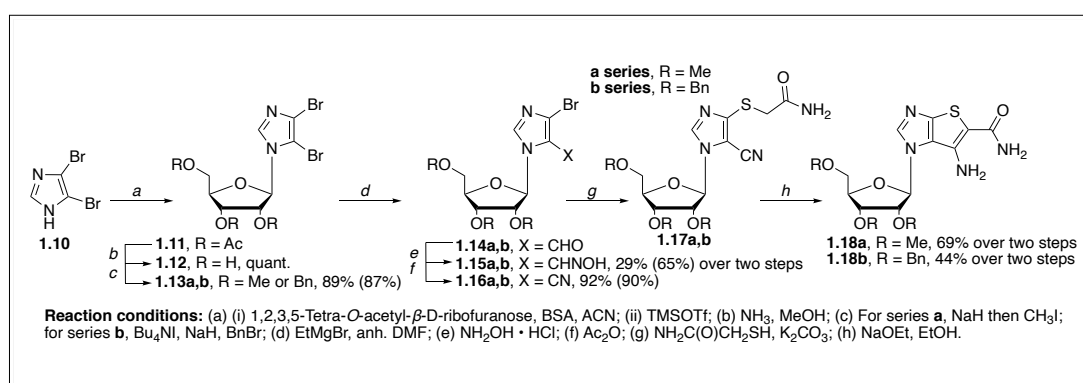
Scheme 1. Proposed synthetic route to distal flex-adenosine (**1.1**).

However, although both tricyclic heterobase **1.4** and the analogous guanine analogue were successfully achieved, attempts at the subsequent coupling proved fruitless due to solubility issues.(Seley, Zhang et al. 2001) Instead, Seley-Radtke turned to using the thiomethyl intermediate **1.7** for coupling in order to overcome solubility issues (**Scheme 2**), as previously shown by Leonard (Leonard, Morrice et al. 1975, Morrice, Sprecker et al. 1975, Leonard and Hiremath 1986) and others in the synthesis of *lin*-benzo nucleoside analogues.(Seley, Zhang et al. 2001) Both products **1.8** and **1.9** were expected, based on coupling at either the desired N3 or at N1, respectively.(Seley, Zhang et al. 2001) However, NMR characterization revealed that only the N1 product was obtained and thus attention was turned to a linear approach.(Seley, Zhang et al. 2001)



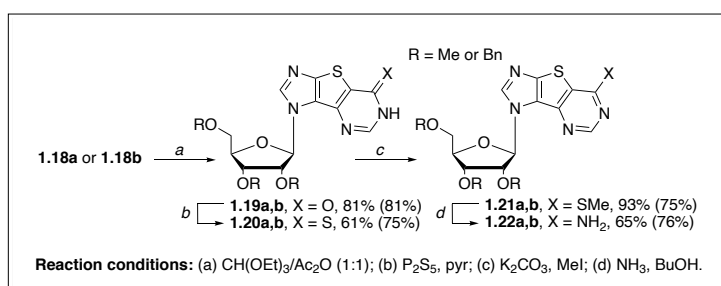
Scheme 2. Tricyclic intermediates **1.8** and **1.9**.

When investigating potential heterobases to use in the synthesis of fleximers **1.1** and **1.2**, 4,5-dibromimidazole **1.10** was found to be advantageous due to its symmetry which would result in only one product regardless of which nitrogen the coupling occurred. (Seley, Zhang et al. 2001) Additionally, it avoided the need for protecting the free imidazole nitrogen which, in previous attempts, proved to be difficult to deprotect later on. (Seley, Zhang et al. 2001) As shown in **Scheme 3**, acyl-protected intermediate **1.11** was achieved via a glycosidic coupling of 4,5-dibromimidazole **1.10** to a tetraacetate-protected ribose sugar which provided the initial nucleoside scaffold. (Seley, Zhang et al. 2001)



Scheme 3. Synthesis of imidazole-thiophene intermediates **1.18a** and **1.18b** from 4,5-dibromimidazole.

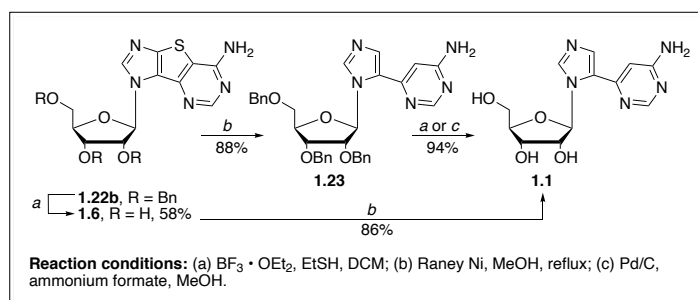
Removal of the acetate groups was achieved using methanolic ammonia, providing intermediate **1.12** in quantitative yield. The free hydroxyl groups were then protected with either methyl groups, for series **a**, or with benzyl groups, for series **b** as shown in **Scheme 3** to afford compounds **1.13a** and **1.13b** in high yields. The reasoning for replacing the labile acetate groups with more robust protecting groups was so that they would withstand the subsequent Grignard treatment to afford intermediates **1.14a** and **1.14b**. Conversion of the Grignard products to oximes **1.15a** and **1.15b** was achieved in low yield for series **a**, and in modest yield for series **b**. Dehydration of the oximes provided nitriles **1.16a** and **1.16b** both in high yields. The thiol side chain was then introduced using thioglycolamide which gave intermediates **1.17a** and **1.17b**. Immediate ring closure resulted in the bicyclic imidazole-thiophene intermediates **1.18a** and **1.18b** (**Scheme 4**). (Seley, Zhang et al. 2001) A 1:1 mixture of acetic anhydride and triethyl orthoformate was then used to close the pyrimidine ring, affording tricyclic intermediates **1.19a** and **1.19b** in high yields as shown in **Scheme 4**. (Seley, Zhang et al. 2001)



Scheme 4. Synthesis of tricyclic nucleoside intermediate **1.22a** and **1.22b**.

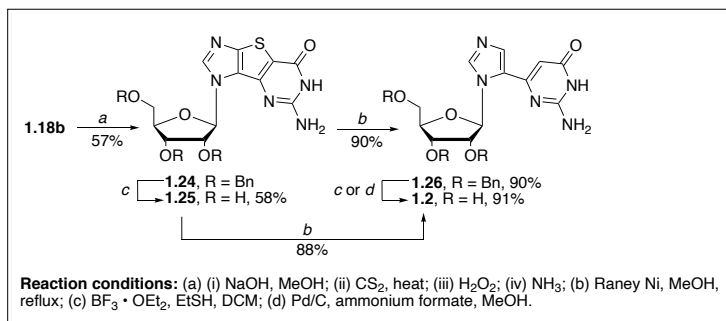
Conversion of carbonyls **1.19a** and **1.19b** to thiocarbonyls **1.20a** and **1.20b** was achieved using phosphorus pentasulfide, as shown in **Scheme 4**. The thiocarbonyls were then immediately methylated to

afford intermediates **1.21a** in high yield and **1.21b** in lower yield. Ammonolysis of the methylated intermediates then provided compounds **1.22a** and **1.22b** (**Scheme 4**). (Seley, Zhang et al. 2001) Attempts to then remove the protecting groups from the hydroxyls of both **1.22a** and **1.22b** proved to be futile. Eventually it was found that by using an excess of boron trifluoride etherate and ethanethiol, the benzyl groups of **1.22b** could be successfully removed, providing compound **1.6** in modest yield (**Scheme 5**). (Seley, Zhang et al. 2001) Reflux of compound **1.6** with Raney nickel resulted in removal of the sulfur in the thiophene spacer ring, providing fleximer **1.1**. (Seley, Zhang et al. 2001) Attempts to improve yield by first removing the sulfur of compound **1.22b** to afford intermediate **1.23** followed by debenzoylation to achieve fleximer **1.1** led to low yields with difficult purification using the same deprotection method. (Seley, Zhang et al. 2001) However, by using palladium on charcoal and ammonium formate to remove the benzyl groups of compound **1.23** instead, fleximer **1.1** was achieved in high yields with facile purification as shown in **Scheme 5**. (Seley, Zhang et al. 2001)



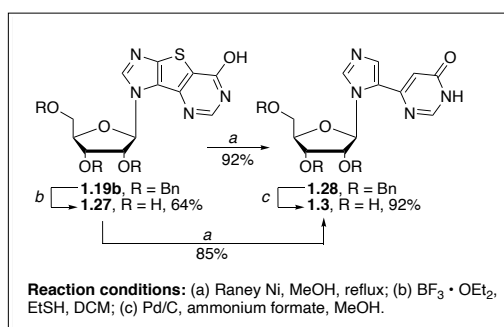
Scheme 5. Synthesis of Flex-adenosine (**1.1**, Flex-A).

The guanosine fleximer **1.2** was achieved by subjecting intermediate **1.18b** to an alternative ring closing procedure to afford compound **1.24** as shown in **Scheme 6**. The benzyl groups were then removed using boron trifluoride etherate, providing intermediate **1.25**. Treatment with Raney Ni then provided fleximer **1.2** in high yield (**Scheme 6**). Again, investigation into the reversal of the sulfur cleavage and deprotection steps saw similar yields for flex-guanosine **1.2**. (Seley, Zhang et al. 2001)



Scheme 6. Synthesis of distal Flex-guanosine (**1.2**, Flex-G).

In parallel, an inosine fleximer analogue was synthesized using methods similar to that of the adenosine fleximer. Starting from intermediate **1.19b** shown in **Scheme 7**, flex-inosine could be achieved using two different methods, as summarized in **Scheme 7**. (Seley, Zhang et al. 2001)



Scheme 7. Synthesis of Flex-inosine (**1.3**).

The first method employed involved treatment of tricyclic **1.19b** with Raney nickel to afford intermediate **1.28** followed by deprotection using palladium on charcoal and ammonium formate to provide inosine fleximer **1.3**. Alternatively, intermediate **1.19b** could be treated with boron trifluoride etherate for deprotection to provide intermediate **1.27** and then converted to flex-inosine **1.3** using the same Raney nickel treatment. However, the former method was preferred due to better yields. (Seley, Zhang et al. 2001)

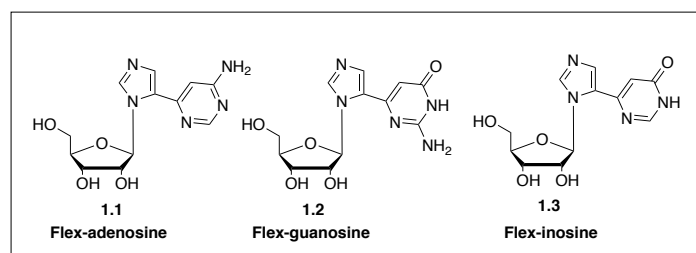


Figure 5. Structures of fleximer analogues of adenosine, guanosine, and inosine.

Initial *ab initio* quantum mechanical structure optimization calculations revealed that all three fleximer analogues, shown in **Figure 5**, had optimized conformations that converged to a similar final conformation. Structural and energetic properties of the calculated conformations are summarized in **Table 1**. (Seley, Zhang et al. 2002)

Table 1. Hartree-Fock Optimized Properties of Fleximer Structures.^a

| | Flex-adenosine (1.1) | Flex-guanosine (1.2) | Flex-inosine (1.3) |
|---|-------------------------|-------------------------|-----------------------|
| total energy (AU) | -1035.5 ± 22 | -1055.4 ± 28 | -1110.5 ± 37 |
| dipole (Debye) | 4.9 | 9.7 | 11.7 |
| dihedral angle (deg) C2' – C1' – N1 – C2 | 223.2 ± 3.4 | 228.7 ± 3.3 | 225.6 ± 2.1 |
| dihedral angle (deg) N1 – C5 – C6' – N1' | -12.9 ± 4.1 | -26.6 ± 5.4 | -19.1 ± 6.6 |
| volume (Å ³) | 305.9 | 302.9 | 317.1 |
| bond (Å) rms dev | 0.009 | 0.007 | 0.004 |
| angles (deg) rms dev | 0.012 | 0.017 | 0.013 |

^a 6-311G* basis set utilized for the optimizations. Values are the average (±SD) of 16 optimized conformations. (Seley, Zhang et al. 2001) Table adapted from Seley et al. (Seley, Zhang et al. 2002)

An optimized structure of flex-adenosine is shown in **Figure 6**, with optimization done using RHF SCF gradient optimization at the 6-311G* level of theory. (Seley, Zhang et al. 2002) All three fleximer analogues adopted high *anti* conformations, with their corresponding dihedral angles all ~225 degrees while the ribose maintained a C2' *endo* conformation. (Seley, Zhang et al. 2002) As shown in **Figure 6**, the pyrimidine ring is rotated out of plane in respect to the imidazole ring. An automated molecular docking study with flex-adenosine revealed that the fleximer analogue adopts a conformation (**Figure 6**) similar to that of the nucleoside inhibitor reported by Turnet et al. in the S-adenosylhomocysteine (SAH) active site, with an RMS deviation of 1.1 Å. This difference is primarily attributed to a 0.4 Å translation of flex-adenosine towards His353 and an overall 12° rotation towards Asp190. (Seley, Zhang et al. 2002) Interestingly, the pyrimidine moiety is nearly perpendicular to the imidazole ring at 87°. (Seley, Zhang et al. 2002)

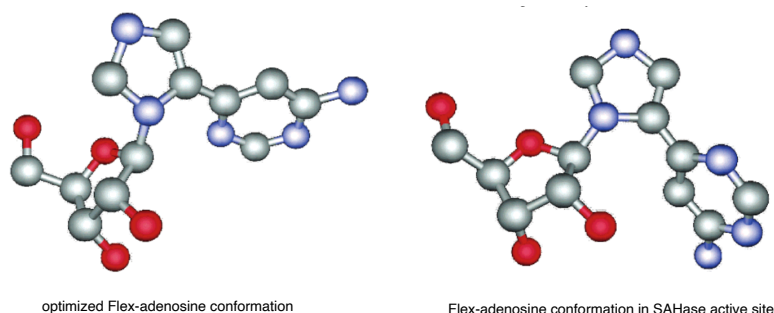


Figure 6. Optimized structure of Flex-adenosine. (Seley, Zhang et al. 2001) Best-fit conformation is shown, corresponding to -60 kcal/mol in the SAHase active site. (Seley, Zhang et al. 2001) Image used with permission from American Chemical Society. (Seley, Zhang et al. 2001)

There have been numerous nucleoside analogues reported to be potent inhibitors of S-adenosyl-L-homocysteine hydrolase (SAHase). (Yin, Yang et al. 2000, Seley, Quirk et al. 2003) SAHase is responsible for cleaving S-adenosylhomocysteine, a byproduct of S-adenosylmethionine (SAM)-promoted methyltransferase reactions, into adenosine and homocysteine using NADH as a cofactor. (Seley, Quirk et al. 2003) Inhibiting SAHase via nucleoside analogues results in NADH depletion and resulting intracellular accumulation of SAH. (Seley, Quirk et al. 2003) The imbalance of the SAH:SAM ratio thus leads to suspension of SAM-dependent methylations, causing DNA to be improperly methylated. (Seley, Quirk et al. 2003) This inhibition of SAHase leading to failed DNA methylation endows these nucleoside analogues antiviral (De Clercq 1994), antiparasitic and anticancer activity. (Chiang 1998) As part of an investigation into SAHase, three parent fleximers (analogues of adenosine, inosine, and guanosine) were tested. First, their structures were optimized using RHF SCF gradient optimization at the 6-311G* level of theory. (Seley, Zhang et al. 2002, Seley, Quirk et al. 2003) The optimized structures were then modelled in SAHase using automated molecular docking (Insight II, Discover/Accelrys) followed by Monte Carlo simulation and simulated annealing. Both adenosine and inosine fleximers occupied the SAHase active site in a similar orientation as shown previously in **Figure 6** with an *anti* conformation. (Seley, Zhang et al. 2002, Seley, Quirk et al. 2003) However, the guanosine fleximer was found to adopt a *syn* conformation as the lowest energy conformation in the SAHase active site (**Figure 7A**). (Seley, Zhang et al. 2002, Seley, Quirk et al. 2003) The pyrimidine moiety displayed such a high degree of twist such that intramolecular hydrogen bonding occurred between the pyrimidine carbonyl and the 5'-hydroxyl of the ribose sugar, as shown in **Figure 7B**. (Seley, Quirk et al. 2003) With this conformation, the amino group on the nucleobase is flipped into the binding pocket, allowing for flex-guanosine to act as an adenosine mimic. (Seley, Quirk et al. 2003)

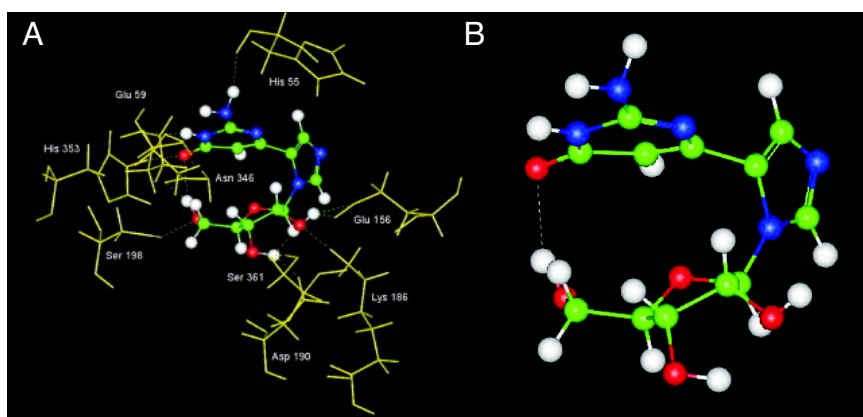


Figure 7. (A) Flex-guanosine showing *syn* conformation in the SAHase active site (yellow). (B) Binding conformation of Flex-guanosine. Images used with permission from Elsevier. (Seley, Quirk et al. 2003)

SAHase assays were also run with the parent fleximers to determine if any could be used as alternative substrates for the enzyme, results of which are summarized in **Table 2**. (Seley, Quirk et al. 2003)

Table 2. SAHase enzyme assays.

| Compound | K_m (μM) ^a | K_{cat} (m^{-1}) ^a | K_i (μM) ^a |
|-------------------------------|--------------------------------------|--|--------------------------------------|
| <i>Synthesis direction</i> | | | |
| Adenosine | 0.82 ± 0.004 | 91.2 ± 0.2 | n.d. ^b |
| Flex-Adenosine (1.1) | 54.4 ± 1.1 | 0.56 ± 0.04 | n.d. ^b |
| Inosine | 2.5 ± 0.03 | 44.2 ± 0.7 | 925 ± 21 |
| Flex-Inosine (1.3) | 421 ± 5.7 | 0.005 ± 0.003 | 422 ± 16 |
| Guanosine | 844 ± 6.6 | 0.06 ± 0.02 | 1472 ± 32 |
| Flex-Guanosine (1.2) | n.s. ^c | n.s. ^c | 217 ± 13 |
| <i>Hydrolysis direction</i> | | | |
| Flex-Guanosine (1.2) | 6.6 ± 0.2 | 28.3 ± 1.2 | 128 ± 18 |

^aValues are mean of three experiments; ^bn.d. not determined; ^cn.s. not a substrate.

Table adapted from Seley et al. (Seley, Quirk et al. 2003)

Both the adenosine and inosine fleximers were recognized as substrates although both were worse than their respective parent nucleosides. The guanosine fleximer, however, had activity in both the synthetic and hydrolytic directions of the SAHase assays, with reported K_i values of 217 and 128 μM respectively. (Seley, Quirk et al. 2003) This was also the first report of a guanosine analogue with SAHase inhibitory activity against an adenosine-metabolizing enzyme. (Seley, Quirk et al. 2003, Polak, Seley et al.

2004) This inhibition may be due to the ability of the guanosine fleximer to adopt a *syn* conformation.(Polak, Seley et al. 2004) Isothermal calorimetry (ITC) was used to determine if the guanosine fleximer formed a stable complex with SAHase, with results being that the interaction between the two is enthalpically driven thereby overcoming the entropic cost of binding. Flex-guanosine bound to SAHase with stoichiometry of 1:1 per monomer and four compound molecules per functional SAHase tetramer. The raw ITC data is shown in **Figure 8** with the binding isotherm shown below. (Seley, Quirk et al. 2003) However, the overall free energy (ΔG) was found to be negative, with a difference of only 2 kcal from the theoretical value. Overall, this preliminary data supported the notion that fleximers would make for a good scaffold given that the entropic loss could be overcome by the ability of fleximers to adopt more favorable conformations, allowing for more binding interactions.(Seley, Quirk et al. 2003)

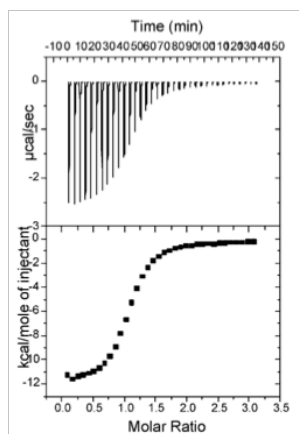


Figure 8. ITC data for flex-guanosine (1.2). Image used with permission from Elsevier.(Seley, Quirk et al. 2003)

Early conformational studies on the first fleximers (adenosine, inosine, and guanosine analogues) were performed to evaluate the degrees of freedom of the novel compounds as well as comparison to their natural counterparts.(Polak, Seley et al. 2004) Normally, the sugar moiety of nucleosides maintains a dynamic pseudorotational equilibrium between two pucker states: north (C3'-*endo*) and south (C2'-*endo*) with the preferred sugar conformation dictated by gauche effects of [O4'-C—C—O3'/2'] fragments, nucleobase anomeric effects, and steric interactions.(Polak, Seley et al. 2004) However, the separation of the nucleobase allows the fleximer analogue to better adapt to binding sites. Conformational equilibria were evaluated via ^1H and 1D difference NOE NMR spectroscopy in both D_2O and $\text{DMSO}-d_6$ solvents at varying temperatures between 298 and 358 K.(Polak, Seley et al. 2004) Pseudorotational analysis found that the fleximer bond, compared to the naturally-occurring parent compounds, led to a significant increase in north-type conformers.(Polak, Seley et al. 2004) The natural nucleosides had a 67-72% preference for south-type at 298 K whereas the fleximer analogues had a 51-64% preference for north-type at the same temperature.(Polak, Seley et al. 2004) This *anti* conformation observed for the fleximers, including flex-guanosine, in solution for NMR analysis differed from the *syn* conformation observed within the enzyme binding site for flex-guanosine.(Seley, Quirk et al. 2003) This tendency for the north:south equilibrium towards the north-type conformers is likely due to the anomeric effect of the fleximer nucleobase. However, since the change is only 2-4%, the fleximer bond gives a small increase in anomeric effect strength and/or small decrease in steric bulk.(Polak, Seley et al. 2004) Potential hydrogen bond formation between the NH_2 of the pyrimidine and the 2'-OH of the sugar moiety may account for the *anti* conformation preference of fleximers.(Polak, Seley et al. 2004)

The guanosine triphosphate fleximer (flex-GTP, **Figure 9**), was used in a study with GTP-L-Fucose pyrophosphorylase (GFPP) published by Quirk et al in 2005.(Quirk and Seley 2005) Both wild-type and various mutant GFPP were utilized in the study, with the K482A mutant showing loss of catalytic activity with a GTP-only substrate.(Quirk and Seley 2005) However, with the same GFPP mutant but flex-GTP as the substrate, k_{cat}/K_m , K_m , and k_{cat} values were found to be nearly identical to that of the wild-type GFPP. On the other hand, a 73.2-fold reduction in k_{cat}/K_m was observed the K478A mutant and flex-GTP substrate but wild-type values with GTP substrate. This confirms that lysine 478 is a catalytically important site for GFPP while also showing that the flexibility of flex-GTP allows the compound to interact with secondary amino acid residues that are typically not part of the binding site mechanisms, as seen with its cross-linking to a lysine out-of-distance to canonical GTP. Additionally, Quirk reported that flex-GTP was a better GFPP substrate compared to GTP as displayed by more than double the catalytic efficiency. Flex-GTP was also found to retain activity despite critical active site residue mutations.(Quirk and Seley 2005)

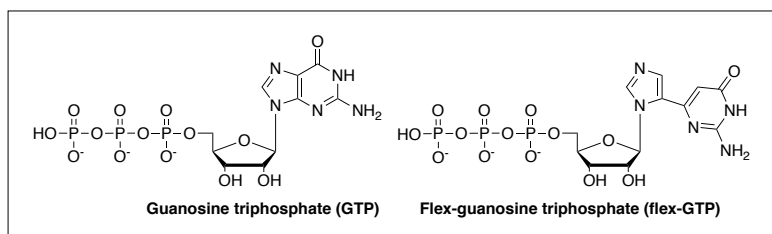


Figure 9. Structures of guanosine triphosphate and flex-guanosine triphosphate.

2. Proximal Fleximers

Inspired by the SAHase inhibitory activity of the initial guanosine distal-fleximer, the Seley-Radtke group explored alternative connectivity of the fleximer bond. The first synthesized fleximers had a carbon-carbon bond between the C-5 of the imidazole and the C-6 of the pyrimidine (Seley, Zhang et al. 2001, Seley, Zhang et al. 2002). These C-4 analogues instead featured the fleximer bond between the C-4 of the imidazole and the C-5 of the pyrimidine, as shown in **Figure 10**, and were named “proximal-fleximers”. (Seley, Salim et al. 2005)

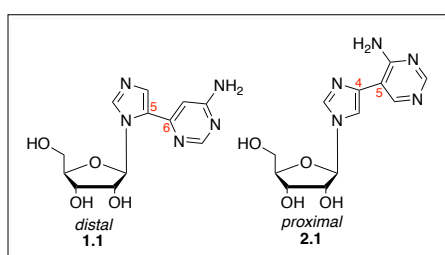
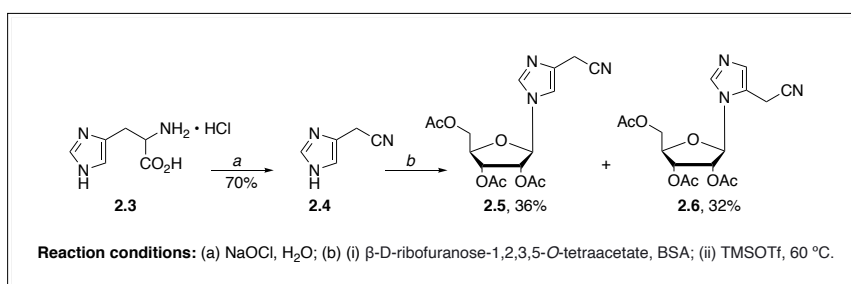


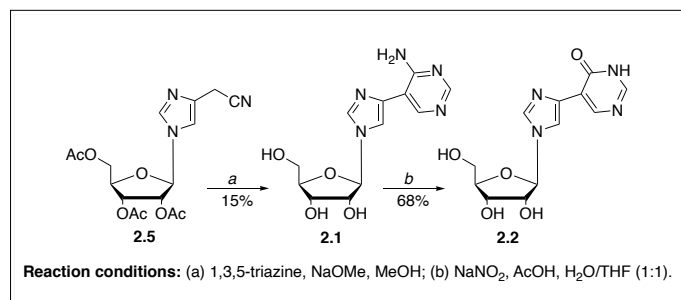
Figure 10. Structure of distal flex-adenosine (1.1, left) versus proximal flex-adenosine (2.1, right).

Initial efforts to synthesize proximal fleximers began with organometallic coupling methods, including Stille, Negishi, and Suzuki cross-couplings. (Seley, Salim et al. 2005) However, efforts to obtain the desired C-4 fleximers failed and were attributed to the electronic deficiency of the pyrimidine system being incompatible with the cross-couplings. (Seley, Salim et al. 2005) Instead, the C-4 imidazole fleximers were obtained via a more linear approach, beginning with histidine hydrochloride **2.3** reacting with sodium hypochlorite to yield intermediate **2.4**, as shown in **Scheme 8**. (Seley, Salim et al. 2005)



Scheme 8. Synthesis of intermediates **2.5** and **2.6** from histidine hydrochloride.

Standard coupling to the tetraacetate-protected ribose was achieved in modest yield, affording compounds **2.5** and **2.6** in 36% and 32% yields respectively. Intermediate **2.5** was followed by a [4 + 2] Diels-Alder cycloaddition with 1,3,5-triazine and immediate retro-Diels-Alder fragmentation to afford the C-4 adenosine fleximer **2.1** in low yield (**Scheme 9**). The overall yield from histidine **2.3** to proximal fleximer **2.1** was only 3.8% in three steps. The C-4 inosine fleximer **2.2** was then achieved via diazotization and subsequent hydrolysis of adenosine fleximer **2.1** using NaNO₂ and acetic acid in a 1:1 mixture of water and THF, as summarized in **Scheme 9**. (Seley, Salim et al. 2005)



Scheme 9. Synthesis of proximal flex-adenosine (**2.1**) and flex-inosine (**2.2**).

Although the overall yields for proximal fleximers **2.1** and **2.2** were very poor, the synthetic routes were short (3 and 4 steps respectively) and utilized readily available and affordable reagents thus opening up a new type of fleximer scaffold. (Seley, Salim et al. 2005)

3. Reverse Fleximers

Following the synthesis of both the early distal and proximal fleximers, the Seley-Radtke group next looked at “reversing” the connectivity of the split purine ring system to further explore how flexibility may improve biological activity. (Sadler, Ojewoye et al. 2008, Zimmermann, Sadler et al. 2011) Previous work by Herdewijn et al. showed C5-substituted pyrimidine ribose analogues with potent activity against HSV-1. (Wigerinck, Pannecouque et al. 1991, De Winter and Herdewijn 1996, Sadler, Ojewoye et al. 2008) Other ribose compounds have also been reported with similar structure to the target compounds shown in **Figure 11**. Among these include substituted pyrimidine analogues synthesized by Tor et al. for use as fluorescent bioprobes in DNA structure studies. (Greco and Tor 2005) Additionally, other carbocyclic scaffolds have shown promising activity for therapeutic use. Thus, the Seley-Radtke group decided to pursue a series of C5-substituted carboxylic uridine analogues using various carboxylic sugar scaffolds as shown in **Figure 11**. (Sadler, Ojewoye et al. 2008, Zimmermann, Sadler et al. 2011)

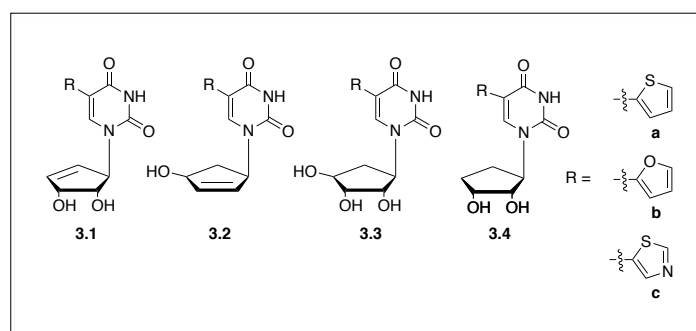
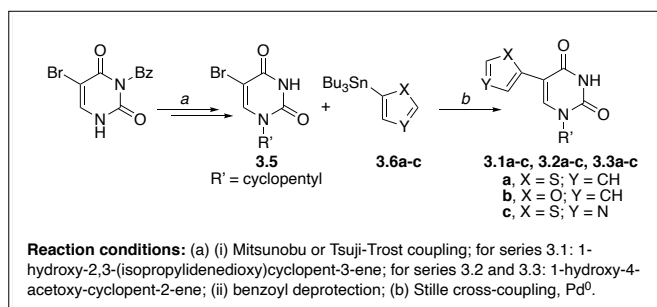


Figure 11. Reverse fleximers featuring various carboxylic sugars.

Initially, the Seley-Radtke group focused on synthesizing the series **3.1**, **3.2**, and **3.3** reverse fleximer analogues (**Figure 11**) which feature 5'-nor, norene, and 4',5'-dideoxy scaffolds. (Sadler, Ojewoye et al. 2008) Synthesis began first with obtaining pyrimidine nucleoside intermediate **3.5** via a Mitsunobu or Tsuji-Trost coupling between 3-benzoyl-5-bromouracil, and the relevant carbocyclic sugar followed by benzoyl deprotection for each series of reverse fleximers. Compounds **3.1a-c**, **3.2a-c**, and **3.3a-c** were then obtained via Stille cross-coupling as outlined in **Scheme 10**. (Sadler, Ojewoye et al. 2008) Preliminary biological testing revealed that compounds **3.2a** and **3.2b** had some activity against DNA methyltransferase (DNA MTase). This was promising as DNA MTase is a necessary enzyme for methylation for both viruses and cancer. (Sadler, Ojewoye et al. 2008)



Scheme 10. Synthesis of reverse fleximers 3.1a-c, 3.2a-c, and 3.3a-c using Stille cross-coupling methods.

Additionally, following leads from previous carbocyclic 5'-nor nucleoside inhibitors of SAHase, the 2',3'-dideoxy reverse carboxylic fleximer analogues (series 3.2) were further pursued (**Figure 12**). (Zimmermann, Sadler et al. 2011) An imidazole analogue was not pursued due to previous failed attempts by Herdewijn to remove the N-methyl group on the imidazole as well as lack of activity. (Wigerinck, Pannecouque et al. 1991, De Winter and Herdewijn 1996, Zimmermann, Sadler et al. 2011) Instead, focus was set on thiophene, furan, and thiazole analogues which had also shown the best biological activity for Herdewijn. (Wigerinck, Pannecouque et al. 1991, De Winter and Herdewijn 1996, Zimmermann, Sadler et al. 2011)

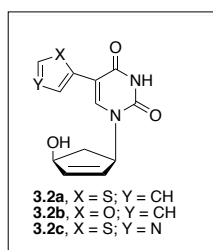
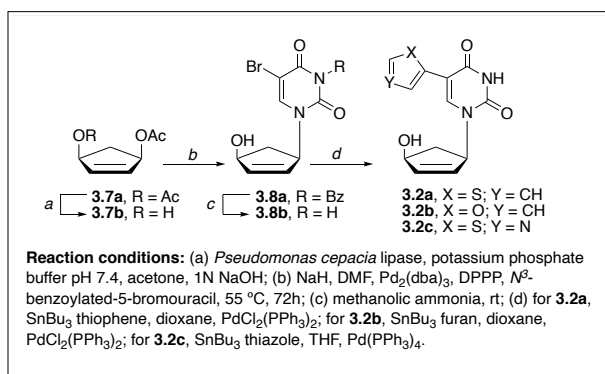


Figure 12. Structure of series 3.2 reverse fleximers.

The syntheses for compounds 3.2a-c are outlined in **Scheme 11**. Beginning with *meso*-diacetate 3.7a, *Pseudomonas cepacia* lipase was used to obtain enantiomer 3.7b. A palladium-catalyzed Tsuji-Trost coupling was used to add the *N*³-benzoyl protected pyrimidine base, affording compound 3.8a. Simple basic deprotection yielded compound 3.8b which was then coupled to various heterocycles using a Stille cross-coupling, resulting in compounds 3.2a-c. Pd(PPh₃)₄ was used as the catalyst for the coupling for compound 3.2c which resulted in better yields due to the increased electron density at the 2-position (and thus better reactivity) compared to the thiophene and furan derivatives. (Zimmermann, Sadler et al. 2011)



Scheme 11. Synthesis of series 3.2 reverse fleximers.

Following synthesis, compounds 3.2a-c were subjected to broad-spectrum antiviral testing; however, unfortunately, none of the compounds showed activity at subtoxic concentrations as summarized in **Table 3**. (Zimmermann, Sadler et al. 2011)

Table 3. Summary of antiviral screening for series 3.2 reverse fleximers.

| Virus | EC ₅₀ (μM) | | | |
|---------------------------------------|-----------------------|------|-------|------------------------|
| | 3.2a | 3.2b | 3.2c | Ribavirin ^a |
| <i>HEL cells</i> | | | | |
| HSV-1 (KOS) | >4 | >100 | >100 | >250 |
| HSV-1 TK ⁻ | >4 | >100 | >100 | >250 |
| HSV-2 (G) | >4 | >100 | >100 | >250 |
| VV | >4 | >100 | >100 | >250 |
| VSV | >4 | >100 | >100 | 146 |
| HCMV (AD-169 & Davis) | 1.8 – 2.0 | – | >20 | – |
| VZV (OKA & 07/1) | 1.6 – 1.7 | – | 47-56 | – |
| <i>HeLa cells</i> | | | | |
| VSV | 4 | >100 | >100 | 29 |
| Coxsackie B4 | >4 | >100 | >100 | 146 |
| RSV | >4 | >100 | >100 | 10 |
| <i>CEM cells</i> | | | | |
| HIV-1 (III _B) HIV-2 (ROD) | >2 | >100 | >50 | >50 |
| <i>Vero cells</i> | | | | |
| Parainfluenza-3 | >4 | >100 | >100 | 85 |
| Reovirus-1 | >4 | 100 | >100 | >250 |
| Sindbis | >4 | 100 | >100 | >250 |
| Coxsackie B4 | >4 | >100 | >100 | >250 |
| Punta Toro | >4 | 20 | >100 | 126 |
| <i>MDCK cells</i> | | | | |
| Influenza (AH3N2) | >0.8 | – | >20 | 9 |
| Influenza A (H1N1) | >0.8 | – | >20 | 9 |
| Influenza B | >0.8 | – | >20 | 9 |

^aPositive control. Table adapted from Zimmermann et al.(Zimmermann, Sadler et al. 2011)

Additionally, although **3.2a** had inhibitory activity against HCMV and VZV at EC₅₀ of 1.6-2.0 μM, it was found to be cytotoxic at 4 – 20 μM against HEL, HeLa, Vero, and MDCK cells (**Table 4**).(Zimmermann, Sadler et al. 2011)

Table 4. Summary of cytotoxicity against various cell lines.

| Cell line | MCC ^a (μM) | 3.2a | 3.2b | 3.2c | Ribavirin ^b |
|-----------|-----------------------|------|------|------|------------------------|
| HEL | ≥4 | >100 | – | ≥100 | >250 |
| HeLa | 20 | >100 | – | >100 | >250 |
| Vero | 20 | >100 | – | >100 | >250 |
| MDCK | 4 | – | – | 100 | >100 |

^aMCC, minimum cytotoxic concentration to cause microscopically visible alteration to cell morphology. ^bPositive control. Table adapted from Zimmermann et al.(Zimmermann, Sadler et al. 2011)

Further investigation into reverse fleximers led to synthesis of the series **3.4** (**Figure 13**). Additionally, both series **3.1** and **3.4** reverse fleximer analogues (**Figure 13**) were designed with the goal of inhibiting SAHase; however, assay results revealed that instead of inhibiting SAHase, the compounds were inhibiting adenosine deaminase (ADA), thus serving as a product inhibitor.(Zimmermann, Sadler et al. 2013)

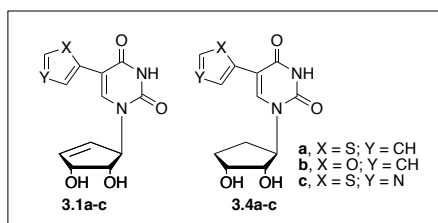
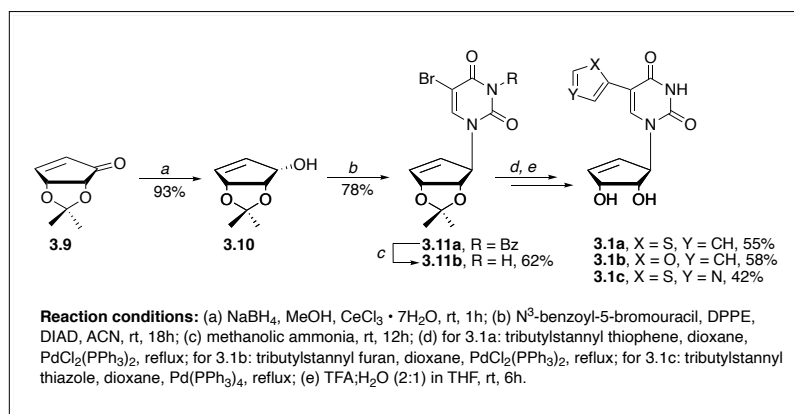


Figure 13. Structures of series 3.1 and series 3.4 reverse fleximers.

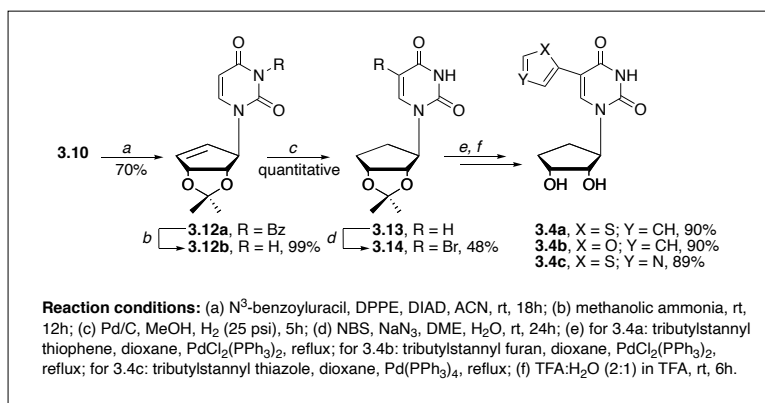
Synthesis of compounds **3.1a-c** (shown in **Scheme 12**) began with enone **3.9**, which was synthesized from D-ribose. The enone was reduced to form compound **3.10** using a Luche reduction which was then coupled via a Mitsunobu reaction with N³-benzoyl-5-bromouracil, affording compound **3.11a**. Removal of the benzoyl protecting group through standard procedures gave intermediate **3.11b** which was then subjected to a Stille coupling using various tin reagents, followed by deprotection of the 2' and 3' hydroxyls to yield

compounds **3.1a-c** in moderate yields. (Zimmermann, Sadler et al. 2013)



Scheme 12. Synthesis of series **3.1** reverse fleximers.

Series **3.4** was synthesized in an analogous manner, beginning with the same allylic alcohol **3.10** being coupled via a Mitsunobu reaction to N³-benzoyluracil, providing compound **3.12a** (**Scheme 13**). Again, the benzoyl group was removed using methanolic ammonia, affording compound **3.12b**. Reduction of intermediate **3.12b** using catalytic hydrogenation conditions yielded compound **3.13** in a quantitative yield. Subsequent bromination at the C5 position afforded compound **3.14** which was then used in Stille couplings to afford compounds **3.4a-c** in high yields. (Zimmermann, Sadler et al. 2013)



Scheme 13. Synthesis of series **3.4** reverse fleximers.

The synthesized compounds were then screened against SAHase in an assay that used ADA to monitor conversion of adenosine to inosine. The results, summarized in **Table 5**, revealed that the compounds were not inhibiting SAHase but instead inhibiting ADA. (Zimmermann, Sadler et al. 2013) This is notable as ADA has been linked to deactivation of nucleoside drugs, including arabinosyl adenine (AraA) due to deamination. (Zimmermann, Sadler et al. 2013)

Table 5. Percent inhibition and fitness scoring in ADA active site.

| Compound ^a | Percent Inhibition ^b | Fitness Score ^c |
|-----------------------|---------------------------------|----------------------------|
| Inosine | 31% | 50.00 |
| 3.1a | 48% | 54.78 |
| 3.1b | 55% | 53.62 |
| 3.1c | 49% | 51.90 |
| 3.4a | 36% | 50.90 |
| 3.4b | 35% | 48.70 |
| 3.4c | 28% | 47.29 |

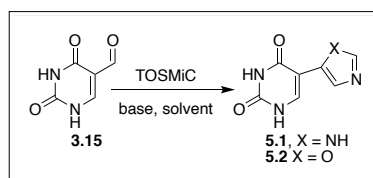
^aCompounds dissolved in DMSO at 100μM concentration; ^bCalculated as [1 – (reaction rate of inhibited ADA ÷ reaction rate of uninhibited ADA)] * 100%. Rates determined by monitoring decrease in absorbance at 265nm for conversion of adenosine to inosine; ^cAnalogues constructed in Chem3D then transferred to Sybyl for analysis. Fitness score is relative affinity of ligand to binding site. Table adapted from Zimmermann et al. (Zimmermann, Sadler et al. 2013)

Computational studies of the compounds in bovine ADA crystallized with transition state analogue 6-hydroxy-1,6-dihydropurine ribose showed that, other than compounds **3.4b** and **3.4c**, all had better fitness

scores than inosine, the product of the normal reaction with adenosine (**Table 5**). Looking at the adenosine binding site of ADA, there is another binding pocket adjacent to this site. In this pocket, it was shown that the furan analogue **3.1b** is able to have additional bonding interactions due to the flexibility and length of the substituted furan ring. (Zimmermann, Sadler et al. 2013) As a result, it is possible that perhaps these analogues are acting as product inhibitors rather than substrate inhibitors. The compounds were also subjected to antiviral screening against viruses including HSV-1, HSV-2, vaccinia, and influenza types A and B; however, activity for all compounds was inferior to that of the positive control, ribavirin. (Zimmermann, Sadler et al. 2013)

Inspired by the reverse fleximers of the Seley-Radtke group, Herdewijn et al. sought to introduce imidazoles to the uridine system. (Mattelaer, Van et al. 2020) It has been previously shown that this can lead to functionalization of DNA to obtain a more stable ribozyme. (Mattelaer, Van et al. 2020) Herdewijn et al. also aimed to avoid the use of protection groups which led to the development of a metal-free route for synthesis of 5-imidazolyl-uracil via Van Leusen reaction. (Mattelaer, Van et al. 2020)

Previously, reverse fleximers were synthesized by first coupling the pyrimidine ring to the desired sugar, either through a Mitsunobu reaction or Tsuji-Trost coupling, and then using a Stille coupling to attach the pendant ring system. (Sadler, Ojewoye et al. 2008, Zimmermann, Sadler et al. 2011, Zimmermann, Sadler et al. 2013) The approach by Herdewijn et al. instead focused on forming the heterocyclic base first and then coupling to the desired sugar. (Mattelaer, Van et al. 2020) Formation of the heterocyclic base began with 5-formyluracil (**3.15**) which was then subjected to a Van Leusen reaction using tosylmethyl isocyanide (TOSMIC) to form the imidazole moiety, providing flex-bases **5.1** and **5.2**, as shown in **Scheme 14**. (Mattelaer, Van et al. 2020)



Scheme 14. Synthesis of flex-bases **5.1** and **5.2** using Van Leusen reactions.

Herdewijn et al. tried various combinations of bases and solvents, of which 7M NH₃ in methanol was found to give the best yields with facile product isolation, as shown in **Table 6**. Attempts at using ammonium hydroxide solution yielded similar results but purification was significantly more tedious leading to product loss. Additionally, other bases were attempted in order to obtain the oxazole analogue, but all proved to be unsuccessful. (Mattelaer, Van et al. 2020)

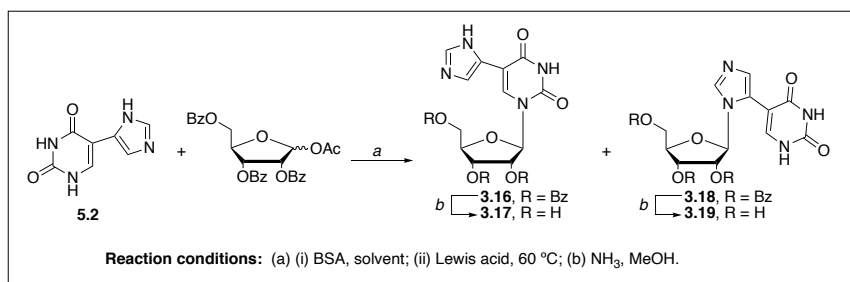
Table 6. Van Leusen Reaction Conditions.

| Entry | TOSMIC [equiv.] | Base (equiv) | Solvent | Scale [g] | Yield ^a [%] | |
|-------|-----------------|------------------------------------|------------------|-----------|------------------------|-------------------|
| | | | | | 5.1 | 5.2 |
| 1 | 3 | NH ₃ (6) | MeOH | 0.125 | 40 | — |
| 2 | 1.6 | NH ₃ (3) | MeOH | 0.125 | 48 | — |
| 3 | 1.6 | NH ₃ (3) | MeOH | 0.125 | 59 | — |
| 4 | 1.6 | NH ₃ (3) | MeOH | 0.25 | 66 | — |
| 5 | 1.6 | NH ₃ (3) | MeOH | 0.5 | 85 | — |
| 6 | 1.6 | NH ₄ OH (3) | MeOH | 1 | 23 | — |
| 7 | 1.6 | NH ₄ OH (3) | H ₂ O | 0.25 | Deg ^b | — |
| 8 | 1.6 | K ₂ CO ₃ (3) | MeOH | 0.25 | — | m.s. ^c |
| 9 | 1.6 | <i>t</i> BuOK (3) | MeOH | 0.25 | — | m.s. ^c |
| 10 | 1.6 | Et ₃ N (3) | MeOH | 0.25 | — | m.s. ^c |
| 11 | 1.6 | DBU (3) | MeOH | 0.25 | — | n.r. ^d |

^aisolated yield; ^bdeg, deradation of starting materials; ^cm.s., multiple spots, multiple products (monitored by TLC, MS); ^dn.r., no reaction. Table adapted from Mattelaer et al. (Mattelaer, Van et al. 2020)

Once flex-base **5.1** was obtained, the nucleobase was then protected using trimethylsilyl groups followed immediately by reaction with 1-O-acetyl-2,3,5-tri-O-benzoyl-D-ribofuranose in a one-pot Vorbrüggen reaction (**Scheme 15**). (Mattelaer, Van et al. 2020) Initial attempts used acetonitrile as a solvent; however, upon switching solvent to dichloroethane (DCE), a product ratio was shifted towards **3.17**. Both THF and DMF solvents were found to be incompatible with the reaction. Additionally, using SnCl₄ as an alternative Lewis acid did not significantly increase product formation from using TMSOTf. Removal of the benzoyl protecting groups using methanolic ammonia provided major product **3.17** and minor product

3.19.(Mattelaer, Van et al. 2020).



Scheme 15. Synthesis of reverse fleximer **3.17** (major product) and fleximer **3.19** (minor product).

The X-ray crystallography structure of compound **3.19** as an HCl salt is shown in **Figure 14**, with the ribose ring showing a C3'-*endo* pucker and overall *anti* conformation.(Mattelaer, Van et al. 2020)

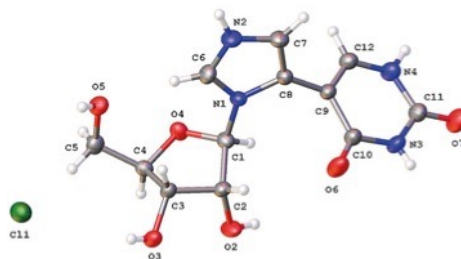


Figure 14. X-ray crystallography structure of fleximer **3.19** HCl salt. Image used with permission from WILEY-VCH Verlag GmbH & Co.(Mattelaer, Van et al. 2020)

The steady-state spectroscopy of compounds **3.17** and **3.19** were also investigated due to similarity to the furan- and oxazole-containing fluorescent probes synthesized by Tor et al.(Greco and Tor 2005, Mattelaer, Van et al. 2020) Absorption maxima for **3.17** and **3.19** in varying solvents are summarized in **Table 7**. The S₀ → S₁ band for **3.17** was found to be very similar in the differing solvents whereas this transition was at lower, slightly more varying wavelengths for compound **3.19**. Fluorescence was also observed for **3.17** but not for **3.19**.(Mattelaer, Van et al. 2020)

Table 7. Absorption maxima for **3.17** and **3.19**.

| Solvent | λ _{abs} [nm] | |
|---------|-----------------------|-------------|
| | 3.17 | 3.19 |
| ACN | 306 | 270 |
| DCM | 305 | 276 |
| MeOH | 307 | 275 |
| PBS | 308 | 272 |

Table adapted from Mattelaer et al.(Mattelaer, Van et al. 2020)

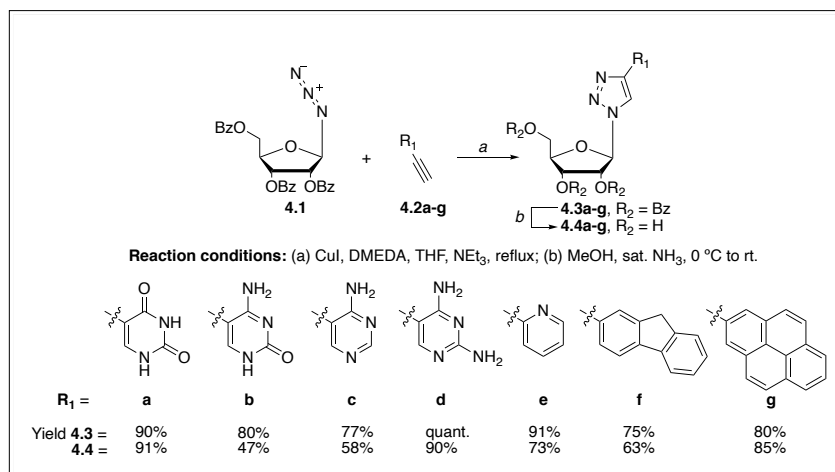
Overall, the metal-free route proposed by Herdewijn et al. provides a facile, shorter, and more economic method for synthesizing imidazole-substituted uridine fleximers.(Mattelaer, Van et al. 2020)

4. Click Fleximers and Other Triazole Fleximers

Earlier efforts to synthesize both *distal* and *proximal* fleximers were challenging; seeking alternative routes to synthesizing other fleximer analogues, Hudson et al. introduced “Click” fleximers in 2012.(St. Amant, Bean et al. 2012) Previous work in the Hudson lab focused on using a copper-catalyzed azide-alkyne Huisgen cycloaddition (CuAAC) to produce 5-ethynyl-2'-deoxycytidine derivatives. Based on structural similarity of these compounds to fleximers, Hudson et al. applied the CuAAC method to fleximer synthesis. Instead of the imidazole ring found in early Seley-Radtke fleximers, Hudson et al. employed a 1,2,3-triazole in order to utilize the CuAAC method.(St. Amant, Bean et al. 2012)

A ribose sugar **4.1** (**Scheme 16**) was chosen to take advantage of the β-directing ability of the 2'-hydroxyl for formation of the glycosyl azide. Various alkynes were considered; uracil **4.2a**, cytosine **4.2b**, and 4-aminopyrimidine **4.2c** were chosen due to accessibility. 2,4-diaminopyrimidine **4.2d** was chosen due to its similarity with diaminopurine riboside whereas 2-pyridinyl **4.2e** was selected because of the potential to act

as a bidentate ligand for metal chelation.(St. Amant, Bean et al. 2012) Both fluorene **4.2f** and pyrene **4.2g** alkynes were chosen with the intention to act as fluorescent reporters and potential for intercalation complexes.(St. Amant, Bean et al. 2012) Actual formation of the click fleximers required stronger conditions than typical click reactions; after optimization, the best condition found was CuI paired with *N,N'*-dimethylethylenediamine (DMEDA) in refluxing THF, as shown in **Scheme 16**. This produced compounds **4.3a-g** in yields ranging from 75% to quantitative. Removal of the benzoyl protecting groups was accomplished using saturated methanolic ammonia, providing final compounds **4.4a-g**.(St. Amant, Bean et al. 2012)



Scheme 16. General click synthesis of fleximers **4.4a-g**.

Initial characterization attempts of the synthesized compounds revealed that compounds **4.3a-c** were organo-gelators, forming reversible gels in CHCl₃, EtOAc, and DMSO. Surprisingly, compound **4.3d** was not found to gelate CHCl₃ despite similarity to compound **4.3c**.(St. Amant, Bean et al. 2012)

Other initial studies with the synthesized compounds included evaluation of fluorescence properties for compounds containing known luminophores, as shown in **Table 8**.(St. Amant, Bean et al. 2012)

Table 8. Fluorescence data of luminophore-containing compounds.

| Compound | Excitation λ_{max} (nm) | Emission λ_{max} (nm) | Φ_F | |
|-------------|---|---|----------|------------------|
| | | | EtOH | H ₂ O |
| 4.3f | 292 | 317 | 0.16 | — |
| 4.3g | 352 | 383 | 0.16 | — |
| 4.4d | 311 | 356 | 0.48 | 0.05 |
| 4.4f | 311 | 331 | — | 0.06 |
| 4.4g | 346 | 382 | — | 0.46 |

Table adapted from St. Amant et al.(St. Amant, Bean et al. 2012)

Of the compounds examined, compound **4.4d** had surprising results with purple fluorescence observed under long-wavelength (360 nm) UV light on TLC. The other nucleobase triazoles did not have observed emission. Additionally, **4.4d** was found to be much more strongly emissive in EtOH than in H₂O; such a difference may be of interest for future studies of interactions with enzymes or incorporation into oligomers.(St. Amant, Bean et al. 2012)

Conformational studies were also carried out using DFT (density functional theory) methods Bb3lyp/6-31+G**, implemented by Gaussian 09. Compounds **4.4a-d** had the typical 3'-endo-like ring pucker found in ribosides. Compounds **4.4a**, **4.4c**, and **4.4d** had preference for the *anti* conformation as the lowest energy structures. These *anti*-conformations are likely stabilized by hydrogen bonding between the 5' hydroxyl and N-2. However, compound **4.4b** had slight preference for the *syn* conformation instead, as shown in **Table 9**.(St. Amant, Bean et al. 2012)

Table 9. Conformational study of compounds **4.4a-d**.

| Compound | Glycosidic conformation (kcal mol ⁻¹) | | Minimum barrier to rotation of heterobiaryl bond (kcal mol ⁻¹) |
|-------------|--|---------------|---|
| | <i>syn</i> - | <i>anti</i> - | |
| 4.4a | 0.509 | 0 | 11.9 |

| | | | |
|-------------|--------|---|-----|
| 4.4b | -1.338 | 0 | 4.8 |
| 4.4c | 1.965 | 0 | 7.1 |
| 4.4d | 2.167 | 0 | 6.1 |

Table adapted from St. Amant et al. (St. Amant, Bean et al. 2012)

This is accounted for by the nonconventional hydrogen bonding between the 5' hydroxyl and C⁵-H (triazole) which was found to be preferred only in compound **4.4b** despite being a possible interaction in all the fleximer compounds. (St. Amant, Bean et al. 2012) The preferred conformations for these compounds are shown in **Figure 15**.

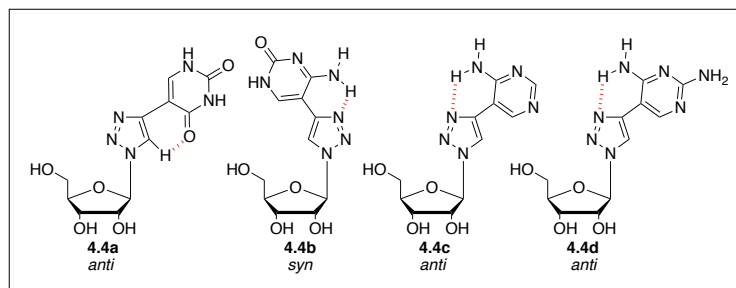


Figure 15. Preferred conformations for compounds **4.5a-d**.

Other fleximers featuring a triazole ring include the β -hydroxyphosphonate ribonucleoside analogues synthesized by Peyrottes et al. as shown in **Figure 16**. (Nguyen Van, Hospital et al. 2016)

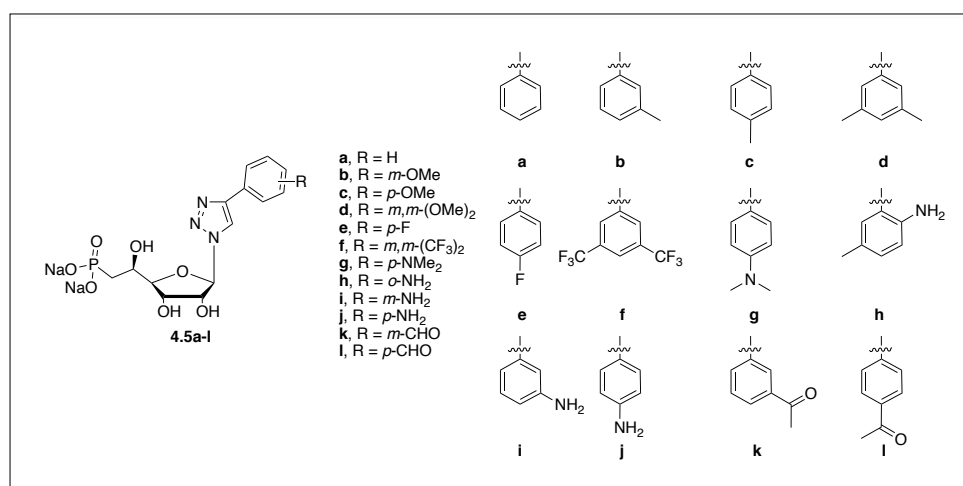
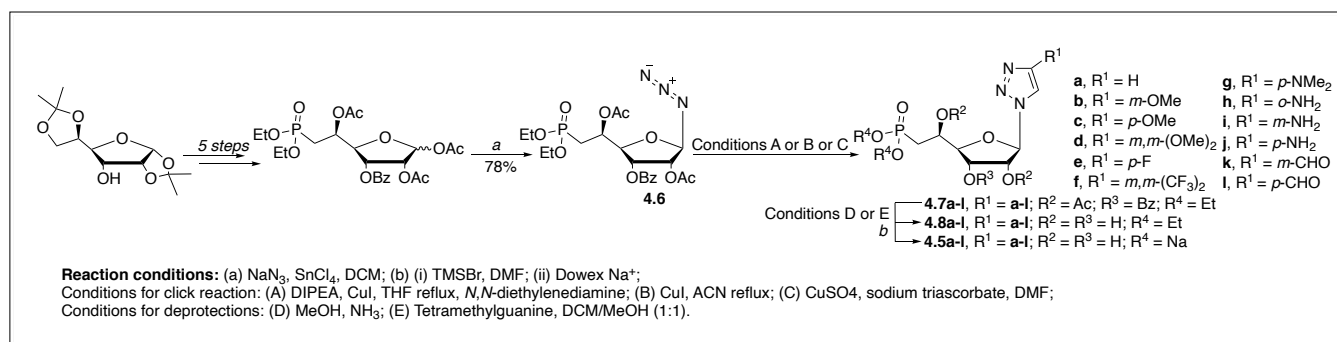


Figure 16. Series of triazole fleximers synthesized by Peyrottes et al.

These triazole fleximers were also synthesized using the CuAAC reaction utilized by Hudson et al. using intermediate **4.6** (obtained from diacetone D-allofuranose) and various alkynes, catalyzed by CuI or CuSO₄ as outlined in **Scheme 17**. (St. Amant, Bean et al. 2012, Nguyen Van, Hospital et al. 2016)



Scheme 17. Synthesis of triazole fleximers **4.5a-l** using click methodologies.

Following deprotection, the nucleoside phosphate analogues were obtained as their sodium salts in

varying yields, from 21% up to 77% as shown in **Table 10**.(Nguyen Van, Hospital et al. 2016)

Table 10. Yields of series 4.5 fleximers.

| Compound | Conditions | Total yield (%) |
|-------------|------------|-----------------|
| 4.5a | A, D | 66 |
| 4.5b | A, D | 44 |
| 4.5c | A, D | 73 |
| 4.5d | A, D | 54 |
| 4.5e | A, D | 40 |
| 4.5f | A, D | 71 |
| 4.5g | A, D | 77 |
| 4.5h | C, D | 45 |
| 4.5i | C, D | 39 |
| 4.5j | C, D | 41 |
| 4.5k | B, E | 36 |
| 4.5l | B, E | 21 |

Table adapted from Nguyen Van et al. (Nguyen Van, Hospital et al. 2016)

The compounds were then screened for inhibition against human 5'-nucleotidase. Most compounds required high concentrations (>1 mM) to reduce enzyme activity by only moderate amounts, thus indicating poor binding. However, both compounds **4.5i** and **4.5h** exhibited >50% inhibition at 1 mM concentration as shown in **Table 11**.(Nguyen Van, Hospital et al. 2016)

Table 11. Human 5'-nucleotidase inhibition screening.

| Compound | % Inhibition at 1 mM | Docking score / NHA | Number of Heavy Atoms (NHA) | Docking score (crude) |
|-------------|----------------------------------|---------------------|-----------------------------|-----------------------|
| 4.5a | n.d. ^a (precipitated) | 6.32 | 25 | 158 |
| 4.5b | 23 ± 19 | 5.91 | 27 | 159.6 |
| 4.5c | 31 ± 3 | 5.64 | 27 | 153.4 |
| 4.5d | 29 ± 13 | 5.45 | 29 | 158.2 |
| 4.5e | 36 ± 1 | 5.85 | 26 | 152.1 |
| 4.5f | 36 ± 14 | 4.71 | 33 | 155.6 |
| 4.5g | 42 ± 0.5 | 5.73 | 28 | 160.5 |
| 4.5h | 64 ± 7 | 5.96 | 26 | 155 |
| 4.5i | 60 ± 8 | 5.94 | 26 | 154.6 |
| 4.5j | 44 ± 10 | 5.68 | 26 | 147.6 |
| 4.5k | 34 ± 1 | 5.97 | 27 | 161.2 |
| 4.5l | 34 ± 0.5 | 5.85 | 27 | 157.9 |

^an.d., not determined; table adapted from Nguyen Van et al.(Nguyen Van, Hospital et al. 2016)

Overall, the work of both Hudson et al.(St. Amant, Bean et al. 2012) as well as the Peyrottes group(Nguyen Van, Hospital et al. 2016) introduced an alternative way of obtaining fleximer analogues by application of click chemistry.

5. Fleximer Bases

Another application of the fleximer technology has been with fleximer base analogues. To date, numerous flex-bases have been synthesized, as shown in **Figure 17**.(Vichier-Guerre, Dugué et al. 2014, Ku, Lopresti et al. 2019, Mattelaer, Van et al. 2020)

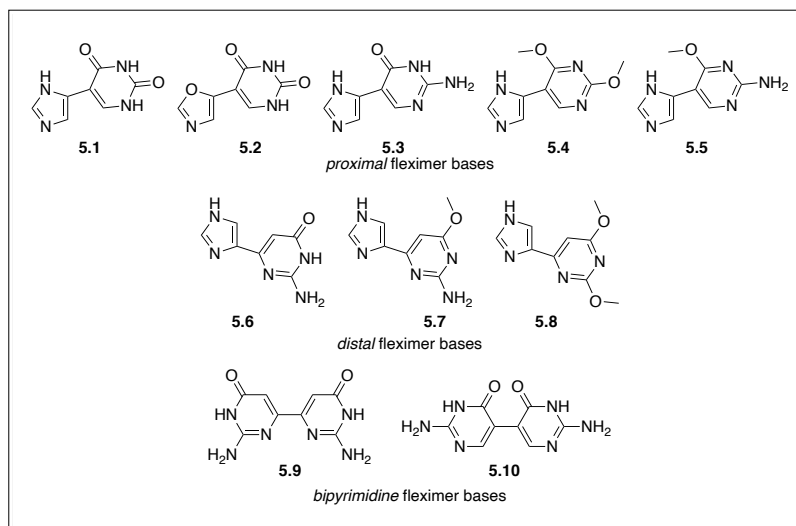


Figure 17. Fleximer base analogues.

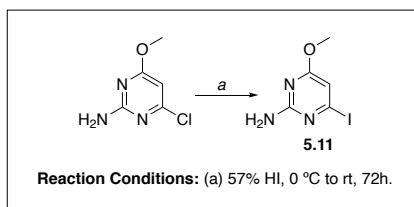
As mentioned in the previous section, Herdewijn et al. synthesized flex-bases **5.1** and **5.2** from 5-formyluracil using a Van Leusen reaction.(Mattelaer, Van et al. 2020) However, the first reported flex-bases were compounds **5.3**, **5.6**, **5.9**, and **5.10** which were designed and synthesized by Seley-Radtke et al. with the goal of being active against the HIV-1 nucleocapsid protein, NC.(Ku, Lopresti et al. 2019) Using previous structural studies on NC in which guanosine consistently showed stacking with the W37 residue of the protein(Mori, Dietrich et al. 2010, Mori, Manetti et al. 2011), Seley-Radtke et al. focused on guanine fleximer analogues.(Ku, Lopresti et al. 2019) Earlier results revealed that the fleximer base moiety was of significance whereas the sugar moiety appeared to provide little benefit. Thus, Seley-Radtke et al. turned focus on synthesizing fleximer base analogues, which had the additional benefit of markedly shorter synthetic routes.(Ku, Lopresti et al. 2019) These initial analogues (**5.3**, **5.6**, **5.9**, **5.10**), shown in **Figure 17**, were analyzed computationally using a protocol by Botta et al. against the NMR structure of NC.(Ku, Lopresti et al. 2019) Compared to guanine, the fleximer analogues had excellent structural overlay while also showing H-bonding with key residues within the hydrophobic pocket.(Ku, Lopresti et al. 2019) The flex-bases additionally showed similar stacking with residue W37 as is observed with guanine. A notable difference with the fleximer analogues is that the flexible bond allowed for extension into the solvent area and interactions with neighboring residues, as seen with the interaction between compound **5.5** and residue K47.(Ku, Lopresti et al. 2019) Additionally, based on FRED (fast, rigid, exhaustive docking) scoring (**Table 12**) using Chemgauss4 function, although *distal* flex-base **5.1** was predicted to have stronger binding than both *proximal* flex-base **5.3** and parent guanine, the scoring among the compounds were comparable and thus observed differences among the compounds may not be significant.(Ku, Lopresti et al. 2019) Additionally, the bipyrimidine compounds **5.4** and **5.5** had promising scores, although slightly less than the purine analogues as shown in **Table 12**.(Ku, Lopresti et al. 2019)

Table 12. FRED scores.

| Compound | FRED score (Chemgauss 4 function) ^a |
|-------------|--|
| Guanine | -6.36 |
| 5.3 | -6.26 |
| 5.6 | -6.77 |
| 5.9 | -6.08 |
| 5.10 | -6.14 |

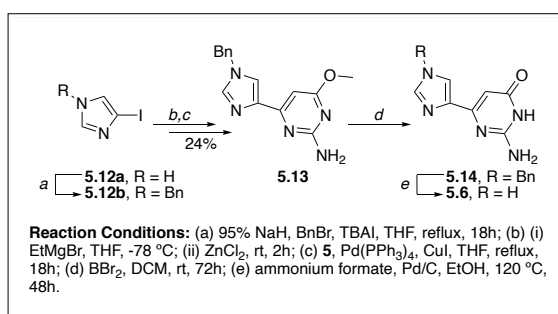
^aA dimensional, lower score = higher affinity. Table adapted from Ku et al.(Ku, Lopresti et al. 2019)

The primary synthetic route to achieve the fleximer base analogues employed a series of organometallic coupling reactions, beginning with the iodination of commercially available 2-amino-6-chloro-4-methoxypyrimidine (**Scheme 18**) to afford pyrimidine **5.11**.(Ku, Lopresti et al. 2019)



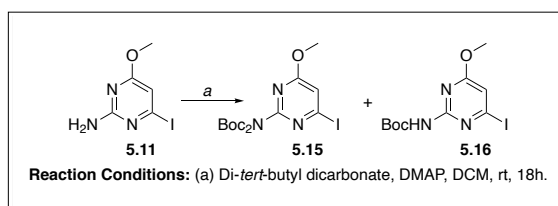
Scheme 18. Iodination of 2-amino-6-chloro-4-methoxypyrimidine to form compound **5.11**.

Attempts to then convert compound **5.11** to an organostannane for subsequent Stille couplings or into a boronic ester for Suzuki couplings proved to be fruitless, with issues such as lack of product formation or high instability. (Ku, Lopresti et al. 2019) Instead, attention was turned to using Negishi conditions by first benzyl protecting iodoimidazole to afford compound **5.12b** which was then coupled to pyrimidine **5.11**, affording protected intermediate **5.13** in low yield (**Scheme 19**). Removal of the methyl protecting group was achieved using boron tribromide in DCM, affording intermediate **5.14**. This was then heated at high temperature with ammonium formate and Pd/C in EtOH to remove the benzyl protecting group, yielding desired compound **5.6**. (Ku, Lopresti et al. 2019)



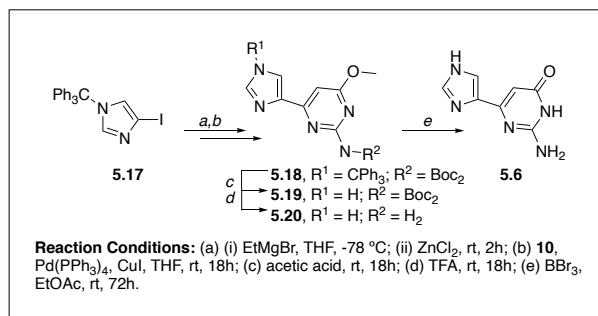
Scheme 19. Synthesis of flex-base **5.6**.

However, due to difficulties in purification arising from the high polarity of these compounds, alternative protecting groups were explored to ease purification. Instead, a *tert*-butyloxycarbonyl (Boc) was employed to protect the exocyclic amine of pyrimidine **5.11**, providing compounds **5.15** and **5.16** (**Scheme 20**) while a trityl protecting group was used to protect the free amine of the imidazole (compound **5.17**, **Scheme 21**). (Ku, Lopresti et al. 2019)



Scheme 20. BOC-protection of pyrimidine **5.11**.

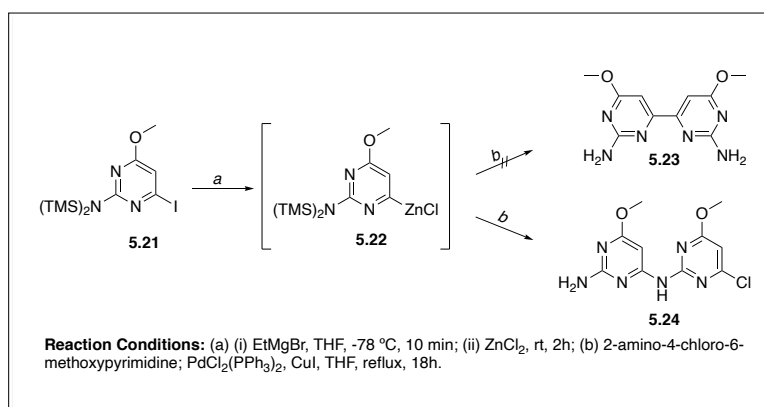
Using these protected compounds instead, the Negishi coupling was more facile and able to be carried out at room temperature. Deprotection of the trityl group was achieved using acetic acid whereas the Boc group was removed utilizing trifluoroacetic acid (TFA) to afford flex-base **5.6**, shown in **Scheme 21**. (Ku, Lopresti et al. 2019)



Scheme 21. Synthesis of flex-base **5.6** using BOC and trityl protecting groups.

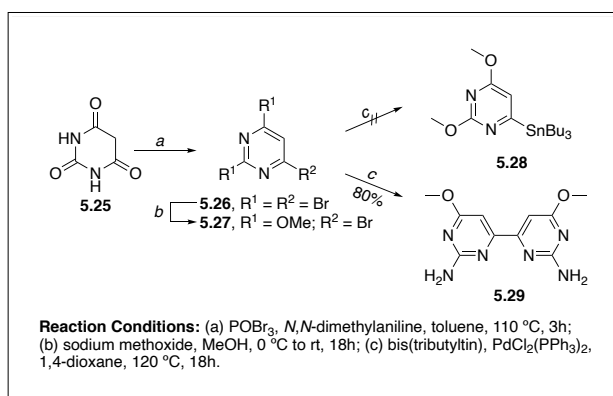
Initial ¹H NMR studies were performed using compound **5.6** and NC. The ¹H NMR spectra of NC in D₂O was first recorded. Then, a one molar equivalent of flex-base **5.6** (dissolved in DMSO-*d*₆) was added to the sample. However, no significant changes to the NC signals were detected. If compound **5.6** did bind to NC, then shifts in the aromatic region would have been observed. Thus, it was concluded that the interaction between **5.6** and NC was either nonexistent or very weak and thus undetectable via NMR. (Ku, Lopresti et al. 2019) The flex-base was also sent for screening against HIV-1 but disappointingly did not show significant activity. (Ku, Lopresti et al. 2019)

After success at synthesizing compound **5.6**, Seley-Radtke et al. envisioned achieving the bipyrimidine **5.9** in similar fashion as outlined in **Scheme 22**. However, instead amine-linked compound **5.24** was achieved likely due to a Buchwald-Hartwig amination due to the presence of the palladium catalyst, shown in **Scheme 22**. (Ku, Lopresti et al. 2019)



Scheme 22. Synthesis of compound **5.24** due to Buchwald-Hartwig amination.

Other attempts to achieve bipyrimidine **5.9** utilizing Stille conditions proved fruitless, as the organostannane could not be obtained although bipyrimidine **5.23** was recovered in good yields (80%), shown in **Scheme 23**. (Ku, Lopresti et al. 2019)

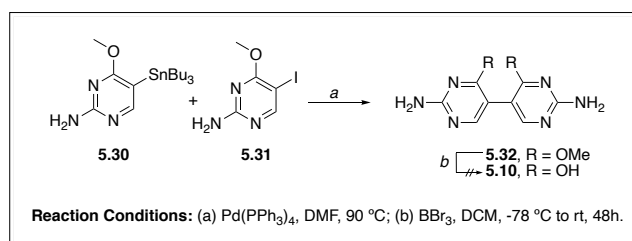


Scheme 23. Synthesis of organostannane **5.28** and recovery of bipyrimidine **5.29**.

Attempts to then utilize compound **5.29** to obtain compound **5.9** were also fruitless. Initially, POCl₃

was used to remove the methyl protecting groups followed by chlorination; however, the chlorinated intermediate could not be isolated due to purification difficulties. Additionally, attempts to convert the methoxy groups to amines were unsuccessful, likely due to the harsh reaction conditions. Inspired by the homocoupling compound **5.29**, Seley-Radtke et al. utilized the same Stille conditions using pyrimidine **5.11** instead to achieve its homocoupled product (as verified by mass spectrometry; however, the product was not isolatable). (Ku, Lopresti et al. 2019)

Focus then turned towards the *proximal* flex-base analogues. Utilizing Stille conditions, intermediate **5.32** was achieved (**Scheme 24**). However, again purification and solubility issues were encountered making it impossible to achieve compound **5.10**. (Ku, Lopresti et al. 2019)



Scheme 24. Synthesis of proximal flex-base **5.10**.

Attempts at synthesizing fleximer base **5.3** were also met without success when employing Negishi cross-coupling methods. This was attributed to the placement of the halogen on the electron-rich C-5 which was speculated to not have reacted with the palladium catalyst due to palladium having reactivity preference for electron-deficient carbons. (Ku, Lopresti et al. 2019)

The synthesis of other proximal (compounds **5.4** and **5.5**, **Figure 17**) and distal (compounds **5.7** and **5.8**, **Figure 17**) flex-bases were achieved through the use of microwave-assisted Suzuki-Miyaura cross-couplings. (Vichier-Guerre, Dugué et al. 2014) These bases were then utilized in enzymatic glycosylation reactions to afford the fleximer nucleoside analogues. Initially, the capability of the *N*-deoxyribosyl-transferase (NDT II) from *Lactobacillus leichmannii*, LINDT, was evaluated to see if it would recognize the fleximer nucleobases as substrates. (Vichier-Guerre, Ku et al. 2020) Because the flex-bases had low water solubility, transferase reactions were carried out in the presence of 5% v/v DMSO at 37 °C to optimize enzyme activity and isolate all possible products. Glycosylation rates were monitored via analytical reverse-phase HPLC, the results of which are summarized in **Table 13**. (Vichier-Guerre, Ku et al. 2020)

Table 13. Glycosylation rates of flex-bases.

| | Acceptor (Flex-Base) | L/NDT (μL) | Incubation time (h) | Starting material | Product (%) ^b | |
|----|-------------------------|---------------|------------------------|----------------------|--------------------------|---------------------|
| | | | | | N1- glycosylated | N3- glycosylated |
| 1 | 5.4 | 1.25 | 3 | 61 | 17 | 22 |
| 2 | | 1.25 | 10 | 53 | 28 | 20 |
| 3 | | 2.5 | 3 | 40 | 74 | 13 |
| 4 | | 2.5 | 10 | 24 | 65 | 6 |
| 5 | | 5.0 | 3 | 15 | 80 | 5 |
| 6 | | 5.0 | 10 | 10 | 88 | 2 |
| 7 | | 7.5 | 3 | 12 | 86 | 2 |
| 8 | | 7.5 | 10 | 10 | 89 | 1 |
| 9 | | 10.0 | 3 | 11 | 87 | 2 |
| 10 | | 10.0 | 10 | 10 | 89 | 1 |
| 11 | 5.5 | 1.25 | 3 | 24 | 30 | 46 |
| 12 | | 1.25 | 10 | 17 | 45 | 58 |
| 13 | | 2.5 | 3 | 18 | 42 | 40 |
| 14 | | 2.5 | 10 | 10 | 78 | 12 |
| 15 | 5.7 | 1.25 | 0.5 | 0 | 100 | — |
| 16 | | 0.63 | 0.5 | 18 | 82 | — |
| 17 | | 0.15 | 3 | 40 | 60 | — |
| 18 | 5.8 | 1.25 | 3 | 70 | 30 | — |
| 19 | | 1.25 | 10 | 20 | 80 | — |
| 20 | | 2.5 | 3 | 7 | 93 | — |
| 21 | | 2.5 | 10 | 4 | 96 | — |

(a) Reaction conditions: 1 μmol acceptor in 5% v/v DMSO; 4 μmol thymidine in 10 mM citrate buffer (pH 6.5; 0.1 mL) in presence of *L*/NDT at 37 °C; (b) Determined by reverse-phase HPLC analysis of aliquot of incubation mixture monitored at 254 nm. Table adapted from Vichier-Guerre et al. (Vichier-Guerre, Ku et al. 2020)

As seen in **Table 13**, regioselectivity is possible with some of the C4-substituted imidazole derivatives. (Vichier-Guerre, Ku et al. 2020) Formation of both the N1 and N3-glycosylated products is achieved in a 1:1 ratio at 37 °C after 3h in the reaction between **5.4** and thymidine using 1.25 $\mu\text{L}/\mu\text{mol}$ NDT (**Table 13**, entry 1). (Vichier-Guerre, Ku et al. 2020) However, it was observed that the N3-glycosylated isomer was being converted to the more stable N1-glycosylated isomer. Increasing the enzyme concentration to 10.0 $\mu\text{L}/\mu\text{mol}$ resulted in nearly complete conversion at 89% product produced with the N1-glycosylated product being the only product (**Table 13**, entries 7 and 8). (Vichier-Guerre, Ku et al. 2020) This same trend was observed with reactions using flex-base **5.5**. It should also be noted that fleximer base **5.5** is possibly a better substrate for NDT due to lower enzyme concentrations being needed for complete conversion (**Table 13**, entries 11-14). Interestingly, with flex-bases **5.7** and **5.8**, only the N1-glycosylated isomer was observed (**Table 13**, entries 15-17 and 18-21). The desired *distal* fleximer nucleosides (N3-glycosylation) were not detected. (Vichier-Guerre, Ku et al. 2020)

Escherichia coli purine nucleoside phosphorylase (PNP) was also evaluated for its ability to utilize flex-bases **5.4** and **5.5** as substrates for ribonucleotide synthesis. (Vichier-Guerre, Ku et al. 2020) For this, reaction mixtures containing the fleximer base (10 mM), adenosine (20 mM), and PNP (0.2 U μmol^{-1}) in a 10 mM phosphate buffer (pH 7.4) were incubated initially at 50 °C. (Vichier-Guerre, Ku et al. 2020) Conversion of both flex-bases **5.4** and **5.5** were slow. Both N1- and N3-glycosylation products were formed, with the target N1-glycosylation product being the major product. Incubation at lower temperatures (37 °C) resulted in more formation of the N3-glycosylation product. It is important to note that previous chemical glycosylation attempts have afforded only the N3-glycosylation product. (Seley, Zhang et al. 2002, Vichier-Guerre, Ku et al. 2020) Overall, it can be concluded that flex-bases are capable of being used as substrates for both *L*/NDT and PNP and regioselectivity can be achieved to give facile access to *proximal* fleximer analogues. (Vichier-Guerre, Ku et al. 2020)

Later, the Khandazhinskaya group also synthesized a series of C3-heteroarylpyrrole flex-base analogues using Suzuki-Miyaura cross-coupling reactions, shown in **Figure 18**. (Matyugina, Khandazhinskaya et al. 2020)

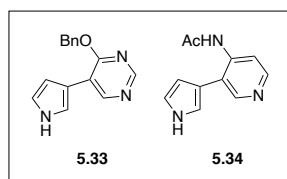
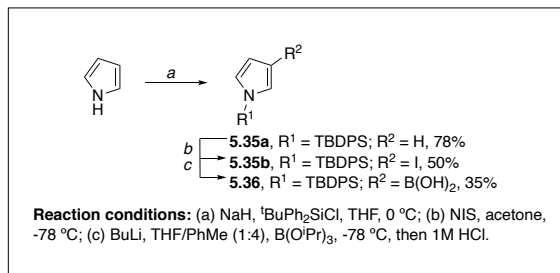


Figure 18. Structures of flex-bases **5.33** and **5.34**.

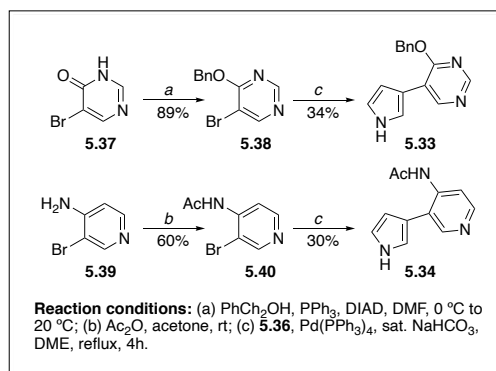
To achieve selective substitution at the C3 site of the pyrrole ring, a bulky substituent could be employed to help block the more reactive C2 site. This was achieved by protecting the amine with a *tert*-butyl(diphenyl)silyl group affording compound **5.35a**, shown in **Scheme 23**. Selective iodination at the C3 site using *N*-iodosuccinimide (NIS) afforded compound **5.35b** in modest yields (**Scheme 23**). Attempts at installing a bromine at the C3 position of compound **5.35a** using Br_2 or *N*-bromosuccinimide (NBS) resulted in a mixture of the desired 3-bromopyrrole product along with significant amounts of 3,4-dibromopyrrole and thus was not used. Instead, boronation of iodopyrrole **5.35b** afford boronic acid **5.36** in low yield (**Scheme 25**). (Matyugina, Khandazhinskaya et al. 2020)



Scheme 25. Synthesis of intermediate **5.36**.

Attempts to couple compound **5.36** to the unprotected heteroarenes **5.37** or **5.39** (**Scheme 26**)

resulted in only trace amounts of the desired coupled products with mostly starting material being recovered. (Matyugina, Khandazhinskaya et al. 2020) Instead, heteroarene **5.37** was first O-benzylated to provide compound **5.38** which was then subjected to a Suzuki coupling using boronic acid **5.36** to afford desired product **5.33** in low yield (**Scheme 26**). Similarly, heteroarene **5.39** was N-acetylated to provide protected compound **5.40** which was coupled to **5.36** to afford flex-base **5.34** in slightly lower yield (**Scheme 26**). (Matyugina, Khandazhinskaya et al. 2020)



Scheme 26. Synthesis of flex-bases **5.33** and **5.34**.

Khandazhinskaya et al. also reported the synthesis of a series of pyrazole-containing adenosine fleximer analogues that utilized synthesized flex-bases (compounds **5.44a-c**, **Figure 19**) and both chemical and enzymatic glycosylation methods to afford the desired fleximer analogues. (Khandazhinskaya, Eletskaya et al. 2021)

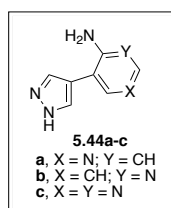
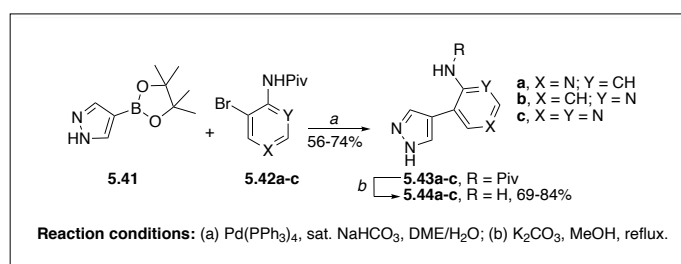


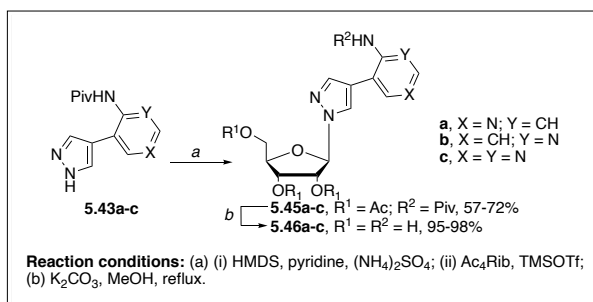
Figure 19. Flex-bases **5.44a-c**.

Synthesis of the desired fleximer bases began with commercially available pinacol ether **5.41** which was subjected to a Suzuki-Miyaura cross-coupling using either pyridines **5.42a-b** or pyrimidine **5.42c**, affording protected bases **5.43a-c** (**Scheme 27**) in modest yields (56-74%). (Khandazhinskaya, Eletskaya et al. 2021) Simple deprotection using potassium carbonate and refluxing in methanol afforded flex-bases **5.44a-c** in yields of 69-84%. (Khandazhinskaya, Eletskaya et al. 2021)



Scheme 27. Synthesis of flex-bases **5.44a-c**.

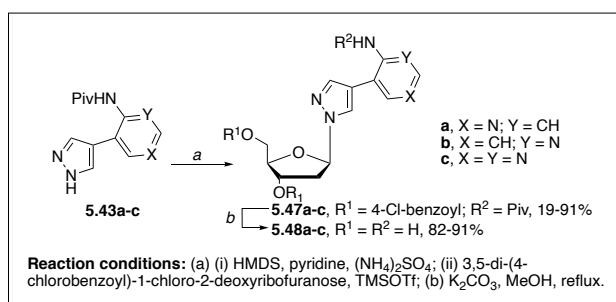
A series of 8-aza-7-deaza fleximers were chemically synthesized via glycosylation of protected flex-bases **5.43a-c** with tetraacetyl-protected ribofuranose, as outlined in **Scheme 28**, using a Vorbrüggen procedure. The flex-bases were first refluxed in hexamethyldisilazane (HMDS) with pyridine and ammonium sulfate. Subsequent reaction with β -D-ribofuranose-1,2,3,4-tetraacetate (Ac_4Rib) with TMSOTf provided intermediates **5.45a** in 72% yield, intermediate **5.45b** in 57% yield, and intermediate **5.45c** in 68% yield (**Scheme 28**). (Khandazhinskaya, Eletskaya et al. 2021)



Scheme 28. Synthesis of fleximers **5.46a-c**.

The protected intermediates were then deprotected using the same procedure with potassium carbonate in refluxing methanol, affording target fleximers **5.46a-c** in near-quantitative yields (95-98%) as shown in **Scheme 28**.(Khandazhinskaya, Eletskaia et al. 2021)

Similarly, a series of 2'-deoxyribonucleoside analogues were synthesized (**Scheme 29**). Again, protected flex-bases **5.43a-c** were refluxed with HMDS in the presence of pyridine and ammonium sulfate and then coupled to 3,5-di-(4-chlorobenzoyl)-1-chloro-2-deoxyribofuranose in 1,2-dichloroethane (DCE) at room temperature, yielding intermediates **5.47a-c** as mixtures of β - and α -anomers.(Khandazhinskaya, Eletskaia et al. 2021) Intermediate **5.47a** was obtained in a 4:1 ratio with an overall yield of 19%. Intermediate **5.47b** had a significantly higher yield of 91% with a 3:2 ratio whereas intermediate **5.47c** was achieved in 63% yield with a 3:1 ratio. The anomeric mixtures of intermediates **5.47b** and **5.47c** were separable via preparative liquid chromatography. The desired fleximer analogues **5.48a-c** were then achieved in high yields (82-91%) by deprotection of intermediates **5.47a-c** using potassium carbonate in refluxing methanol (**Scheme 29**). (Khandazhinskaya, Eletskaia et al. 2021)



Scheme 29. Synthesis of fleximers **5.48a-c**.

Although Khandazhinskaya et al. were able to achieve the desired fleximer analogues in high yields, the syntheses required protection steps that complicated overall product isolation and purification and provided anomeric mixtures, thus lowering product yields.(Khandazhinskaya, Eletskaia et al. 2021) To overcome this issue with chemical synthesis, Khandazhinskaya et al. sought to enzymatically synthesize the target fleximers using recombinant *E.coli* PNP.(Khandazhinskaya, Eletskaia et al. 2021) This enzyme was chosen due to its broad substrate specificity, allowing it to recognize a variety of purine nucleobases shown in **Figure 20**.(Khandazhinskaya, Eletskaia et al. 2021)

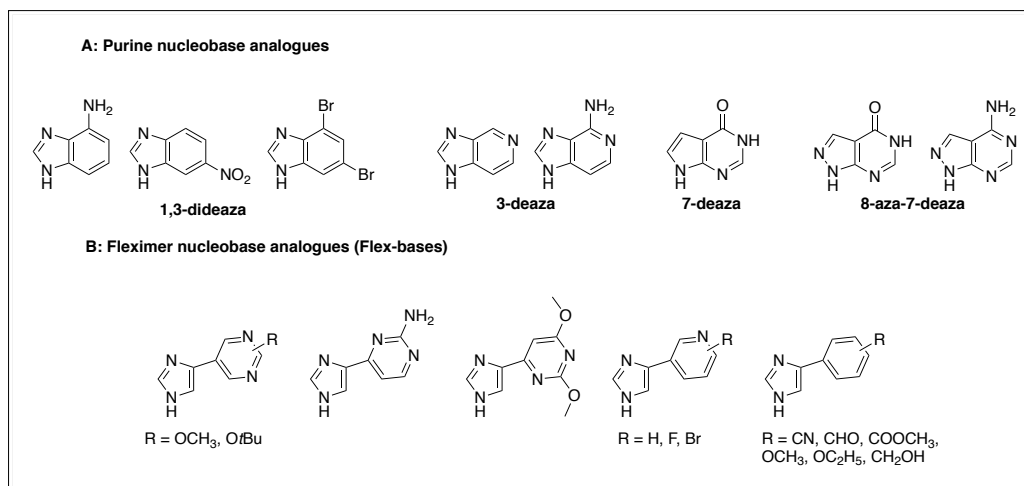


Figure 20. Various heterocyclic base substrates of *E. coli* PNP.

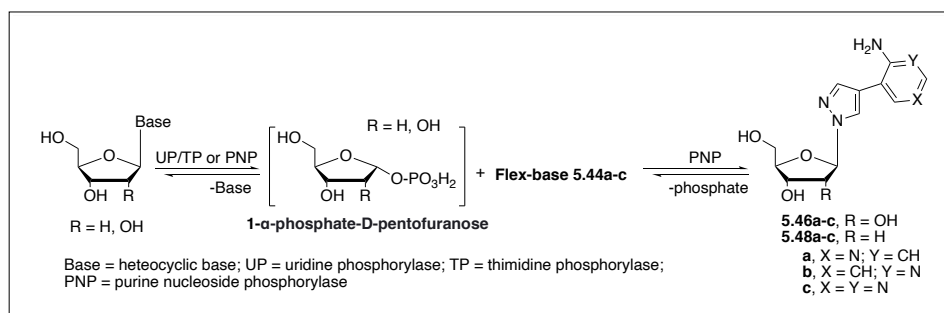
The affinity of flex-bases **5.44a-c** to the two active sites of *E. coli* PNP was evaluated, along with k_{cat} and k_{cat}/K_M values. This data is summarized in **Table 14**. (Khandazhinskaya, Eletskaya et al. 2021) It was found that compared to natural substrate adenine, the K_M values for all three flex-bases were an entire order of magnitude lower; however, their K_M values were 3-7 times higher compared to the close structural analogue 8-aza-7-deazaadenine (**Table 14**). Additionally, the k_{cat} values of the flex-bases did not significantly differ from 8-aza-7-deazaadenine but were three orders of magnitude slower compared to adenine, as seen in **Table 14**. Thus, it was concluded that the reaction rate is strongly influenced by the position of the nitrogen in the pentacyclic ring. (Khandazhinskaya, Eletskaya et al. 2021)

Table 14. Kinetic parameters of the formation of 2-deoxyribosides **5.46a-c** according to the two-interacting site model.

| Substrate/Product | K_{M1}^a (mM) | K_{cat1}^a (s ⁻¹) | K_{cat1}/K_{M1} (s ⁻¹ M ⁻¹) | K_{M1}^b (mM) | K_{cat1}^b (s ⁻¹) | K_{cat1}/K_{M1} (s ⁻¹ M ⁻¹) |
|----------------------|--------------------|------------------------------------|---|--------------------|------------------------------------|---|
| 5.44a / 5.46a | 0.97 ± 0.17 | 2.0 ± 0.3 | 2.1 × 10 ³ | 3.0 ± 0.5 | 11 ± 2 | 3.7 × 10 ³ |
| 5.44b / 5.46b | 0.44 ± 0.06 | 3.7 ± 0.5 | 8.4 × 10 ³ | 2.6 ± 0.4 | 26 ± 4 | 1.0 × 10 ⁴ |
| 5.44c / 5.46c | 0.57 ± 0.14 | 1.8 ± 0.4 | 3.2 × 10 ³ | 3.0 ± 0.7 | 13 ± 3 | 4.3 × 10 ³ |
| 8-Aza-7-deazaadenine | 0.14 ± 0.02 | 1.9 ± 0.3 | 1.4 × 10 ⁴ | 0.66 ± 0.09 | 13 ± 2 | 2.0 × 10 ⁴ |
| Adenine | 0.071 ± 0.015 | 2700 ± 600 | 3.8 × 10 ⁷ | 0.27 ± 0.06 | 3400 ± 700 | 1.3 × 10 ⁷ |

^a K_{M1} and k_{cat1} are kinetic parameters of the active site to which the substrate binds first; ^b K_{M2} and k_{cat2} are kinetic parameters of the active site to which the substrate binds if the adjacent active site is occupied. Table adapted from Khandazhinskaya et al. (Khandazhinskaya, Eletskaya et al. 2021)

Flex-bases **5.44a-c** were then found to be substrates for *E. coli* PNP, allowing for synthesis of fleximer analogues **5.46a-c** and **5.48a-c** in high yields as shown in **Scheme 30**. (Khandazhinskaya, Eletskaya et al. 2021)



Scheme 30. Enzymatic synthesis of flex-adenosine analogues **5.46a-c** and **5.48a-c**.

However, the overall rate of conversion was slow. (Khandazhinskaya, Eletskaya et al. 2021) *E. coli* cell lines overexpressing PNP and thymidine phosphorylase (TP) were then used but overall yields for the fleximer analogues were akin to that of normal *E. coli* PNP. It should be noted though that the amount of

target fleximer per mL of substrate mixture was 10 times higher (**Table 15**). Additionally, in *E. coli* cells overexpressing PNP or TP, reaction times were significantly shorter.(Khandazhinskaya, Eletskaya et al. 2021) *E. coli* cell lines overexpressing PNP and TP were then used but overall yields for the fleximer analogues were similar to that of normal *E. coli* PNP.

Table 15. Comparison of chemical synthesis and enzymatic synthesis methods.

| | Chemical synthesis | Isolated enzymes, PNP + UP | | <i>E. coli</i> cells overexpressing PNP and <i>E. coli</i> cells overexpressing UP or TP | | |
|--------------|---------------------------------|---|------------------------|--|------------------------|-------------------------|
| Compound | Isolated yield ^a (%) | Isolated product (mg/mL reaction mixture) | Isolated yield, mg (%) | Isolated product (mg/mL reaction mixture) | Isolated yield, mg (%) | Purity ^b (%) |
| 5.46a | 71 | 0.21 | 29 (30) | 1.63 | 51 (28) | 99.8 |
| 5.46b | 55 | 0.26 | 16 (44) | 2.66 | 36 (46) | 98.6 |
| 5.46c | 65 | 0.32 | 20 (55) | 3.31 | 205 (54) | 99.9 |
| 5.48a | 18 ^c | 0.14 | 22 (51) | 2.69 | 73 (45) | 99.9 |
| 5.48b | 82 ^d | 0.29 | 18 (52) | 2.26 | 43 (45) | 97.7 |
| 5.48c | 57 ^e | 0.35 | 22 (64) | 2.83 | 43 (51) | 99.5 |

^aPurity >95%, according to NMR data; ^bPurity according to HPLC data; ^cMixture of β - and α -anomers in 4:1 ratio; ^dMixture of β - and α -anomers in 3:2 ratio; ^eMixture of β - and α -anomers in 3:1 ratio. Table adapted from Khandazhinskaya et al.(Khandazhinskaya, Eletskaya et al. 2021)

Preliminary biological evaluation of fleximers **5.46a-c** and **5.48a-c** revealed that none of the synthesized fleximer analogues undergo deamination *in vitro*. Additionally, no significant effects on cell growth were observed in concentrations up to 100 μ M.(Khandazhinskaya, Eletskaya et al. 2021) More detailed studies on the biological activities of the fleximer analogues are currently underway.(Khandazhinskaya, Eletskaya et al. 2021)

II. Sugar Modifications

The sugar moiety is a common site of interest, with changes being able to be made at each carbon, such as removal of hydroxyl groups to provide deoxy derivatives or inclusion of other groups such as fluorine or methyl.(Seley-Radtke 2018, Yates and Seley-Radtke 2019) Additionally, the furanose ring oxygen can be substituted for a carbon, giving carboxylic analogues, or changed to another heteroatom such as sulfur or nitrogen.(Seley-Radtke 2018, Yates and Seley-Radtke 2019)

6. 2' Modifications

Following the success of Flex-GTP to maintain potency following mutation of a critical amino acid in the GFPP active site, the Seley-Radtke group pursued a series of 2'-deoxy fleximer analogues both with distal and proximal connectivity (**Figure 21**). (Wauchope, Velasquez et al. 2012)

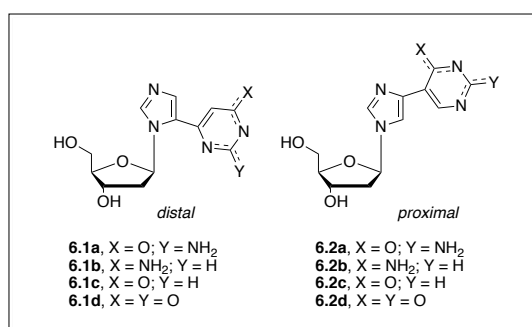
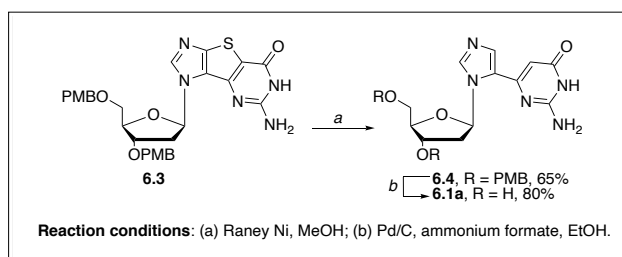


Figure 21. Structures of 2'-deoxy fleximer analogues.

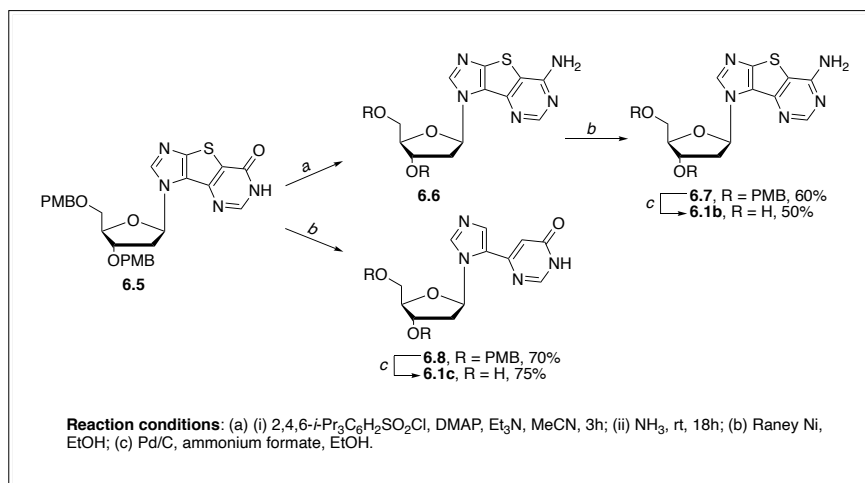
The 2'-deoxy distal fleximers **6.1a-d** were synthesized using the same methods for the distal ribofuranose fleximers (Wauchope, Velasquez et al. 2012) discussed in a previous section in which a tricyclic intermediate is first synthesized.(Seley, Zhang et al. 2001, Seley, Zhang et al. 2002) After synthesis of tricyclic compound **6.3** according to previously established methods (Seley, Zhang et al. 2001, Seley, Zhang et al. 2002), sulfur was removed via Raney nickel to afford protected intermediate **6.4** (**Scheme 31**). (Wauchope, Velasquez et al. 2012) The *p*-methoxybenzyl (PMB) protecting group was then removed to provide the

desired 2'-deoxy distal fleximer **6.1a** in good yield. (Wauchope, Velasquez et al. 2012)



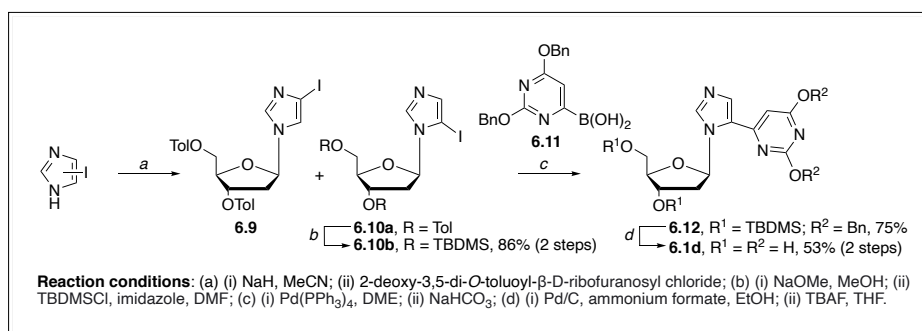
Scheme 31. Synthesis of 2'-deoxy distal fleximer **6.1a**.

The next two fleximers, **6.1b** and **6.1c**, were synthesized starting from the same tricyclic intermediate **6.5** as shown in **Scheme 32**. (Wauchope, Velasquez et al. 2012)



Scheme 32. Synthesis of 2'-deoxy distal fleximers **6.1b** and **6.1c**.

Similar to the synthesis of fleximer **6.1a**, intermediate **6.5** was treated with Raney nickel to provide compound **6.8** in good yield which was subsequently deprotected to give fleximer **6.1c** in 75% yield (**Scheme 32**). (Wauchope, Velasquez et al. 2012) Conversion of the carbonyl of tricyclic **6.5** to an amine afforded intermediate **6.6** which was then treated with Raney nickel to give PMB-protected intermediate **6.7** in 60% yield. Deprotection of **6.7** then provided fleximer **6.1b** in modest yield. (Wauchope, Velasquez et al. 2012)

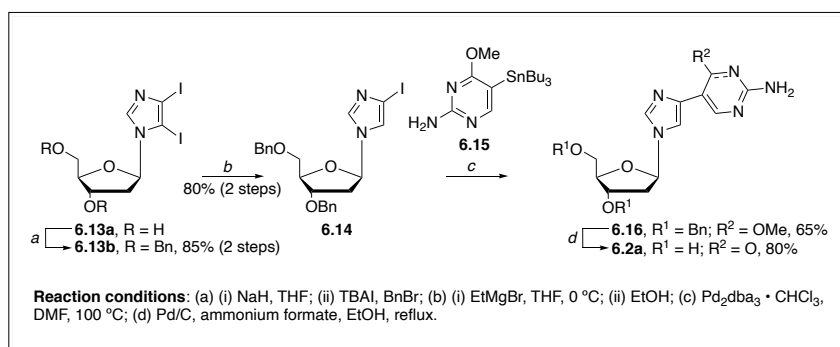


Scheme 33. Synthesis of 2'-deoxy distal fleximer **6.1d**.

The synthesis of xanthosine fleximer **6.1d** began with a glycosylation reaction between Hoffer's chlorosugar and iodoimidazole, affording an isomeric mixture of **6.9** and **6.10a** (**Scheme 33**). (Wauchope, Velasquez et al. 2012) Deprotection of intermediate **6.10a** and immediate re-protection using tert-butyldimethylsilyl (TBDMS) chloride provided compound **6.10b** in high yield. A Suzuki coupling with boronic acid **6.11** afforded protected compound **6.12**. Removal of the protecting groups gave desired 2'-deoxy distal fleximer **6.1d** (**Scheme 33**). (Wauchope, Velasquez et al. 2012)

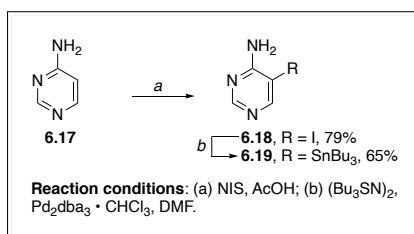
The syntheses of the 2'-deoxy proximal fleximers were more facile, compared to the distal analogues. The expanded purine tricyclic intermediate was not necessary, as it was for the distal fleximers. Instead, after glycosylation of the 2'-deoxy sugar with iodinated imidazole, the desired pyrimidine could be attached via a

Stille or Suzuki coupling reaction.(Wauchope, Velasquez et al. 2012), as shown with the synthesis of 2'-deoxy proximal fleximer **6.2a** in **Scheme 34**.(Wauchope, Velasquez et al. 2012)



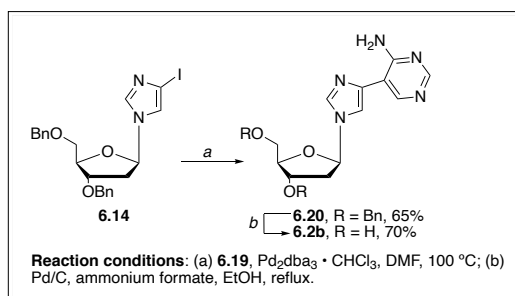
Scheme 34. Synthesis of 2'-deoxy proximal fleximer **6.2a**.

Synthesis of **6.2a** began with benzyl protection of intermediate **6.13a** to provide **6.13b** (**Scheme 34**). Intermediate **6.13b** was then selectively de-iodinated at the 5 position to provide compound **6.14** in high yield. A Suzuki coupling with boronic acid **6.15** afforded protected intermediate **6.16** in modest yield. Removal of the benzyl and methyl protecting groups provided desired proximal fleximer **6.2a** in high yield.(Wauchope, Velasquez et al. 2012) For fleximer **6.2b**, synthesis first began with formation of the desired tributylstannyl reagent **6.19** (**Scheme 35**) to be used in a Stille cross-coupling reaction.(Wauchope, Velasquez et al. 2012)



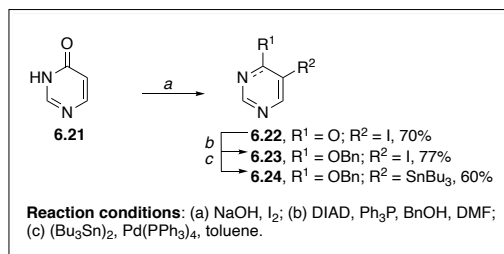
Scheme 35. Synthesis of Stille reagent **6.19**.

Synthesis of Stille reagent **6.19** began with commercially available 4-aminopyrimidine **6.17** which was iodinated to afford intermediate **6.18** in high yield (**Scheme 35**). Addition of the tributylstannyl group at the 5 position was achieved using a palladium-catalyzed reaction in DMF, providing compound **6.19** in modest yield.(Wauchope, Velasquez et al. 2012) This was then used in a Stille coupling with compound **6.14** to provide the protected intermediate **6.20** (**Scheme 36**). Removal of the benzyl groups using Pd/C and ammonium formate in ethanol gave desired fleximer **6.2b** in 70% yield.(Wauchope, Velasquez et al. 2012)

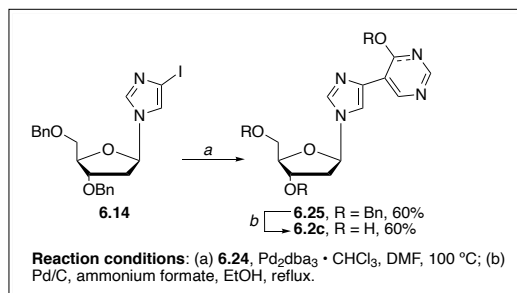


Scheme 36. Synthesis of 2'-deoxy proximal fleximer **6.2b**.

Fleximer **6.2c** was obtained in a similar fashion, beginning with synthesis of the desired 5-(tributylstannyl)pyrimidine intermediate as outlined in **Scheme 37**.(Wauchope, Velasquez et al. 2012) Commercially available pyrimidine **6.21** was iodinated, yielding intermediate **6.22** which was then benzyl protected using Mitsunobu conditions to afford intermediate **6.23** in high yield (**Scheme 37**). Reaction of **6.23** with bis(tributyltin) in toluene, catalyzed by palladium tetrakis, provided Stille reagent **6.24** in 60% yield.(Wauchope, Velasquez et al. 2012) This was then used in a Stille coupling reaction with compound **6.14** to provide intermediate **6.25** (**Scheme 38**). Again, removal of the benzyl groups provided the desired 2'-deoxy proximal fleximer **6.2c** in modest yield.(Wauchope, Velasquez et al. 2012)

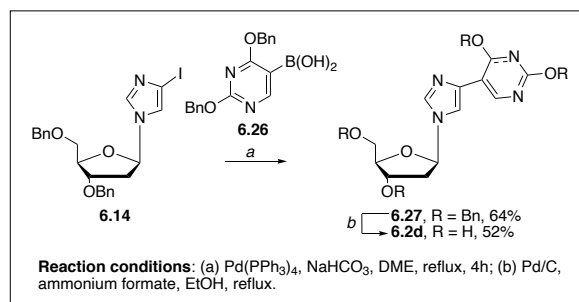


Scheme 37. Synthesis of Stille reagent **6.24**.



Scheme 38. Synthesis of 2'-deoxy proximal fleximer **6.2c**.

Lastly, the xanthosine proximal fleximer analogue **6.2d** was achieved by coupling boronic acid **6.26** with compound **6.14** using Suzuki coupling conditions, affording protected intermediate **6.27** in modest yield (**Scheme 39**). Deprotection of **6.27** provided desired fleximer **6.2d** in 52% yield. (Wauchope, Velasquez et al. 2012)



Scheme 39. Synthesis of 2'-deoxy proximal fleximer **6.2d**.

In addition to 2'-deoxy distal fleximers **6.1a-d** and 2'-deoxy proximal fleximers **6.2a-d**, Khandazhinskaya et al. also synthesized fleximers featuring 2'-deoxy modifications (compounds **5.48a-c**, **Scheme 30**) as shown in a previous section. Biological testing for these compounds has yet to be reported.

7. 3' Modifications

Another common position on the sugar ring for modification is the 3' position. (Deval, Powdrill et al. 2007, Deval 2009, Seley-Radtke and Yates 2018, Yates and Seley-Radtke 2019) This position is particularly of interest for modification due to the role it plays in recognition and incorporation into the growing nucleic acid chain. Nucleoside analogues are incorporated via the 3' hydroxyl of the template chain interacting with the 5' hydroxyl of the next incoming nucleotide. (Deval, Powdrill et al. 2007, Deval 2009, Seley-Radtke and Yates 2018, Yates and Seley-Radtke 2019) Thus, if the 3' hydroxyl were absent or replaced by a different moiety, the DNA chain elongation could theoretically be interrupted. Modifications at this position led to the 'chain terminator' class of nucleoside analogues. (Deval, Powdrill et al. 2007, Deval 2009, Seley-Radtke and Yates 2018, Yates and Seley-Radtke 2019)

Modifications at the 3' position are similar to those made at the 2' position, such as addition of methyl or fluoro groups. (Seley-Radtke and Yates 2018, Yates and Seley-Radtke 2019) Among the first modifications made though were removal of the 3' hydroxyl group in addition to the 2' hydroxyl, resulting in 2',3'-dideoxy nucleoside analogues. Early compounds with this modification include zalcitabine (ddC) and didanosine (ddI), as shown in **Figure 22**. Both ddC and ddI have been FDA-approved for use as nucleoside reverse

transcriptase inhibitors (NRTIs) for human immunodeficiency virus (HIV). (Seley-Radtke and Yates 2018)

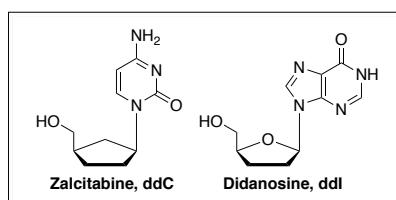


Figure 22. Structures of Zalcitabine (ddC) and Didanosine (ddI).

A 2',3'-dideoxy modification has been incorporated into a series of reverse fleximers, as shown in a previous section with the carbocyclic 5'-nor reverse fleximers (compound series **3.2**, Figure **11**). Unfortunately, unlike ddC and ddI, the series **3.2** compounds were found to be inactive against HIV during *in vitro* evaluation. (Zimmermann, Sadler et al. 2011)

8. Carboxylic Modifications

Another nucleoside structural modification found to be particularly fruitful in producing potent antiviral and anticancer drugs are the carbocyclic nucleosides. (Seley-Radtke and Yates 2018, Yates and Seley-Radtke 2019) These modified nucleosides lack the furanose oxygen within the sugar moiety, possessing instead a methylene group. This change results not only in significant stability of the glycosidic bond but also increases overall lipophilicity. Some notable carbocyclic nucleosides include Neplanocin A (NpcA, **Figure 23**) and Aristeromycin (Ari), both of which are naturally occurring adenosine analogues with potent antiviral, anticancer, and antiparasitic activity. (Seley-Radtke and Sunkara 2009, Zimmermann, O'Neill et al. 2014)

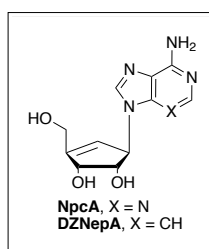


Figure 23. Structures of Neplanocin (NpcA) and deaza-neplanocin (DZNepA).

However, both NpcA and Ari have major issues with cytotoxicity stemming from intracellular conversion to their active triphosphate forms by adenosine kinase and recognition and metabolism by adenosine deaminase. (Zimmermann, O'Neill et al. 2014) This cytotoxicity can be significantly reduced by forming truncated versions of the nucleoside analogues via removal of the 4'-CH₂OH, as shown in **Figure 24**. (Zimmermann, O'Neill et al. 2014)

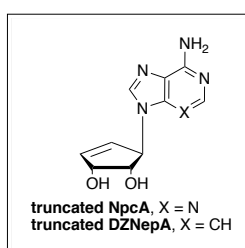


Figure 24. Structures of truncated NpcA and DZNepA.

Additionally, it has been found that 3-deazadenosine analogues of truncated NpcA and Ari exhibit greater inhibition levels than the parent compounds. (Zimmermann, O'Neill et al. 2014) These truncated 3-deaza compounds have shown potent activity against chloroquine-resistant and -susceptible strains of *P. falciparum*, a protozoan parasite. (Zimmermann, O'Neill et al. 2014)

In 2014, Seley-Radtke reported the synthesis of a series of truncated 3-deaza NpcA fleximer analogues as shown in **Figure 25**. (Zimmermann, O'Neill et al. 2014)

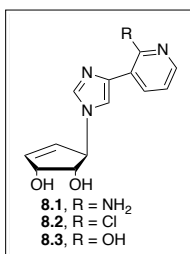
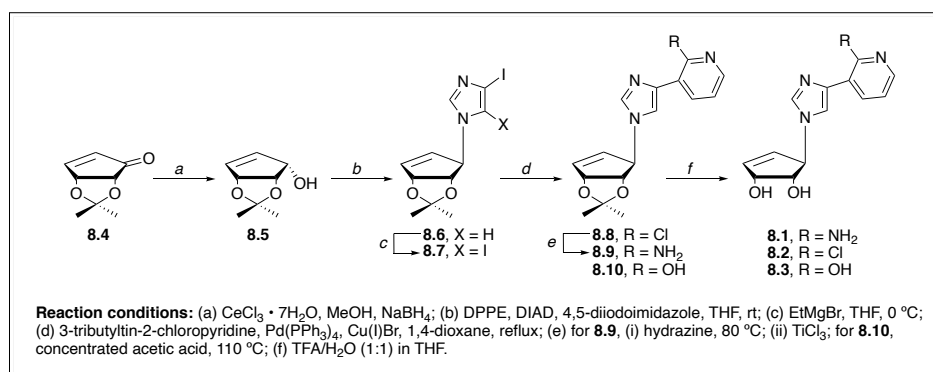


Figure 25. Structures of truncated DZNepA fleximer targets.

Synthesis of these compounds, as outlined in **Scheme 31**, began with D-cyclopentanone **8.4** which was subjected to a Luche reduction to afford cyclopentanol **8.5**. Compound **8.6** was obtained via standard Mitsunobu coupling conditions using diisopropylazodicarboxylate (DIAD) and 1,2-bis(diphenylphosphino)ethane (DPPE). The 5-iodo was then removed using EtMgBr, affording compound **8.7** which was then used in a Stille coupling to provide intermediate **8.8**. Deprotection gave desired NpcA fleximer **8.2**. Initial attempts to transform the chloro group of the pyridine ring to the required azide for compound **8.1** using sodium or lithium azide were unsuccessful. Additionally, attempts to follow a palladium catalyzed procedure developed by Hartwig using sodium-*t*-butoxide were also unsuccessful. Even attempts to make the catalyst *in situ* as initially developed by Buchwald were fruitless. However, use of titanium chloride proved to be successful and following deprotection, compound **8.1** was achieved. Conversion of the chloro group of intermediate **8.8** to compound **8.10** was done using concentrated acetic acid. Deprotection of compound **8.10** then produced the desired inosine fleximer analogue **8.3**. (Zimmermann, O'Neill et al. 2014)



Scheme 40. Synthesis of fleximers **8.1**, **8.2**, and **8.3**.

The NpcA fleximer analogues **8.1-8.3** were screened against *Trypanosoma brucei* (Lister 427 strain) with all three compounds having EC₅₀ values around 200 μM (**Table 16**). (Zimmermann, O'Neill et al. 2014)

Table 16. *Trypanosoma brucei brucei* screening.

| Compound | Average EC ₅₀ (μM) |
|-------------|----------------------------------|
| 8.1 | 216 ± 21 |
| 8.2 | 212 ± 31 |
| 8.3 | 287 ± 24 |
| pentamidine | 0.0044 ± 0.0001 |

Table adapted from Zimmermann et al. (Zimmermann, O'Neill et al. 2014)

These low levels of activity were attributed to lack of recognition of the fleximers by *T. b. brucei* nucleoside transporters. This was confirmed using fleximers that most closely resembled the original nucleoside substrates for *T. b. brucei* nucleoside transporters P1 and P2 (**Table 17**). Overall, fleximers appear to have approximately two orders of magnitude less affinity for *T. b. brucei* nucleoside transporters, thus limiting their uptake. The loss in Gibbs free energy for the fleximer-transporter interaction (compared to parent nucleosides) may be due to increased entropy caused by the orientation the fleximer assumes within the binding pocket and/or the larger base of the fleximer analogue. (Zimmermann, O'Neill et al. 2014)

Table 17. K_i values for *T. b. brucei* nucleoside transporters P1 and P2.

| | P1 K_i (μ M) | | | P2 K_i (μ M) | | |
|-----------|---------------------|--------------|-------------------------------|---------------------|------------|-------------------------------|
| | Nucleoside | Fleximer | $\delta(\Delta G^0)$ (kJ/mol) | Nucleoside | Fleximer | $\delta(\Delta G^0)$ (kJ/mol) |
| Adenosine | 0.36 ± 0.05 | 35 ± 11 | 11.4 | 0.91 ± 0.29 | 37 ± 3 | 9.2 |
| Guanosine | 1.8 ± 0.3 | 251 ± 75 | 12.2 | >500 | >500 | – |
| Inosine | 0.44 ± 0.10 | 387 ± 30 | 16.8 | >500 | >500 | – |

Table adapted from Zimmermann et al.(Zimmermann, O'Neill et al. 2014)

This same sugar moiety has also been used in the previously discussed reverse fleximer series **3.1** compounds (**Figure 11**). Additionally, other carboxylic sugars have also been used in reverse fleximer synthesis, such as with series **3.2**, **3.3** and **3.4** compounds (**Figure 11**) shown previously. Any further developments in fleximers featuring a carboxylic sugar will be reported as data becomes available.

9. Acyclic Modifications

A common sugar modification that has proven successful in multiple FDA approved nucleoside drugs is the use of an acyclic sugar moiety.(Seley-Radtke and Yates 2018) Acyclic sugars were first introduced in the 1970s by Eric De Clercq and Antonín Holý. They lack the 2' and/or the 3' carbons on the sugar moiety.(Clercq and Holý 2005, Seley-Radtke and Yates 2018) One of the first acyclic nucleosides to exhibit antiviral activity was acyclovir (ACV), a guanosine nucleoside analogue, which was approved for treatment of HSV and varicella zoster virus (VZV) and acts as an obligate chain terminator against the herpes viral DNA polymerase.(O'Brien and Campoli-Richards 1989) It has even exhibited antiviral activity against other DNA viruses such as Epstein-Barr virus (EBV) and cytomegalovirus (CMV).(Andersson, Sköldenberg et al. 1985, O'Brien and Campoli-Richards 1989, Barkholt, Lewensohn-Fuchs et al. 1999) Combining the fleximer nucleoside technology with the acyclic sugar of acyclovir, the Seley-Radtke lab produced a novel series of doubly flexible nucleoside analogues (Flex-ACV analogues, **Figure 26**) in hopes of having broad spectrum antiviral activity similar to that of acyclovir.(Peters, Jochmans et al. 2015)

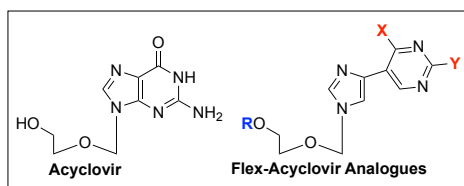
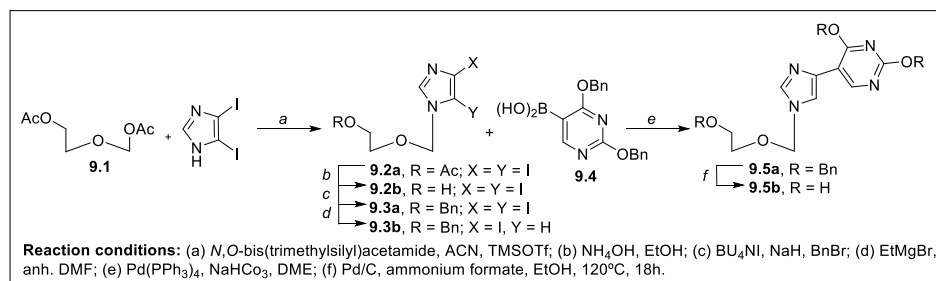


Figure 26. Structure of acyclovir vs. Flex-acyclovir analogues. *R*, *X*, and *Y* represent the various locations for potential modifications.

Synthesis of the acyclic fleximers began with a literature procedure to make the sugar moiety of acyclovir via a modified Vorbruggen reaction of 2-acetoxyethyl acetoxymethylether (**9.1**) and diiodoimidazole to give intermediate **9.2a** as seen in **Scheme 41**. The acetate protecting group was removed to give **9.2b**, followed by a protection with benzyl groups (**9.3a**). Compound **9.3a** could then be selectively deiodinated with EtMgBr to give intermediate **9.3b**.(Peters, Jochmans et al. 2015)

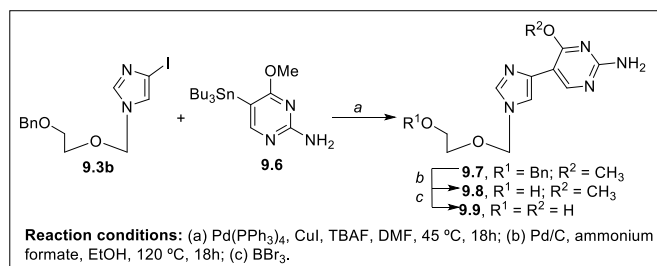


Scheme 41. Synthesis of the Flex-ACV sugar intermediates and the first Flex-ACV nucleosides.

This intermediate (**9.3b**) was then used in various Suzuki-Miyaura cross coupling reactions. The first coupling partner **9.4** was synthesized via literature procedures without purification and used in the coupling reaction to give compound **9.5a** (**Scheme 41**). The benzyl groups on this compound were removed with Pd/C to give the flex acyclic xanthosine nucleoside **9.5b** in a 26% yield (**Scheme 41**). (Peters, Jochmans et al. 2015) When the temperature was lowered to 60°C, the pyrimidine on **9.5b** was deprotected, but the sugar moiety was not. This modification would allow for future functionalization on the pyrimidine moiety.(Peters,

Jochmans et al. 2015)

The first attempts to make the guanosine analogue via the synthesis of the diamino pyrimidine were not successful. (Peters, Jochmans et al. 2015) The guanosine analogue was still pursued via a Stille cross-coupling method that utilized an organotin reagent. Compound **9.3b** was coupled to compound **9.6** (**Scheme 42**), which was prepared via literature procedures with 2-amino-5-chloro-6-methoxy pyrimidine. (Peters, Jochmans et al. 2015) The reaction of **9.3b** and **9.6** yielded nucleoside **9.7**, which was then benzyl deprotected with Pd/C in an ammonium formate/EtOH reflux (**9.8**, 24%). The methyl group on the pyrimidine was then removed via BBr₃ to give the guanosine analogue **9.9** in a 24% yield (**Scheme 42**). (Peters, Jochmans et al. 2015)



Scheme 42. Continued synthesis of various Flex-ACV nucleoside analogues.

By the time the compounds were synthesized multiple outbreaks of human and zoonotic coronaviruses had occurred across the globe. (Docea, Tsatsakis et al. 2020) Efforts were unsuccessful in finding an antiviral drug that targets the coronaviruses, making these viral targets highly attractive to the Seley-Radtke lab. (Tan, Ooi et al. 2004, Peters, Jochmans et al. 2015) Therefore, the Flex-ACV analogues (**9.5b**, **9.8**, and **9.9**) were tested for antiviral activity against three different coronaviruses, HCoV-NL63, MERS-CoV, and SARS-CoV in various types of cells. The results are summarized in **Table 18**. (Peters, Jochmans et al. 2015) Most notable, compound **9.8** showed antiviral activity against HCoV-NL63 and MERS-CoV, whereas the parent compound acyclovir was found to be completely inactive. (Peters, Jochmans et al. 2015) The best activity was seen against HCoV-NL63 on Vero cells with an EC₅₀ of 8.8 ± 1.5 µM. Compound **9.8** also demonstrated high CC₅₀ values, showing it did have selectivity towards the viruses. It is important to note that the Flex-ACV analogues were the first modified nucleoside analogues to exhibit antiviral activity against coronaviruses. (Peters, Jochmans et al. 2015)

Table 18. Anti-coronavirus activity of Flex-ACV analogues

| Compound | HCoV-NL63 on Vero118 | | MERS-CoV on Huh7 | | MERS-CoV on Vero | | SARS-CoV on VeroE6 | |
|------------------|-----------------------|-----------------------|-----------------------|-----------------------|-----------------------|-----------------------|-----------------------|-----------------------|
| | EC ₅₀ (µM) | CC ₅₀ (µM) | EC ₅₀ (µM) | CC ₅₀ (µM) | EC ₅₀ (µM) | CC ₅₀ (µM) | EC ₅₀ (µM) | CC ₅₀ (µM) |
| 9.5b | 92 ± 68 | >200 | n.d. | n.d. | n.d. | n.d. | n.d. | n.d. |
| 9.8 | 8.8 ± 1.5 | 120 ± 37 | 13.5 ± 0.0 | 54.0 ± 1.7 | 10.1 ± 1.2 | 77.2 ± 50.1 | 28.1 ± 0.2 | 90.8 ± 7.1 |
| 9.9 | >200 | >200 | n.d. | n.d. | n.d. | n.d. | n.d. | n.d. |
| Acyclovir | >100 | >100 | >1000 | >1000 | >1000 | >1000 | >1000 | >1000 |

EC₅₀: effective concentration showing 50% inhibition of virus-induced CPE; CC₅₀: cytotoxic concentration showing 50% inhibition of cell survival; n.d.: not determined. Table adapted from Peters et al. (Peters, Jochmans et al. 2015)

Based on the antiviral activities of **9.8** and **9.9**, it was possible the methoxy group on **9.8** was acting as a prodrug, which had been shown in other nucleoside analogues. (McGuigan, Madela et al. 2010, Peters, Jochmans et al. 2015) This inspired the Seley-Radtke lab to pursue other prodrugs such as McGuigan Protides on the Flex-ACV analogues. A prodrug is an inactive compound that can be converted to an active drug via metabolism. (Najjar and Karaman 2019) Many prodrugs are utilized to overcome drug delivery issues, especially for phosphate compounds that have poor stability and negative charges that make membrane permeability difficult. As previously mentioned, the first phosphorylation step is the rate limiting step in the cell. To overcome permeability and phosphorylation issues, Professor Chris McGuigan introduced a prodrug technology called the McGuigan Protide. (McGuigan, Cahard et al. 1996, McGuigan, Hassan-Abdallah et al. 2006, Mehellou, Rattan et al. 2018) The general structure of the Protide is shown in **Figure 27**. (Slusarczyk, Serpi et al. 2018) The amino acid ester group and the aryl group are used to mask the negative charges on the monophosphate to allow the nucleoside to cross the cell membrane. Once the nucleoside crosses the cell membrane, the amino acid ester group and aryl group are removed via cellular

metabolism. This leaves the monophosphate nucleotide, which can then be phosphorylated to give the active triphosphate drug. (Mehellou, Rattan et al. 2018) The development of the phosphoramidate Protide technology has proven successful in various drugs such as tenofovir alafenamide and GS-5734. (Slusarczyk, Serpi et al. 2018)

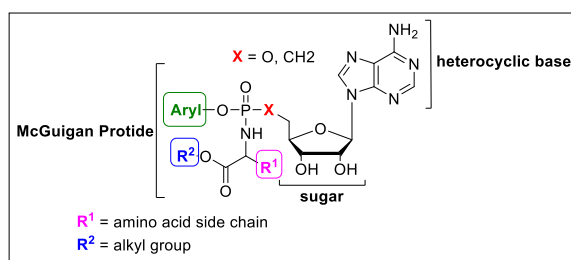
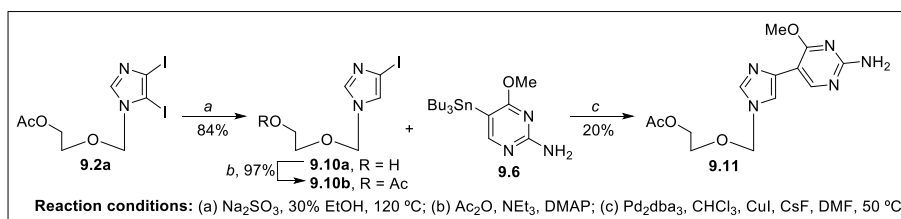


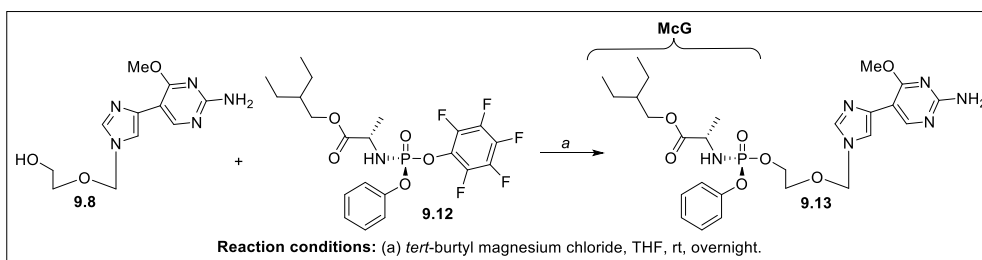
Figure 27. General scaffold of a McGuigan Protide.

The Flex-ACV analogues continued to be pursued and the Seley-Radtke lab utilized the Protide technology on these analogues, as well as an acetate prodrug on the sugar moiety. (Yates, Raje et al. 2017) Synthesis of the Flex-ACV prodrugs began with compound **9.2a**, which was simultaneously deacetylated and deiodinated in 30% ethanol with sodium sulfite to give compound **9.10a**. This compound could then be acetylated (**9.10b**) to give the correct sugar moiety needed for the acetate prodrug synthesis (Scheme 43). (Yates, Raje et al. 2017) The same Stille reagent that was previously synthesized (**9.6**) was utilized in Stille cross-coupling methods to give the desired nucleoside analogues. Coupling of compounds **9.10a** and **9.6** yielded final compound **9.8**, while coupling of compound **9.10b** with compound **9.6** yielded the acetate prodrug **9.11**. (Yates, Raje et al. 2017)



Scheme 43. Synthesis of the acetate prodrug.

Synthesis of the Flex-ACV McGuigan Protide began with a literature procedure from L-alanine to make the phosphoramidate intermediate **9.12** (Scheme 44). (Ross, Ganapati Reddy et al. 2011) Nucleoside **9.8** and compound **9.12** were then treated with *tert*-butyl magnesium chloride to give the Protide **9.13** in a 69% yield. (Yates, Raje et al. 2017)



Scheme 44. Synthesis of the McGuigan protide.

Given the anti-coronavirus activity previously exhibited by the Flex-ACV analogues and the antiviral activity seen by other nucleosides that utilize the McGuigan Protide technology, the Seley-Radtke lab evaluated compounds **9.8**, **9.11**, and **9.13** for anti-filovirus activity. (Yates, Raje et al. 2017) At the time there were no FDA approved treatments for filoviruses like Ebola. The Flex-ACV analogues were screened against Ebola virus (EBOV), Marburg virus (MARV), and Sudan Ebola virus (SUDV), as well as hemorrhagic fevers such as Lassa virus and Rift Valley fever. The results of these studies are summarized in Table 19 and Table

Table 19. Anti-filovirus screening of compounds **9.8**, **9.11**, and **9.13**.

| Compound | EBOV on HeLa | | SUDV on HeLa | | MARV on HeLa | |
|-------------|-----------------------|-----------------------|-----------------------|-----------------------|-----------------------|-----------------------|
| | EC ₅₀ (μM) | CC ₅₀ (μM) | EC ₅₀ (μM) | CC ₅₀ (μM) | EC ₅₀ (μM) | CC ₅₀ (μM) |
| 9.8 | >100 | >100 | >100 | >100 | >100 | >100 |
| 9.11 | 44 ± 13 | >100 | 20 ± 10 | >100 | 70 ± 27 | >100 |
| 9.13 | 29 ± 9 | >100 | 7 ± 2 | >100 | 62 ± 13 | >100 |

Table adapted from Yates et al.(Yates, Raje et al. 2017)

Table 20. Anti-filovirus screening of compounds **9.8** and **9.13**.

| Compound | EBOV on Huh7 | | Lassa Virus on Huh7 | | Rift Valley Fever on Huh7 | |
|-------------|-----------------------|-----------------------|-----------------------|-----------------------|---------------------------|-----------------------|
| | EC ₅₀ (μM) | CC ₅₀ (μM) | EC ₅₀ (μM) | CC ₅₀ (μM) | EC ₅₀ (μM) | CC ₅₀ (μM) |
| 9.8 | 2.2 ± 0.3 | >50 | >50 | >50 | >50 | >50 |
| 9.13 | 27.2 ± 2.2 | >50 | >50 | >50 | >50 | >50 |

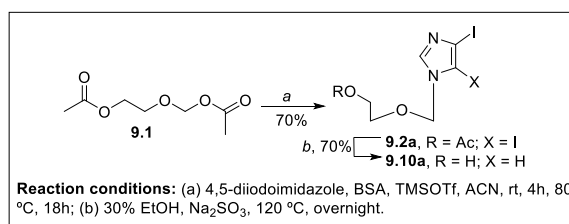
Table adapted from Yates et al.(Yates, Raje et al. 2017)

The Flex-ACV McGuigan Protide **9.13** exhibited activity against all tested filoviruses with the best EC₅₀ value of 7 ± 2 μM against SUDV. While compound **9.8** had no activity against EBOV in Hela cells, it did exhibit single digit micromolar activity against EBOV in Huh7 cells (2.2 ± 0.3 μM). Compound **9.11** did exhibit weak antiviral activity against EBOV, MARV, and SUDV.(Yates, Raje et al. 2017)

The broad-spectrum antiviral activity of the Flex-ACV analogues prompted the Seley-Radtke lab to further investigate the analogues against other families of viruses and explore the mechanism of action of the compounds to determine how the antiviral activity was occurring and what enzymes the compounds were interacting with.(Thames, Waters et al. 2020) The 2-amino-4-methoxy Flex-ACV nucleoside (**9.8**) and its prodrugs continued to be investigated, along with the dimethoxy nucleoside and its prodrug analogues, in which the synthesis will be detailed below.

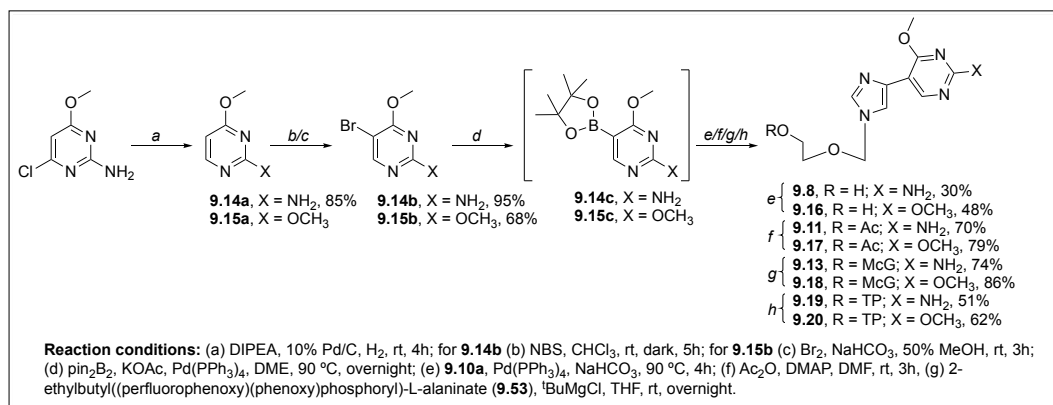
Previous synthesis of the Flex-ACV analogues utilized Stille cross coupling conditions that required an organotin reagent.(Peters, Jochmans et al. 2015, Yates, Raje et al. 2017) Unfortunately, purification to remove residual tin was very tedious and resulted in very low yields of final compounds. More recently the synthesis of the Flex-ACV nucleoside analogues was optimized. It was found that a different organometallic coupling method resulted in better yields.(Thames, Waters et al. 2020)

Before the nucleoside could be synthesized, first the sugar moiety was made via previously established modified Vorbruggen methods outlined in **Scheme 45** to give the important intermediate **9.10a**.(Peters, Jochmans et al. 2015, Yates, Raje et al. 2017, Thames, Waters et al. 2020)

**Scheme 45.** Flex-ACV sugar synthesis.

To achieve the desired pyrimidine moiety for the 2-amino-4-methoxy Flex-ACV nucleoside series, synthesis began with a dechlorination of commercially available 2-amino-4-chloro-6-methoxy pyrimidine in the presence of H₂ gas and Pd/C to give compound **9.14a** in an 85% yield. Compound **9.14a** was then brominated with NBS to give the pyrimidine (**9.14b**) in a 95% yield. To achieve the brominated dimethoxy pyrimidine **9.15b**, commercially available 2,4-dimethoxy pyrimidine (**9.15a**) was brominated with Br₂ in a 68% yield.(Thames, Waters et al. 2020)

Both brominated pyrimidines were then utilized in a one-pot, two-step Suzuki-Miyaura cross coupling reaction and converted to the corresponding boronic ester intermediate (**9.14c** and **9.15c**). The boronic esters were coupled with the sugar moiety **9.10a** to achieve the parent nucleoside analogues **9.11** and **9.23** in 30% and 48% yields, respectively (**Scheme 46**). (Thames, Waters et al. 2020)



Scheme 46. Optimized synthesis of the Flex-ACV analogues, including prodrugs and triphosphate analogues.

The acetate prodrugs were achieved differently than previously published.(Yates, Raje et al. 2017) Instead of the acetate group being present before coupling, it was added to the nucleoside after the organometallic coupling reaction. Both the 2-amino-4-methoxy series and the 2,4-dimethoxy series utilized the parent nucleosides **9.8** and **9.16** in the presence of acetic anhydride and DMAP in DMF to give the acetate prodrugs (**9.11** and **9.17**) in 70% and 79% yields respectively (**Scheme 46**). (Thames, Waters et al. 2020) The yield reported for the acetate prodrug **9.17** was higher than the previously reported yield.(Yates, Raje et al. 2017) As previously reported, the McGuigan Protide of the parent nucleosides could be achieved via a typical McGuigan Protide synthesis.(Yates, Raje et al. 2017) As seen in **Scheme 46**, the parent nucleosides were reacted with intermediate **9.12** in the presence of *tert*-butyl magnesium chloride to give the prodrugs in high yields (**9.13**- 74% and **9.18**- 86%). The yield of compound **9.13** was also higher than the previously reported synthesis.(Yates, Raje et al. 2017, Thames, Waters et al. 2020)

As previously stated, the triphosphate analogues of nucleoside drugs tend to be the active form of the drug.(Périgaud, Gosselin et al. 1992, De Clercq 2002, Seley-Radtke and Yates 2018, Yates and Seley-Radtke 2019) Therefore, it was important to synthesize the triphosphates of the Flex-ACV nucleosides to elucidate the mechanism of action. The triphosphate analogues were achieved via a modified procedure published by Hollenstein et. al. which utilized the parent nucleosides **9.8** and **9.16** in the presence of tributylammonium pyrophosphate and 2-chloro-1,3,2-benzo-dioxaphosphorin-4-one (Sal-PCI) (**Scheme 46**). After rigorous purification, the triphosphates **9.19** and **9.20** were achieved in 51% and 62% yields, respectively.(Thames, Waters et al. 2020)

The parent Flex-ACV nucleosides and the corresponding prodrug analogues were then tested against various flaviviruses.(Thames, Waters et al. 2020) The viruses within this family such as Dengue virus (DENV), Zika virus (ZIKV), and Yellow Fever virus (YFV) cause severe diseases with high health burden across the globe. With no FDA approved treatments, the *Flaviviridae* family became of interest to the Seley-Radtke lab.(Pierson and Diamond 2020) The Flex-ACV analogues were initially tested for their anti-DENV, YFV, and ZIKV activity on Vero76 cells. The results are summarized in **Table 21**.(Thames, Waters et al. 2020) Several of the compounds were highly potent against the tested flaviviruses, with compound **9.8** having nanomolar levels of activity against DENV (EC₅₀= 0.057 µM) and YFV (EC₅₀= 0.37 µM). Compound **9.8** showed promise as a broad spectrum therapeutic, especially due to previous coronavirus and filovirus activity. Additionally, preliminary maximum tolerated dose studies in mice of compound **9.8** showed no toxicity up to 250 mg per kg.(Thames, Waters et al. 2020)

Table 21. Antiviral activity of the Flex-ACV analogues against flaviviruses.

| Compound | DENV on Vero76 | | ZIKV on Vero76 | | YFV on Vero76 | |
|-------------|--------------------------|--------------------------|--------------------------|--------------------------|--------------------------|--------------------------|
| | EC ₅₀ (µM) | CC ₅₀ (µM) | EC ₅₀ (µM) | CC ₅₀ (µM) | EC ₅₀ (µM) | CC ₅₀ (µM) |
| 9.8 | 0.057 | 1.20 | >1.80 | >1.80 | 0.37 | 1.7 |
| 9.11 | 6.1 | 65 | >100 | >100 | >57 | 57 |
| 9.13 | >57 | 57 | >31 | 31 | >55 | 55 |
| 9.16 | >50 | 50 | >76 | 76 | >58 | 58 |
| 9.17 | 17 | 53 | 79 | >100 | >58 | 58 |
| 9.18 | >53 | 53 | >56 | 56 | >53 | 53 |

Table adapted from Thames et al.(Thames, Waters et al. 2020)

Once in hand, triphosphates **9.19** and **9.20** were evaluated for the ability to inhibit the flavivirus RdRp and/or the flavivirus MTase. Both the RdRp and the MTase are found on the same protein NS5, which is used in viral replication and capping, making these enzymes favorable enzymatic targets.(Pierson and Diamond 2020) Using DENV RdRp, the Flex-ACV triphosphate analogues were tested for their ability to be incorporated into the growing strand of viral RNA. Only very weak inhibition was observed for compound **9.19** at high concentrations (1.1 mM) in the presence of all four NTPs and the absence of GTP, and thus the compound does not act as a chain terminator. Incorporation of compound **9.20** was not observed and therefore it can be concluded that the RdRp is not highly targeted by these compounds and is not responsible for the antiviral activity.(Thames, Waters et al. 2020)

Next the compounds were tested for inhibition of the flaviviral MTase, which is highly conserved on the NS5 protein, unlike the RdRp which has high rates of mutations.(Pierson and Diamond 2020) Both the 2-amino-4-methoxy Flex-ACV series and the 2,4-dimethoxy Flex-ACV series were tested for activity, which is summarized in **Figure 28**.(Thames, Waters et al. 2020) The triphosphate analogues **9.19** and **9.20** were able to decrease the activity of ZIKV and DENV MTase, with **9.20** having the greatest inhibitory effect against ZIKV as seen with a decrease in MTase activity to 9%. It is important to note that none of the analogues were able to inhibit the human N7 MTase, suggesting that the Flex-ACV analogues are selective towards viral enzymes.(Thames, Waters et al. 2020)

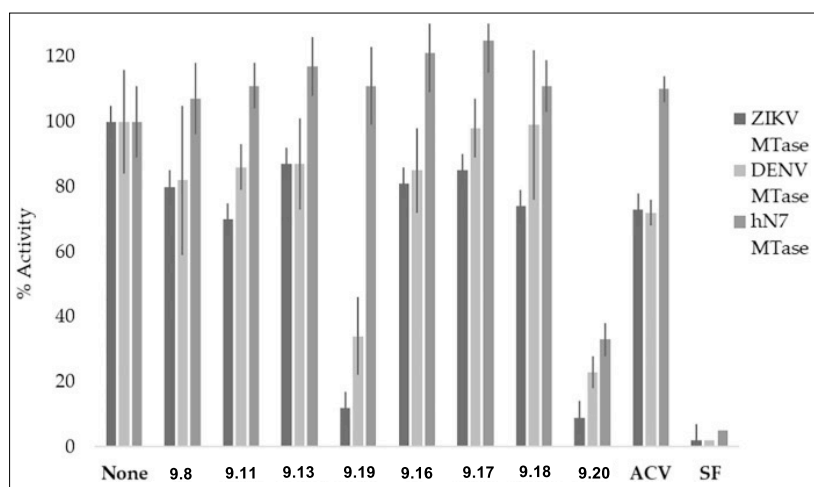


Figure 28. Antiviral activity of the 2-amino-4-methoxy series and the 2,4-dimethoxy series against ZIKV, DENV, and hN7 MTases. Figure adapted with permission from Elsevier.(Thames, Waters et al. 2020)

Compounds **9.19** and **9.20** were further evaluated against ZIKV, DENV, and human N7 MTase to determine the IC_{50} (concentration of compound needed for 50% inhibition) of the triphosphate analogues. The results are summarized in **Table 22**.(Thames, Waters et al. 2020) As seen with the MTase inhibition data in **Figure 28**, the triphosphates are able to inhibit the viral MTases (single digit μM values) while there is very weak inhibition of the human N7 MTase (49 μM). (Thames, Waters et al. 2020) This data suggests that the anti-flaviviral activity exhibited with the 2-amino-4-methoxy Flex-ACV analogue **9.8** is due to MTase inhibition and not inhibition of viral RdRp. This was not expected since many modified nucleoside analogues inhibit viral polymerases like the parent nucleoside acyclovir.(Thames, Waters et al. 2020)

Table 22. IC_{50} for compounds **9.19** and **9.20** against DENV, ZIKV, and hN7 MTases.

| Compound | ZIKV MTase | DENV MTase | hN7 MTase |
|-------------|-----------------------|-----------------------|-----------------------|
| | IC_{50} (μM) | IC_{50} (μM) | IC_{50} (μM) |
| 9.19 | 1.7 | 8.4 | 49 |
| 9.20 | 0.15 | 1.1 | 13 |

Table adapted from Thames et al.(Thames, Waters et al. 2020)

To further explore the mechanism of action of the Flex-ACV triphosphate analogues **9.19** and **9.20**, computational molecular modeling studies were carried out.(Thames, Waters et al. 2020) Predicted binding of the compounds to the cap/GTP binding site of DENV (PDB ID 4V0R), ZIKV (PDB ID 5GOZ), YFV (PDB ID 3EVD), and human N7 (PDB ID 5E9W) MTases were studied in crystal structure docking simulations. Binding of **9.19** and **9.20** in the ZIKV MTase binding site are seen in **Figure 29**.(Thames, Waters et al. 2020) Key hydrogen bonding interactions of the free amine group of compound **9.19** with Met19 and Leu16 and the oxygen in the sugar moiety of the Flex-Acv triphosphate with Lys13 are similar to that of GTP. The switch to

a methoxy group at position 2 in compound **9.20** instead of the free amine resulted in the loss of hydrogen bonding with Met19 and Leu16, but the fleximer triphosphate analogue could still interact with Phe24. Therefore, both the 2-amino-4-methoxy Flex-ACV triphosphate **9.19** and the 2,4-dimethoxy Flex-ACV triphosphate **9.20** occupied the ZIKV MTase binding site in a similar fashion to that of GTP.(Thames, Waters et al. 2020)

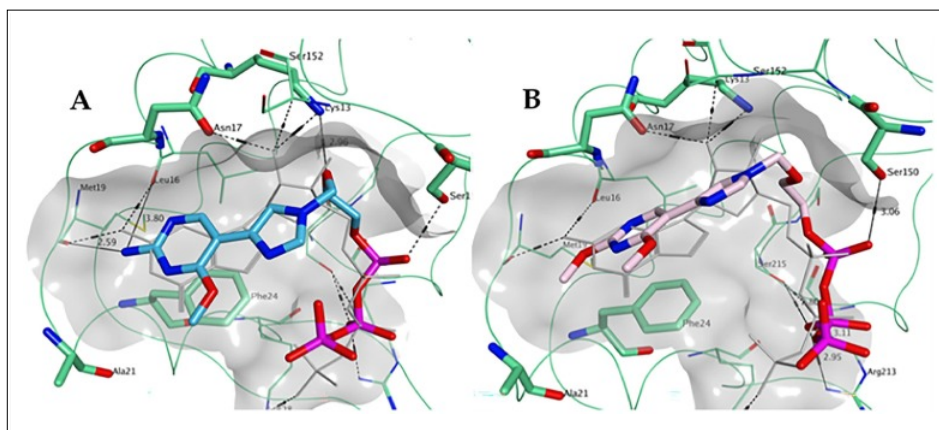


Figure 29. Binding of **9.19** (A) and **9.20** (B) within the GTP pocket of ZIKV NS5 MTase. Image used with permission from Elsevier.(Thames, Waters et al. 2020)

Next the interaction of the triphosphate analogues was explored in the DENV MTase binding site (**Figure 30**). (Thames, Waters et al. 2020) This time important hydrogen bonding interactions with the methoxy group of compound **9.19** were seen with the amino acid residue Arg22. This interaction may explain the increased antiviral activity against DENV compared to the other flaviviruses. This same interaction was seen with the 4-methoxy group on **9.20**. Once again loss of hydrogen bonding at Leu17 and Leu20 was seen for **9.20** due to the replacement of the amino group with a methoxy group at position 2 of the nucleobase. Both triphosphate analogues had similar binding to that of GTP in the DENV MTase binding site. These results suggest that the 2-amino group is essential for the anti-flaviviral activity seen with compound **9.8** and its corresponding triphosphate analogue **9.19**.(Thames, Waters et al. 2020)

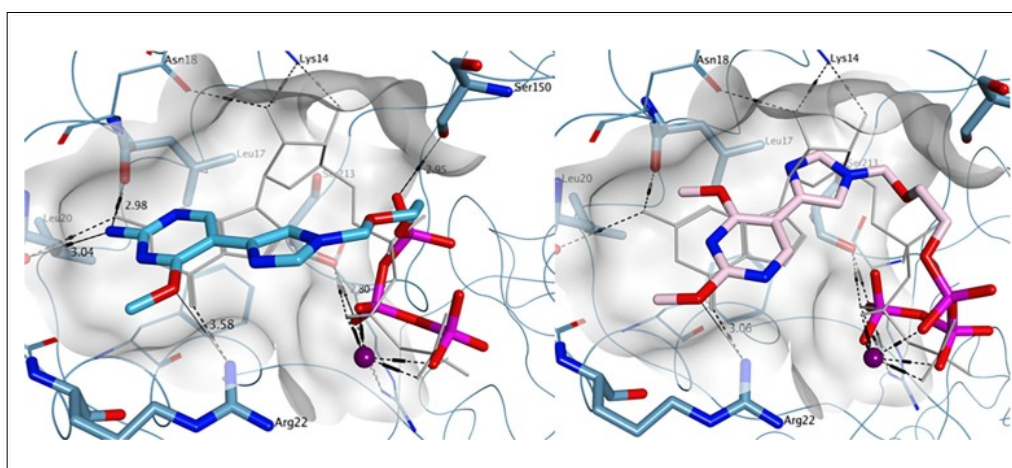


Figure 30. Binding of **9.19** (A) and **9.20** (B) within the GTP pocket of DENV NS5 MTase. Image used with permission from Elsevier.(Thames, Waters et al. 2020)

Next the interactions of the triphosphate analogues in the YFV MTase binding site compared to GTP were explored (**Figure 31**). (Thames, Waters et al. 2020) Once again the 2-amino group of **9.19** had hydrogen bonding interactions with Leu residues 16 and 19, similar to DENV and ZIKV MTase. But the distance between Lys21 and the 4-methoxy group of **9.19** was too far to maintain important interaction and therefore supports the decrease in activity against YFV for the Flex-ACV analogues. Compound **9.20** had no hydrogen bonding interactions with the important Leu and Lys residues.(Thames, Waters et al. 2020)

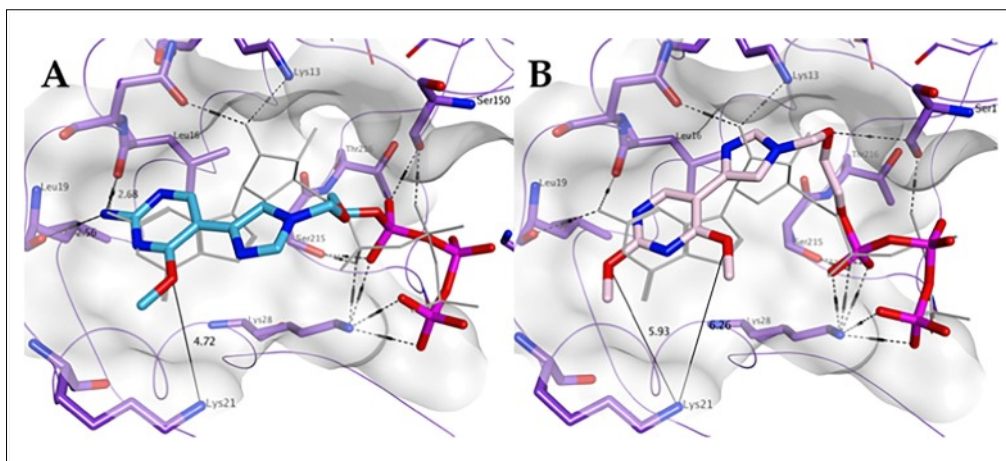


Figure 31. Binding of **9.19** (A) and **9.20** (B) within the GTP pocket of YFV NS5 MTase. Image used with permission from Elsevier.(Thames, Waters et al. 2020)

Finally, the interactions of the triphosphate analogues in the human N7 MTase binding site were investigated (**Figure 32**). (Thames, Waters et al. 2020) It is important to note that the human N7 MTase binding site is very different from that of the flaviviral MTases. It was predicted that the triphosphate analogues would not have strong binding in the human N7 MTase corresponding with the antiviral activity shown earlier. It was found that **9.19** occupied a larger space than GTP and does not have important hydrogen bonding interaction in the binding site. Compound **9.20** appeared to have better binding in the human N7 MTase binding site. The two methoxy groups present on this compound allowed for hydrogen bonding with Asn176. (Thames, Waters et al. 2020)

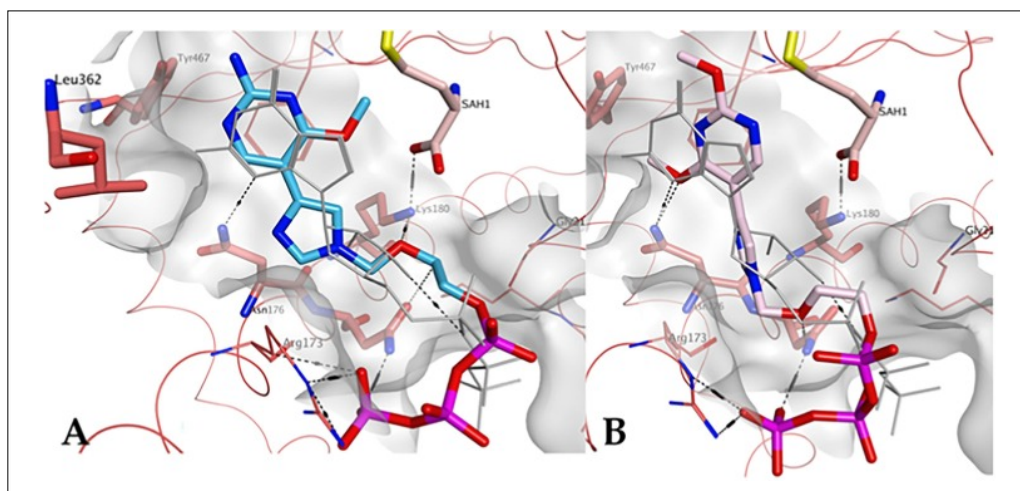


Figure 32. Binding of **9.19** (A) and **9.20** (B) within human N7 MTase pocket. Image used with permission from Elsevier.(Thames, Waters et al. 2020)

Overall, these studies suggest that the Flex-ACV analogues could be potential broad-spectrum antiviral therapeutics against not just the flaviviruses tested in this study but could also have activity against other flaviviruses and other families of viruses.

The Seley-Radtke lab carried out a small SAR study on the Flex-ACV analogues to elucidate the effect of hydrogen bond donor and hydrogen bond acceptor groups on the pyrimidine moiety, as well as various acetate protecting groups on the sugar moiety, on antiviral activity. (Yates, Chatterjee et al. 2019) **Figure 33** depicts the various analogues synthesized in this study.

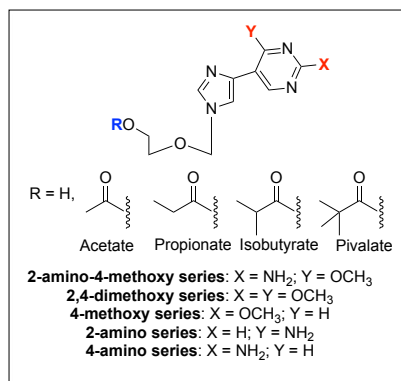
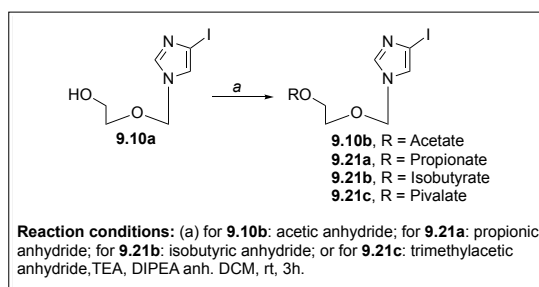


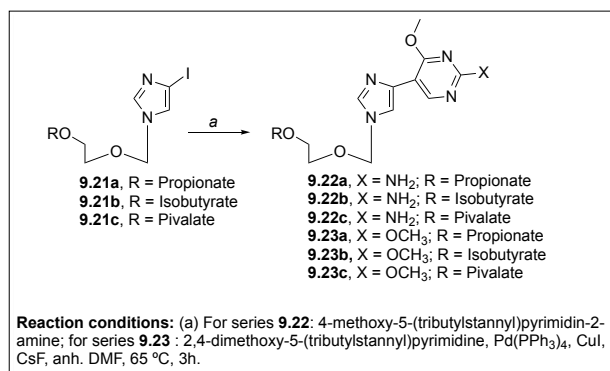
Figure 33. Various series of compounds synthesized in the Flex-ACV SAR study.

The SAR featured compounds that had previously been synthesized in the lab, as well as new novel Flex-ACV analogues. Synthesis of the sugar intermediate **9.10a**, as well as the synthesis of **9.8**, **9.11**, **9.16**, and **9.17** had previously been reported in other publications and will not be detailed in this portion of this paper. (Peters, Jochmans et al. 2015, Yates, Raje et al. 2017, Thames, Waters et al. 2020) Synthesis of all ester protecting intermediates was achieved via the reaction of the monoiodo sugar **9.10a** with the appropriate anhydride compound, TEA, and DIPEA (**Scheme 47**) to yield compounds **9.10b**, **9.21a**, **9.21b**, and **9.21c**. (Yates, Chatterjee et al. 2019) The ester intermediates could then be used in Stille coupling conditions previously established. (Peters, Jochmans et al. 2015, Yates, Raje et al. 2017)



Scheme 47. Synthesis of the various acetate protected sugar intermediates.

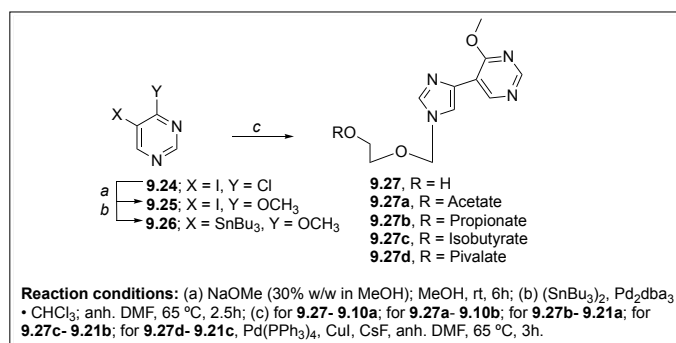
To synthesize the remaining three ester-protected (propionate, isobutyrate, pivalate) 2-amino-4-methoxy analogues, the appropriate stannyl pyrimidine was coupled to the corresponding ester sugar intermediate in a Stille reaction to give compounds **9.22a**, **9.22b**, and **9.22c** in good yields (**Scheme 48**). (Yates, Chatterjee et al. 2019) The remaining ester-protected 2,4-dimethoxy analogues **9.23a**, **9.23b**, and **9.23c** were achieved in good yields under similar Stille conditions (**Scheme 48**). (Yates, Chatterjee et al. 2019)



Scheme 48. Synthesis of the 2-amino-4-methoxy Flex-ACV series, as well as the 2,4-dimethoxy Flex-ACV series.

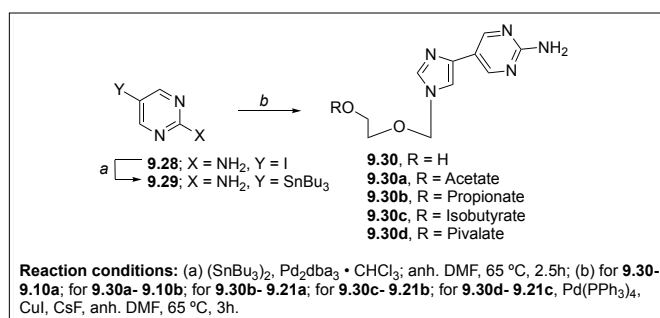
The next series of Flex-ACV nucleosides to be synthesized were the 4-methoxy pyrimidine analogues. Synthesis began with the formation of the stannyl pyrimidine starting from commercially available 4-chloro-5-iodopyrimidine (**9.24**). In the presence of sodium methoxide, the chlorine on position 4 could be

converted to a methoxy group to give compound **9.25** in good yields (**Scheme 49**). (Yates, Chatterjee et al. 2019) This compound was then treated with tributyltin and a palladium catalyst with mild heating to give the 4-methoxy stannyl pyrimidine **9.26**. As seen in **Scheme 49**, the stannyl pyrimidine was then used in various couplings of the sugar moieties to yield the following compounds: **9.27**, **9.27a**, **9.27b**, **9.27c**, and **9.27d** in 30% to 45% yields. (Yates, Chatterjee et al. 2019)



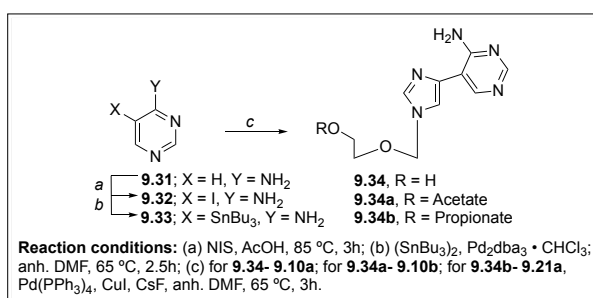
Scheme 49. Synthesis of the 4-methoxy Flex-ACV series.

The next Flex-ACV nucleoside series to be synthesized was the 2-aminopyrimidine series, which began with commercially available 2-amino-5-iodopyrimidine (**9.28**) and was converted to the stannyl pyrimidine using similar methods described above to give compound **9.29**. This pyrimidine could then be used in Stille conditions to achieve compounds **9.30-9.30d** in greater than 50% yields (**Scheme 50**). (Yates, Chatterjee et al. 2019) This was much higher than that observed for the 2-amino-4-methoxy series. (Yates, Chatterjee et al. 2019)



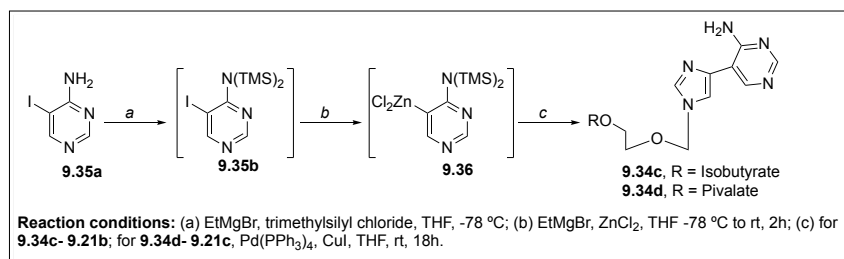
Scheme 50. Synthesis of the 2-amino Flex-ACV series.

The final pyrimidine series explored on the Flex-ACV analogues were the 4-aminopyrimidine analogues. Synthesis began with commercially available 4-aminopyrimidine (**9.31**) that was iodinated at position 5 (**9.32**) in the presence of N-iodosuccinamide in acetic acid. This compound was then converted to the stannyl pyrimidine (**9.33**) via previously described methods (**Scheme 51**). (Yates, Chatterjee et al. 2019) Stille cross coupling conditions realized compounds **9.34-9.34b**, all in very low yields due to residual tin impurities that were difficult to remove. (Yates, Chatterjee et al. 2019) Various attempts to remove the tin impurities were unsuccessful, so potential protecting groups for the 4-amino group proved to be necessary for the coupling reactions of this series. First a di-boc protection of the 4-amino group was attempted with di-tert-butyl dicarbonate, which was successful, but later attempts to convert this pyrimidine compound to the stannyl intermediate were unsuccessful. Efforts to convert the protected pyrimidine to a boronic ester under Suzuki coupling conditions proved fruitless. (Yates, Chatterjee et al. 2019)



Scheme 51. Synthesis of the first set of 4-amino Flex-ACV analogues.

To achieve the protected amino group on the pyrimidine, an *in situ* protection was carried out with chlorotrimethylsilane to give compound **9.35b** (Scheme 52). (Yates, Chatterjee et al. 2019) This compound was complexed with ZnCl₂ in Negishi type coupling conditions to afford intermediate **9.36**. The addition of the isobutyrate and pivalate sugar moieties to the zinc intermediate gave the respective nucleosides **9.34c** and **9.34d**. (Yates, Chatterjee et al. 2019) Purification of the analogues proved to be difficult due to streaking on silica columns. This was resolved with the addition of NH₄OH to the solvent gradient used for chromatography purification to give the final compound in decent yields. (Yates, Chatterjee et al. 2019)



Scheme 52. Synthesis of the remaining 4-amino Flex-ACV analogues.

All synthesized compounds were tested for antiviral activity against EBOV-Makona in Huh7 cells at the Centers for Disease Control (CDC). The EC₅₀ and cell viability were determined for each compound. The results are summarized in Table 23. (Yates, Chatterjee et al. 2019) It is important to note that none of the modified Flex-ACV analogues tested in this study exhibited cytotoxicity up to 100 μM. Compound **9.8** still demonstrated single digit micromolar activity against EBOV as previously established in other antiviral testing. It was also demonstrated that the pyrimidine modifications, as well as the various ester protecting groups led to trends in antiviral activity. (Yates, Chatterjee et al. 2019)

Table 23. Antiviral screening for the Flex-ACV SAR compounds against EBOV.

| R Group | 2-amino-4-methoxy analogues | 2,4-dimethoxy analogues | 4-methoxy analogues | 2-amino analogues | 4-amino analogues |
|-------------|-----------------------------|-------------------------|-----------------------|-----------------------|-----------------------|
| | EC ₅₀ (μM) | EC ₅₀ (μM) | EC ₅₀ (μM) | EC ₅₀ (μM) | EC ₅₀ (μM) |
| H | 1.49 ± 0.98 | 23.44 ± 20.28 | 78.88 ± 17.14 | >100 | >100 |
| acetate | >100 | 16.34 ± 11.46 | 35.36 ± 20.37 | 52.89 ± 28.25 | >100 |
| propionate | 62.18 ± 18.99 | >100 | 51.87 ± 19.58 | >100 | >100 |
| isobutyrate | >100 | 31.96 ± 9.12 | 38.29 ± 28.15 | 53.99 ± 23.74 | >100 |
| pivalate | 7.21 ± 1.85 | 81.34 ± 10.15 | 51.40 ± 10.01 | 34.42 ± 20.01 | 72.29 ± 18.74 |

Table adapted from Yates et al. (Yates, Chatterjee et al. 2019)

The antiviral activity revealed that a change from the hydrogen donating 2-amino group on compound **9.8** to a hydrogen accepting 2-methoxy group on compound **9.16** decreased anti-EBOV activity from 1.49 μM to 23.44 μM respectively. When only a hydrogen atom is present at position 2 of the pyrimidine moiety, antiviral activity decreased again. When only an amino group was present on the pyrimidine moiety i. e. compounds **9.30** and **9.34**, anti-EBOV activity was not observed. For the 2-amino, 4-amino, and 4-methoxy series, activity was improved depending on the ester group present on the sugar. (Yates, Chatterjee et al. 2019) The ester protected 4-methoxy compound **9.27a** had an EC₅₀ of 35.36 μM, while its non-protected parent analogue **9.27** had decreased antiviral activity (78.88 μM). But the ester protecting group did not affect all Flex-ACV series the same. Some had better activity than the parent analogues, while others did not. (Yates, Chatterjee et al. 2019) The other ester protecting groups also gave variable activity across all analogues. It is important to note that even with ester protection, the 4-amino series did not see a statistically significant increase in anti-EBOV activity, which when paired with the results from the active compounds, suggest that the 4-methoxy group is necessary for antiviral activity to occur. (Yates, Chatterjee et al. 2019)

To determine if the decrease in antiviral activity was due to lipophilicity or branching of the ester groups (i.e. acetate vs. propionate vs. isobutyrate vs pivalate), logP of the acetate protecting groups was determined (Table 24). (Yates, Chatterjee et al. 2019) The greater the logP value, the more lipophilic the compound. To no surprise the parent analogues that contained R group = H, were the least lipophilic. The lowest lipophilicity was observed with the 2-amino and 4-amino pyrimidine series. The larger the ester protecting group, the larger the logP value. (Yates, Chatterjee et al. 2019) It is important to note that the

lipophilicity can predict antiviral activity, but if a compound is too lipophilic, this hinders the antiviral activity. This is suggested when comparing the activity of the isobutyrate protected analogues to the pivalate protected analogues. Those analogues containing the pivalate had decreased antiviral activity i.e., compound **9.30c** vs **9.30d**.(Yates, Chatterjee et al. 2019)

Table 24. logP values for the Flex-ACV analogues.

| R Group | logP | | | | |
|--------------------|-----------------------------|-------------------------|---------------------|-------------------|-------------------|
| | 2-amino-4-methoxy analogues | 2,4-dimethoxy analogues | 4-methoxy analogues | 2-amino analogues | 4-amino analogues |
| H | 0.02 | 0.7 | 0.31 | -0.57 | -0.36 |
| acetate | 0.25 | 0.93 | 0.54 | -0.34 | -0.14 |
| propionate | 0.9 | 1.58 | 1.2 | 0.31 | 0.52 |
| isobutyrate | 1.47 | 2.15 | 1.76 | 0.88 | 1.09 |
| pivalate | 2.18 | 2.85 | 2.47 | 1.59 | 1.79 |

Table adapted from Yates et al.(Yates, Chatterjee et al. 2019)

Previous NMR studies conducted with the Seley-Radtke lab found that fleximer analogues prefer to be in anti-conformation in solution, which is the typical conformation of nucleosides.(Polak, Seley et al. 2004) Similar studies were pursued with the Flex-ACV analogues. Compounds were analyzed in 1% DMSO-*d*₆/D₂O via Nuclear Overhauser Effect Spectroscopy experiments.(Yates, Chatterjee et al. 2019) It was confirmed for compound **9.8**, **9.11**, **9.16**, and **9.17** that the anti-conformation was preferred as seen by the NMR conformation that the aromatic protons H6 and H11 are spatially apart from each other.(Yates, Chatterjee et al. 2019) The 4-amino parent nucleoside **9.34** and its acetate protected counterpart **9.34a** preferred syn-conformation in solution, which could explain the lack of anti-EBOV seen with these compounds. Further testing needs to be performed on the other pyrimidine series.(Yates, Chatterjee et al. 2019)

Overall, this SAR study, along with the antiviral activity previously discussed for the Flex-ACV analogues, it is possible that these analogues may serve as broad spectrum antiviral therapeutics against a wide variety of viral families such as flaviviruses, filoviruses, and coronaviruses. Further elucidation on the mechanism of action of the compounds, as well as *in vivo* testing of the active analogues will need to be performed. Further modifications across the Flex-ACV scaffold as well as new prodrugs will also be investigated at a later date.

E. Conclusion

Since its first introduction back in 2001(Seley, Zhang et al. 2001), the fleximer technology has been applied to a wide range of nucleoside analogues, proving its versatility.(Seley-Radtke 2018, Chudinov 2020) The fleximer bond can be inserted between the C-5 of the imidazole moiety and the C-6 of the pyrimidine to afford *distal* fleximer analogues (Seley, Zhang et al. 2001, Seley, Zhang et al. 2002) or between the C-4 of the imidazole and C-5 of the pyrimidine, providing *proximal* fleximer analogues.(Seley, Salim et al. 2005) This fleximer bond can even be 'reversed' in which the pyrimidine ring forms the glycosidic bond with the sugar moiety instead, resulting in reverse fleximers.(Sadler, Ojewoye et al. 2008, Zimmermann, Sadler et al. 2011)

Additionally, the utilization of various sugar moieties has been applied to fleximers, such as those containing 2' and/or 3' modifications, as observed with the carboxylic fleximer analogues reported by Seley-Radtke et al.(Zimmermann, Sadler et al. 2011, Wauchope, Velasquez et al. 2012, Zimmermann, Sadler et al. 2013) as well as by Khandazhinskaya et al.(Khandazhinskaya, Eletskaia et al. 2021), or even acyclic sugar moieties, as first reported by the Seley-Radtke group in 2015.(Peters, Jochmans et al. 2015) The acyclovir fleximer analogue **9.2** has shown particularly potent activity against coronaviruses (HCoV-NL63, MERS-CoV, SARS-CoV) whereas the parent compound is completely inactive.(Peters 2015, Peters, Jochmans et al. 2015) Additionally, acyclovir fleximer analogues from series **9.2** and **9.13** have proven effective against a number of other viruses, including filoviruses (e.g. EBOV, MARV, SUDV)(Yates, Raje et al. 2017) and flaviviruses (e.g. DENV, ZIKV, YFV)(Thames, Waters et al. 2020), demonstrating the ability of fleximers to exhibit broad-spectrum antiviral activity.

Overall, the fleximer technology with nucleoside analogues has been shown to have great potential and a promising future in nucleoside antiviral drug design. Current efforts are underway to explore new nucleoside scaffolds and endow them with the fleximer technology, the results of which will be reported as they become available.

F. References:

Andersson, J., B. Sköldenberg, I. Ernberg, S. Britton, W. Henle and U. Andersson (1985). "Acyclovir treatment in primary Epstein-Barr virus infection. A double-blind placebo-controlled study." Scand J Infect Dis Suppl **47**: 107-115.

Barkholt, L., I. Lewensohn-Fuchs, B. G. Ericzon, G. Tydén and J. Andersson (1999). "High-dose acyclovir prophylaxis reduces cytomegalovirus disease in liver transplant patients." Transpl Infect Dis **1**(2): 89-97.

Chiang, P. K. (1998). "Biological effects of inhibitors of S-adenosylhomocysteine hydrolase." Pharmacol Ther **77**(2): 115-134.

Chudinov, M. V. (2020). "Nucleoside Analogs with Fleximer Nucleobase." Chem. Heterocycl. Compd. (N. Y., NY, U. S.) **56**(6): 636-643.

Clercq, E. D. and A. Holý (2005). "Acyclic nucleoside phosphonates: a key class of antiviral drugs." Nature Reviews Drug Discovery **4**(11): 928-940.

De Clercq, E. (1994). "Antiviral Activity Spectrum and Target of Action of Different Classes of Nucleoside Analogues." Nucleosides and Nucleotides **13**(6-7): 1271-1295.

De Clercq, E. (2002). "Strategies in the design of antiviral drugs." Natl Rev Drug Discov **1**(1): 13-25.

De Clercq, E. (2005). "Antiviral drug discovery and development: where chemistry meets with biomedicine." Antiviral Res **67**(2): 56-75.

De Clercq, E. (2005). "Recent highlights in the development of new antiviral drugs." Curr Opin Microbiol **8**(5): 552-560.

De Clercq, E. and J. Neyts (2009). "Antiviral agents acting as DNA or RNA chain terminators." Handb Exp Pharmacol(189): 53-84.

De Winter, H. and P. Herdewijn (1996). "Understanding the binding of 5-substituted 2'-deoxyuridine substrates to thymidine kinase of herpes simplex virus type-1." J Med Chem **22**(39(24)): 4727-4737.

Deval, J. (2009). "Antimicrobial strategies: inhibition of viral polymerases by 3'-hydroxyl nucleosides." Drugs **69**(2): 151-166.

Deval, J., M. H. Powdrill, C. M. D'Abramo, L. Cellai and M. Götte (2007). "Pyrophosphorolytic excision of nonobligate chain terminators by hepatitis C virus NS5B polymerase." Antimicrob Agents Chemother **51**(8): 2920-2928.

Docea, A., A. Tsatsakis, D. Albulescu, O. Cristea, O. Zlatian, M. Vinceti, S. Moschos, D. Tsoukalas, M. Goumenou, N. Drakoulis, J. Dumanov, V. Tutelyan, G. Onischenko, M. Aschner, D. Spandidos and D. Calina (2020). "A new threat from an old enemy: Re-emergence of coronavirus (Review)." International Journal of Molecular Medicine.

Fischer, E. (1894). "Einfluss der Configuration auf die Wirkung der Enzyme." Berichte der deutschen chemischen Gesellschaft **27**(3): 2985-2993.

Greco, N. J. and Y. Tor (2005). "Simple Fluorescent Pyrimidine Analogues Detect the Presence of DNA Abasic Sites." J. Am. Chem. Soc. **127**(31): 10784-10785.

Khandazhinskaya, A., B. Eletskaia, I. Fateev, M. Kharitonova, I. Konstantinova, V. Barai, A. Azhayev, M. T. Hyvonen, T. A. Keinänen, S. Kochetkov, K. Seley-Radtke, A. Khomutov and E. Matyugina (2021). "Novel fleximer pyrazole-containing adenosine analogues: chemical, enzymatic and highly efficient biotechnological synthesis." Org. Biomol. Chem.: Ahead of Print.

Koshland, D. E. (1958). "Application of a Theory of Enzyme Specificity to Protein Synthesis." Proc Natl Acad Sci U S A **44**(2): 98-104.

Ku, T., N. Lopresti, M. Shirley, M. Mori, J. Marchant, X. Heng, M. Botta, M. F. Summers and K. L. Seley-Radtke (2019). "Synthesis of distal and proximal fleximer base analogues and evaluation in the nucleocapsid protein of HIV-1." Bioorg. Med. Chem. **27**(13): 2883-2892.

Leonard, N. J. and S. P. Hiremath (1986). "Dimensional Probes of Binding and Activity." Tetrahedron **42**(7): 1917-1961.

Leonard, N. J., A. G. Morrice and M. A. Sprecker (1975). "Linear benzoadenine. Stretched-out analog of adenine." The Journal of Organic Chemistry **40**(3): 356-363.

Mattelaer, H.-P., H. A.-S. Van, J. F. de, d. A. M. Van, M. L. Van, W. Dehaen and P. Herdewijn (2020). "New metal-free route towards imidazole substituted uridine." European J Org Chem.

Matyugina, E. S., A. L. Khandazhinskaya, S. N. Kochetkov and K. L. Seley-Radtke (2020). "Synthesis of 3-hetarylpyrroles by Suzuki-Miyaura cross-coupling." Mendeleev Communications **30**(2): 231-232.

McGuigan, C., D. Cahard, H. M. Sheeka, E. De Clercq and J. Balzarini (1996). "Aryl phosphoramidate derivatives of d4T have improved anti-HIV efficacy in tissue culture and may act by the generation of a novel intracellular metabolite." J Med Chem **39**(8): 1748-1753.

McGuigan, C., A. Hassan-Abdallah, S. Srinivasan, Y. Wang, A. Siddiqui, S. M. Daluge, K. S. Gudmundsson, H. Zhou, E. W. McLean, J. P. Peckham, T. C. Burnette, H. Marr, R. Hazen, L. D. Condreay, L. Johnson and J. Balzarini (2006). "Application of phosphoramidate ProTide technology significantly improves antiviral potency of carbocyclic adenosine derivatives." J Med Chem **49**(24): 7215-7226.

McGuigan, C., K. Madela, M. Aljarah, A. Gilles, A. Brancale, N. Zonta, S. Chamberlain, J. Vernachio, J. Hutchins, A. Hall, B. Ames, E. Gorovits, B. Ganguly, A. Kolykhalov, J. Wang, J. Muhammad, J. M. Patti and G. Henson (2010). "Design, synthesis and evaluation of a novel double pro-drug: INX-08189. A new clinical candidate for hepatitis C virus." Bioorganic & Medicinal Chemistry Letters **20**(16): 4850-4854.

Mehellou, Y., H. S. Rattan and J. Balzarini (2018). "The ProTide Prodrug Technology: From the Concept to the Clinic." Journal of Medicinal Chemistry **61**(6): 2211-2226.

Mori, M., U. Dietrich, F. Manetti and M. Botta (2010). "Molecular Dynamics and DFT Study on HIV-1 Nucleocapsid Protein-7 in Complex with Viral Genome." Journal of Chemical Information and Modeling **50**(4): 638-650.

Mori, M., F. Manetti and M. Botta (2011). "Predicting the Binding Mode of Known NCp7 Inhibitors To Facilitate the Design of Novel Modulators." Journal of Chemical Information and Modeling **51**(2): 446-454.

Morrice, A. G., M. A. Sprecker and N. J. Leonard (1975). "The angular benzoadenines. 9-Aminoimidazo[4,5-f]quinazoline and 6-aminoimidazo [4,5-h]quinazoline." J Org Chem **40**(3): 363-366.

Najjar, A. and R. Karaman (2019). "The prodrug approach in the era of drug design." Expert Opinion on Drug Delivery **16**(1): 1-5.

Nguyen Van, T., A. Hospital, C. Lionne, L. P. Jordheim, C. Dumontet, C. Périgaud, L. Chaloin and S. Peyrottes (2016). "Beta-hydroxyphosphonate ribonucleoside analogues derived from 4-substituted-1,2,3-triazoles as IMP/GMP mimics: synthesis and biological evaluation." Beilstein Journal of Organic Chemistry **12**: 1476-1486.

Ouellette, R. and J. D. Rawn (2018). Nucleosides, Nucleotides, and Nucleic Acid. Organic Chemistry: Structure, Mechanism, Synthesis. London, U.K., Academic Press 973-1000.

O'Brien, J. J. and D. M. Campoli-Richards (1989). "Acyclovir." Drugs **37**(3): 233-309.

Peters, H. L. (2015). The Design, Synthesis, and Biological Evaluation of a Series of Acyclic Fleximer Nucleoside Antivirals. Ph.D, University of Maryland, Baltimore County.

Peters, H. L., D. Jochmans, A. H. de Wilde, C. C. Posthuma, E. J. Snijder, J. Neyts and K. L. Seley-Radtke (2015). "Design, synthesis and evaluation of a series of acyclic fleximer nucleoside analogues with anti-coronavirus activity." Bioorg. Med. Chem. Lett. **25**(15): 2923-2926.

Pierson, T. C. and M. S. Diamond (2020). "The continued threat of emerging flaviviruses." Nature Microbiology **5**(6): 796-812.

Polak, M., K. L. Seley and J. Plavec (2004). "Conformational Properties of Shape Modified Nucleosides - Fleximers." J. Am. Chem. Soc. **126**(26): 8159-8166.

Périgaud, C., G. Gosselin and J. L. Imbach (1992). "Nucleoside Analogues as Chemotherapeutic Agents: A Review." Nucleosides and Nucleotides **11**(2-4): 903-945.

Quirk, S. and K. L. Seley (2005). "Identification of catalytic amino acids in the human GTP fucose pyrophosphorylase active site." Biochemistry **44**(39): 13172-13178.

Ross, B. S., P. Ganapati Reddy, H.-R. Zhang, S. Rachakonda and M. J. Sofia (2011). "Synthesis of Diastereomerically Pure Nucleotide Phosphoramidates." The Journal of Organic Chemistry **76**(20): 8311-8319.

Sadler, J. M., O. Ojewoye and K. L. Seley-Radtke (2008). ""Reverse fleximers": introduction of a series of 5-substituted carbocyclic uridine analogues." Nucleic Acids Symp Ser (Oxf)(52): 571-572.

Seley, K. L., S. Quirk, S. Salim, L. Zhang and A. Hagos (2003). "Unexpected inhibition of S-adenosyl-L-homocysteine hydrolase by a guanosine nucleoside." Bioorg. Med. Chem. Lett. **13**(12): 1985-1988.

Seley, K. L., S. Salim and L. Zhang (2005). ""Molecular Chameleons". Design and Synthesis of C-4-Substituted Imidazole Fleximers." Org. Lett. **7**(1): 63-66.

Seley, K. L., L. Zhang and A. Hagos (2001). ""Fleximers". Design and Synthesis of Two Novel Split Nucleosides." Org. Lett. **3**(20): 3209-3210.

Seley, K. L., L. Zhang, A. Hagos and S. Quirk (2002). ""Fleximers". Design and Synthesis of a New Class of Novel Shape-Modified Nucleosides." J. Org. Chem. **67**(10): 3365-3373.

Seley-Radtke, K. (2018). "Flexibility-Not just for yoga anymore!" Antivir Chem Chemother **26**: 2040206618756788.

Seley-Radtke, K. L. and N. K. Sunkara (2009). "Carbocyclic Thymidine Analogues for Use as Potential Therapeutic Agents." Nucleosides, Nucleotides & Nucleic Acids **28**(5-7): 633-641.

Seley-Radtke, K. L. and M. K. Yates (2018). "The evolution of nucleoside analogue antivirals: A review for chemists and non-chemists. Part 1: Early structural modifications to the nucleoside scaffold." Antiviral Research **154**: 66-86.

Slusarczyk, M., M. Serpi and F. Pertusati (2018). "Phosphoramidates and phosphonamidates (ProTides) with antiviral activity." Antiviral Chemistry and Chemotherapy **26**: 204020661877524.

St. Amant, A. H., L. A. Bean, J. P. Guthrie and R. H. E. Hudson (2012). "Click fleximers: a modular approach to purine base-expanded ribonucleoside analogs." Org. Biomol. Chem. **10**(32): 6521-6525.

Tan, E. L. C., E. E. Ooi, C.-Y. Lin, H. C. Tan, A. E. Ling, B. Lim and L. W. Stanton (2004). "Inhibition of SARS Coronavirus Infection In Vitro with Clinically Approved Antiviral Drugs." Emerging Infectious Diseases **10**(4): 581-586.

Thames, J. E., C. D. Waters, C. Valle, M. Bassetto, W. Aouadi, B. Martin, B. Selisko, A. Falat, B. Coutard, A. Brancale, B. Canard, E. Decroly and K. L. Seley-Radtke (2020). "Synthesis and biological evaluation of novel flexible nucleoside analogues that inhibit flavivirus replication in vitro." Bioorg Med Chem **28**(22): 115713.

Tripathi, A. and V. Bankaitis (2017). "Molecular Docking: From Lock and Key to Combination Lock." J Mol Med Clin Appl **2**(1).

Vichier-Guerre, S., L. Dugué and S. Pochet (2014). "A convenient synthesis of 4(5)-(hetero)aryl-1H-imidazoles via microwave-assisted Suzuki–Miyaura cross-coupling reaction." **55**(46): 6347-6350.

Vichier-Guerre, S., T. C. Ku, S. Pochet and K. L. Seley-Radtke (2020). "An Expedient Synthesis of Flexible Nucleosides through Enzymatic Glycosylation of Proximal and Distal Fleximer Bases." ChemBioChem **21**(10): 1412-1417.

Wauchope, O. R., M. Velasquez and K. Seley-Radtke (2012). "Synthetic routes to a series of proximal and distal 2'-deoxy fleximers." Synthesis **44**(22): 3496-3504.

Wigerinck, P., C. Pannecouque, R. Snoeck, P. Claes, E. De Clercq and P. Herdewijn (1991). "5-(5-Bromothien-2-yl)-2'-deoxyuridine and 5-(5-chlorothien-2-yl)-2'-deoxyuridine are equipotent to (E)-5-(2-bromovinyl)-2'-deoxyuridine in the inhibition of herpes simplex virus type I replication." Journal of Medicinal Chemistry **34**(8): 2383-2389.

Yates, M. K., P. Chatterjee, M. Flint, Y. Arefeayne, D. Makuc, J. Plavec, C. F. Spiropoulou and K. L. Seley-Radtke (2019). "Probing the effects of pyrimidine functional group switches on acyclic fleximer analogues for antiviral activity." Molecules **24**(17): 3184.

Yates, M. K., M. R. Raje, P. Chatterjee, C. F. Spiropoulou, S. Bavari, M. Flint, V. Soloveva and K. L. Seley-Radtke (2017). "Flex-nucleoside analogues - Novel therapeutics against filoviruses." Bioorg Med Chem Lett **27**(12): 2800-2802.

Yates, M. K. and K. L. Seley-Radtke (2019). "The evolution of antiviral nucleoside analogues: A review for chemists and non-chemists. Part II: Complex modifications to the nucleoside scaffold." Antiviral Research **162**: 5-21.

Yin, D., X. Yang, Y. Hu, K. Kuczera, R. L. Schowen, R. T. Borchardt and T. C. Squier (2000). "Substrate binding stabilizes S-adenosylhomocysteine hydrolase in a closed conformation." Biochemistry **39**(32): 9811-9818.

Zimmermann, S. C., E. O'Neill, G. U. Ebiloma, L. J. M. Wallace, H. P. De Koning and K. L. Seley-Radtke (2014). "Design and synthesis of a series of truncated neplanocin fleximers." Molecules **19**(12): 21200-21214, 21215 pp.

Zimmermann, S. C., J. M. Sadler, G. Andrei, R. Snoeck, J. Balzarini and K. L. Seley-Radtke (2011). "Carbocyclic 5'-nor "reverse" fleximers. Design, synthesis, and preliminary biological activity." Medchemcomm **2**(7).

Zimmermann, S. C., J. M. Sadler, P. I. O'Daniel, N. T. Kim and K. L. Seley-Radtke (2013). ""Reverse" Carbocyclic Fleximers: Synthesis of a New Class of Adenosine Deaminase Inhibitors." Nucleosides, Nucleotides Nucleic Acids **32**(3): 137-154.